Spatial Correlation, Trade, and Inequality: Evidence from the Global Climate*

Jonathan I. Dingel
Chicago Booth & NBER

Kyle C. Meng
UC Santa Barbara & NBER

Solomon M. Hsiang
UC Berkeley & NBER

December 2018

Abstract

This paper shows that welfare inequality across a trading network is greater when neighboring locations have more similar productivities. A rise in the global spatial correlation of productivities can raise cross-country welfare dispersion by increasing the correlation between a country's productivity and its gains from trade. To causally examine this mechanism, we study how annual global agricultural trade responds to exogenous changes in the spatial correlation of agricultural productivity driven by a global climatic phenomenon. As predicted, gains from trade over the last half-century were larger for more productive countries and smaller for less productive countries when agricultural productivity was more spatially correlated. In a forecasting application, end-of-century climate change projections that incorporate this general-equilibrium effect exhibit substantially greater global welfare inequality, with higher welfare losses across most of Africa.

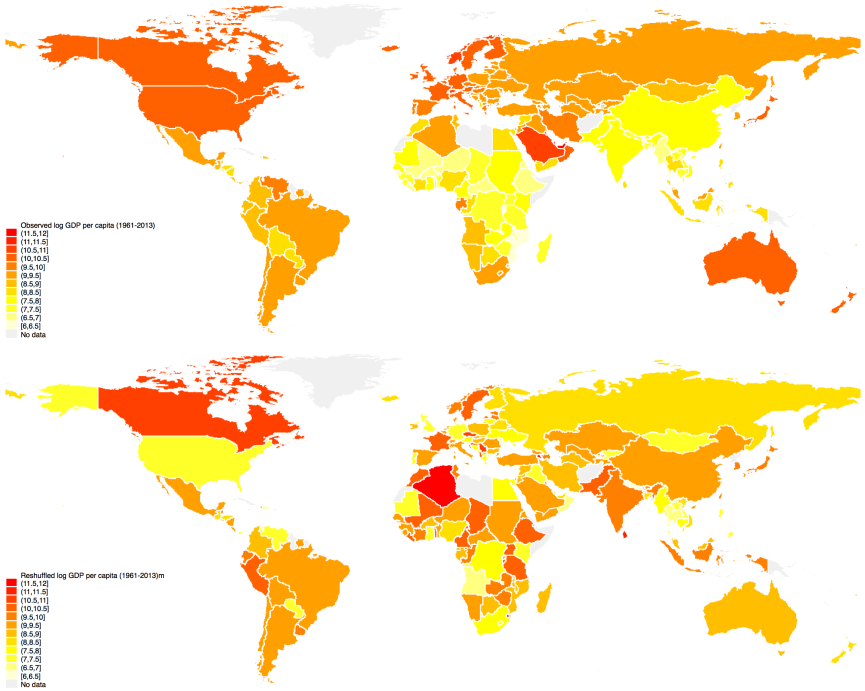
Keywords: gains from trade, spatial correlation, inequality, climate change, El Niño, agricultural trade
JEL codes: F11, F14, F18, O13, Q17, Q54, Q56

*Dingel and Meng contributed equally to this work. We thank Treb Allen, Costas Arkolakis, Mark Cane, Chris Costello, Arnaud Costinot, Tatyana Deryugina, Pedro DiNezio, Dave Donaldson, Robert Feenstra, Kinda Hachem, Christian Hansen, Matthew Kahn, Yuhei Miyauchi, Brent Neiman, Ben Olken, Esteban Rossi-Hansberg, Veronica Rappaport, and Michael Waugh for valuable discussions and suggestions. Thanks to seminar participants at numerous institutions and conferences for helpful comments. Kevin Dano provided excellent research assistance. This work was completed in part with resources provided by the University of Chicago Research Computing Center. Dingel thanks the James S. Kemper Foundation Faculty Research Fund at the University of Chicago Booth School of Business for financial support. A previous version of this paper circulated as "The Spatial Structure of Productivity, Trade, and Inequality: Evidence from the Global Climate." jdingel@chicagobooth.edu, kmeng@bren.ucsb.edu, shsiang@berkeley.edu.

1 Introduction

A striking feature of the global economy is the extent to which economic activity is spatially correlated. This spatial structure is evident in the top panel of Figure 1: low-income countries tend to be near other low-income countries and high-income countries are similarly clustered near one another. Moran's I, a measure of spatial correlation, is 0.247 for log real GDP per capita.[1] By contrast, consider the counterfactual incomes depicted in the bottom panel of Figure 1. This arrangement, which we generated by randomly reassigning the same set of income levels to countries, is spatially uncorrelated, exhibiting a Moran's I statistic of only 0.015.

Figure 1: Average log GDP per capita (1961-2013): observed and reshuffled



NOTES: Top panel shows observed log real GDP per capita averaged over 1961-2013. Bottom panel randomly reshuffles country-level log real GDP per capita from the top panel.

This pattern reflects the fact that many determinants of income are spatially correlated. Neighboring locations often have similar demographics, political institutions, and natural environments, as we document in Table F.1. What are the economic consequences of such spatial correlation? That is, what would happen if the cross-country distribution of productivity had the same mean

[1] Moran's I is a commonly used measure of global spatial correlation that can be computed for any geography endowed with a distance metric. It takes values between -1 and 1. Formally, Moran's I for x_i is

$$I = \frac{N}{\sum_i \sum_{j \neq i} \omega_{ij}} \frac{\sum_i \sum_{j \neq i} \omega_{ij} (x_i - \overline{x}) (x_j - \overline{x})}{\sum_\ell (x_\ell - \overline{x})^2},$$

where N is the number of countries, $\omega_{ij} = \omega_{ji}$ is a spatial weight, and $\overline{x}$ is the cross-sectional average. In all empirical applications, we use spatial weights $\omega_{ij} = 1/(d_{ij} + 1)$, where d_{ij} is the great-circle distance between the two countries' area-weighted centroids.

and variance but looked more like the bottom panel of Figure 1 than the top panel?

In this paper, we show that greater spatial correlation of productivities increases welfare inequality by altering the pattern of international trade. The spatial structure of productivity shapes countries' gains from trade because they trade more with their neighbors than distant countries. We empirically validate this prediction, finding that an observable sufficient statistic for the gains from trade responds to exogenous variation in the spatial correlation of productivities induced by a global climatic phenomenon over the last half century. As a demonstration of how this result can inform empirical research, we show that incorporating changes in spatial correlation into an otherwise standard partial-equilibrium projection of climate-change impacts leads to greater projected inequality.

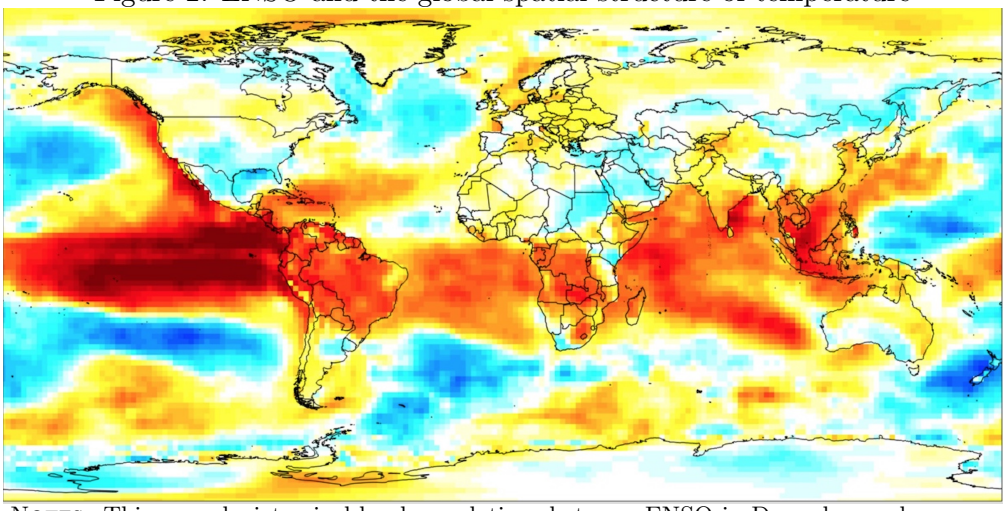
We articulate why the spatial correlation of productivity may influence welfare inequality between trading economies using a standard model of trade. A country benefits by trading with more productive counterparts, which demand more of its exports and sell it cheaper imports. Since trade costs increase with geographic distance (Disdier and Head, 2008), a country enjoys larger gains from trade when its neighbors, rather than distant trading partners, are more productive. Thus, when productivities are spatially uncorrelated, the gains from trade are evenly distributed across space, as all countries are similarly near both more and less productive trading partners. When productivities are spatially correlated, more productive countries gain more from trade because their neighbors are more productive. We prove that greater spatial correlation increases welfare inequality in a four-country model. We then simulate a quantitative trade model with a realistic geography and find that the Moran's I statistic aptly summarizes the model's rich spatial structure. In particular, we show that a reduced-form regression that can be readily taken to data and uses the Moran's I statistic captures more than 93% of the welfare variance generated by the model when productivities are reshuffled.

Our main contribution is to empirically estimate this general-equilibrium relationship. Causal validation of general-equilibrium effects is typically difficult because of a paucity of unaffected control units. This is particularly true when the setting involves international trade and the treatment of interest affects the entire trade network. Under such circumstances, comparisons must be made across equilibria or time. While we cannot experimentally reshuffle productivities as in the bottom panel of Figure 1, we can approximate the experimental ideal using a suitably exogenous phenomenon that varies the global spatial correlation of productivities across time.

To that end, our identification strategy exploits a naturally-occurring climatic phenomenon known as the El Niño-Southern Oscillation (ENSO). In years when ENSO is strong, there are large, spatially contiguous regions of similar temperature conditions. Figure 2 depicts the temperature deviations caused by these ENSO events. Locations near the equator tend to become hotter (red), while mid-latitude locations tend to become cooler (blue). These temperature deviations have consequences for cereal productivity: ENSO increases the global spatial correlation of cereal productivities. We examine the effect of this natural experiment on trade patterns using a sufficient-statistic approach to infer the gains from trade in cereals from observed expenditure shares. In a

broad class of trade models, a country's gains from trade are revealed by the share of its expenditure devoted to imports (Arkolakis, Costinot and Rodríguez-Clare, 2012). As predicted, we find over the last half-century that greater spatial correlation of productivity increases the cross-sectional correlation between productivity and the gains from trade. A one-standard-deviation increase in the spatial correlation of cereal productivities increases the dispersion of welfare attributable to cereal consumption by 2%.

Figure 2: ENSO and the global spatial structure of temperature



NOTES: This map depicts pixel-level correlations between ENSO in December and average temperature during the following February for 1961-2013. Red areas are hotter with warmer ENSO conditions. Blue areas are cooler with warmer ENSO conditions.

Since spatial correlation of economic features is pervasive, this mechanism may be relevant for empirical analyses of many determinants of economic outcomes. Much empirical research looks at the economic consequences of local characteristics without addressing the broader spatial structure of these features. We propose that the spatial correlation of productivity be included in reduced-form exercises to help account for the role of international trade linkages without imposing the full structure of quantitative trade models. To illustrate this approach, we introduce the spatial correlation of cereal productivity into an otherwise standard partial-equilibrium approach for forecasting the economic impacts of anthropogenic climate change. Climate change is expected to substantially alter productivities across the planet, with various general-equilibrium consequences. To examine, in isolation, the general-equilibrium role of spatial correlation, we show that projections that incorporate the change in the spatial correlation of cereal productivity due to climate change predict a 20% greater increase in welfare inequality from cereal consumption by the end of the twenty-first century. Projections that omit this change considerably understate the climate-driven welfare losses for most countries in Africa because these countries jointly experience larger productivity losses. While these projections are not a literal forecast of future climate impacts because they abstract from adaptation, migration, and other possible responses, they demonstrate the value of incorporating spatial correlation into otherwise partial-equilibrium approaches to estimating climate impacts. Similar exercises can be applied, for example, to the literature attributing

differences in cross-country income to local factors and technology by further examining the spatial correlation of these components (Klenow and Rodríguez-Clare, 1997; Caselli, 2005).

This paper relates to the long-running dialogue regarding the influence of environmental and geographic endowments on the well-being of societies (Sachs and Warner, 1997; Easterly and Levine, 2003). Persistent correlations between local geographic endowments and local economic outcomes are often remarkable (Hornbeck, 2012), with prior work articulating numerous potential channels of influence from local conditions to local productivities (Nordhaus, 2006; Bleakley, 2007) and local institutions (Nunn and Puga, 2012). Our analysis advances this literature by exploring the influence of *non-local* geographic endowments, occurring at both neighboring and distant locations, in the determination of local outcomes – an effect that depends critically on the overall spatial structure of endowments. In short, we focus on the general-equilibrium role of geography.

This paper thus contributes to a large literature in international trade and economic geography studying local economic consequences of the geographic distribution of economic activity (Head and Mayer, 2004; Redding and Venables, 2004). Our results link the distribution of the gains from trade to the spatial structure of productivity. In neoclassical trade models, a country's gains from trade depend on its terms of trade – the relative price of its exports compared to its imports. In small-open-economy models, these prices are exogenous, so the terms of trade do not depend on local economic conditions. By contrast, Costinot and Rodríguez-Clare (2014, p.251) say that "one of the main goals of quantitative trade models therefore is to predict the terms-of-trade changes associated with particular shocks." The terms of trade are also important to topics in development and growth.[2] Despite this prominent theoretical role, there is little empirical evidence linking changes in the terms of trade to their economic determinants.[3] We find that expenditure shares respond to local productivity shocks, contrary to the small-open-economy assumption. Higher productivity worsens a country's terms of trade, and this effect is dampened when neighboring countries also have higher productivity.

Spatial correlation in the level of productivity (absolute advantage) is distinct from spatial correlation in the pattern of relative productivities (comparative advantage). Comparative advantage causes countries to gain by specializing and trading with each other. Absolute advantage governs how these gains from trade are divided between countries through the terms of trade. Our prediction concerns the spatial correlation of absolute advantage. In standard quantitative trade models, the pattern of comparative advantage is symmetric across countries (Lind and Ramondo, 2018). If comparative advantage were spatially correlated, neighboring countries would gain less by trading with each other due to the similarity of their relative productivities. Our empirical estimates thus capture the consequences of spatial correlation of absolute advantage as mediated by any spatial correlation in comparative advantage.

[2] For example, in Acemoglu and Ventura (2002), diminishing returns due to terms-of-trade effects govern the dispersion of the world income distribution.

[3] Empirical work, which "typically assumes that countries are small and that the terms of trade are exogenous" (Debaere and Lee, 2003), has primarily focused on the consequences of external shocks to countries' commodity terms of trade. Notable exceptions are Acemoglu and Ventura (2002) and Debaere and Lee (2003), which study the effects of capital accumulation on the terms of trade.

The most closely related study of global agricultural trade is by Costinot, Donaldson and Smith (2016), who examine the consequences of climate change using a model of international trade and an agronomic productivity forecast. While we focus on the spatial correlation of absolute advantage, they focus on changes in comparative advantage and within-country crop switching. While they employ agronomic forecasts to predict changes in trade flows, we empirically estimate the trade effects of historical variation in agricultural productivities.

Finally, this paper speaks to the growing empirical literature examining how anthropogenic climate change may affect inequality across countries, which could provide a new consideration for the long-running discussion of cross-country convergence (Lucas, 1988; Barro, 1991; Johnson and Papageorgiou, 2018). Prior research employing estimates from historical local temperature variation projects increased dispersion in various economic outcomes across countries under climate change (Dell, Jones and Olken, 2012; Burke, Hsiang and Miguel, 2015). This paper shows that projected future welfare inequality may be even greater when projections include general-equilibrium effects due to changes in the spatial structure of productivity. In doing so, this paper advances the climate impacts literature by bringing the reduced-form approach conceptually closer to recent structural macroeconomic analyses exploring the spatial distribution of economic activity under climate change (Brock, Engström and Xepapadeas, 2014; Desmet and Rossi-Hansberg, 2015; Krusell and Smith, 2016).

The rest of the paper is structured as follows: Section 2 introduces our theoretical framework and prediction linking spatial correlation and trade. Section 3 shows that the El Niño-Southern Oscillation affects the spatial correlation of cereal productivity across the world. Section 4 uses temperature- and ENSO-driven variation in cereal productivities to empirically estimate how spatial correlation of productivity affects the pattern of the gains from trade. Section 5 considers implications for projecting the global impacts of anthropogenic climate change. Section 6 concludes.

2 Theoretical framework

This section introduces our theoretical framework that shows how the spatial correlation of productivities may affect welfare inequality and guides our empirical investigation of this prediction.

In any trade equilibrium, a country's welfare can be stated as the sum of its welfare under autarky and its gains from trade. A country's welfare under autarky depends only on its own productivity. Its gains from trade depend on the entire distribution of productivities across the trading network. The variance of welfare across countries is the variance of this sum. It therefore depends on not only the variances of productivity and the gains from trade but also the covariance between these two components.

We investigate how the spatial correlation of productivities influences the covariance between a country's productivity and its gains from trade. This requires an observable outcome that identifies the gains from trade. Across a broad class of models, a country's gains from trade are revealed

by the share of its expenditure devoted to its own output. The less a country spends on its own output, the larger its gains from trade. In autarky, all its expenditure is on its own output. In the trade equilibrium, this expenditure share, when combined with the "trade elasticity" governing how consumers substitute across consumption sources, summarizes the welfare gain from exchange with other locations (Arkolakis, Costinot and Rodríguez-Clare, 2012).

Section 2.1 establishes that within this class of trade models our object of interest is the covariance between a country's productivity and its domestic share of expenditure. Section 2.2 illustrates how this covariance depends on the spatial correlation of the productivity distribution and shows how to identify this *ceteris paribus* prediction in empirical settings. Section 2.3 discusses the role of comparative advantage and describes conditions under which examining one sector in isolation is informative about welfare dispersion in a multi-sector world. Section 2.4 describes the criteria used to select a suitable empirical setting. Details and derivations are available in Appendix A.

2.1 Sufficient statistics for welfare dispersion

We consider a general economic environment within the class of models characterized by Arkolakis, Costinot and Rodríguez-Clare (2012), in which the gains from trade can be inferred from the domestic share of expenditure. We assume perfect competition in the main text, while Appendix A.1 covers the case of monopolistic competition. The world economy is comprised of $j = 1, \ldots, N$ countries.

Preferences. Individuals in country j have preferences with a constant elasticity of substitution $\sigma > 1$ over goods indexed by ω. The accompanying price index is

$$P_j = \left(\int_\omega p_j(\omega)^{1-\sigma} d\omega \right)^{1/(1-\sigma)}.$$

Production. There is one factor of production, and each country j inelastically supplies L_j units of that factor, which earns wage w_j. A country's income is therefore $Y_j = w_j L_j$. The production technology exhibits constant returns to scale and is employed by perfectly competitive firms. The cost of producing in country j depends on productivity A_j. This parameter's microeconomic meaning is model-specific: A_j governs the cost of producing j's good in the Armington model and the location parameter of j's cost distribution for a continuum of goods in the Eaton and Kortum (2002) model.

Trade costs. There are iceberg trade costs, such that selling one unit of a good to j from i requires $\tau_{ij} \geq 1$ units, with $\tau_{ii} = 1$. By the no-arbitrage condition, $p_j(\omega) \leq \tau_{ij} p_i(\omega)$.

Gravity equation. Denote sales from i to j by X_{ij} and j's total expenditure by $X_j \equiv \sum_{i=1}^N X_{ij}$. The share of expenditure by j on goods from i takes the form of a gravity equation:

$$\lambda_{ij} = \frac{X_{ij}}{X_j} = \frac{\chi_i \left(\tau_{ij} w_i\right)^{-\epsilon}}{\sum_{l=1}^N \chi_l \left(\tau_{lj} w_l\right)^{-\epsilon}} = \frac{\chi_i \left(\tau_{ij} w_i\right)^{-\epsilon}}{\Phi_j}, \tag{1}$$

where χ_i is a function of A_i and other structural parameters that are not trade costs, ϵ is the

"trade elasticity", and $\Phi_j \equiv \sum_{l=1}^{N} \chi_l \left(\tau_{lj} w_l\right)^{-\epsilon}$ is the "inward multilateral resistance" term (Head and Mayer, 2014). Φ_j is a (decreasing) transformation of j's price index that summarizes consumers' access to goods from every source.

Equilibrium. In equilibrium, labor-market clearing, goods-market clearing, and budget constraints are satisfied such that total income $Y_i = w_i L_i$ equals total expenditure X_i. Thus, an equilibrium is a set of incomes $\{Y_i\}_{i=1}^{N}$ such that

$$Y_i = \sum_{j=1}^{N} \lambda_{ij} Y_j.$$

In this environment, the results of Arkolakis, Costinot and Rodríguez-Clare (2012) imply that real consumption per capita is

$$\ln\left(C_i/L_i\right) = \ln A_i + \gamma - \frac{1}{\epsilon} \ln \lambda_{ii}, \tag{2}$$

where γ is a constant determined by structural parameters that are not productivity. The former term, $\ln A_i + \gamma$, is per capita welfare in autarky. In the absence of trade, a country's welfare is independent of other countries' conditions and depends only on its own productivity. The latter term, $-\frac{1}{\epsilon} \ln \lambda_{ii}$, is a sufficient statistic for the gains from trade relative to autarky. It is a country's expenditure share on its own goods, mediated by the trade elasticity ϵ that governs how bilateral expenditures respond to changes in bilateral trade costs. Since expenditure shares depend on relative prices, this sufficient statistic is closely linked to the country's terms of trade: a country purchases less from itself when its export price is higher. With this standard equilibrium expression for welfare in hand, we can consider how dispersion in $\ln\left(C/L\right)$ across countries depends on the spatial distribution of productivities.

From equation (2), variance in welfare across countries is governed by the variance of productivity, the covariance of productivities and gains from trade, and the variance of those gains.

$$var\left(\ln\left(C_i/L_i\right)\right) = var\left(\ln A_i\right) + 2cov\left(\ln A_i, \frac{-1}{\epsilon} \ln \lambda_{ii}\right) + var\left(\frac{1}{\epsilon} \ln \lambda_{ii}\right) \tag{3}$$

To examine the role of spatial correlation, consider two productivity distributions – a correlated state c and an uncorrelated state u – in which the unconditional variance in productivities is identical, $var(\ln A_i^c) = var(\ln A_i^u)$. Under this assumption, the difference in welfare dispersion between the correlated and uncorrelated states is

$$\begin{aligned} var\left(\ln\left(C_i^c/L_i\right)\right) - var\left(\ln\left(C_i^u/L_i\right)\right) = &-\frac{2}{\epsilon}\left[cov\left(\ln A_i^c, \ln \lambda_{ii}^c\right) - cov\left(\ln A_i^u, \ln \lambda_{ii}^u\right)\right] \\ &+ \frac{1}{\epsilon^2}\left[var\left(\ln \lambda_{ii}^c\right) - var\left(\ln \lambda_{ii}^u\right)\right]. \end{aligned} \tag{4}$$

The latter term should make only a second-order contribution to the difference in welfare dispersion, since $\frac{1}{\epsilon^2}$ is an order of magnitude smaller than $\frac{2}{\epsilon}$ for empirically relevant values of the trade

elasticity.[4]

The first-order difference in welfare dispersion is governed by the covariance of productivities and domestic shares of expenditure. We expect this covariance to be positive. A more productive country produces greater output, so the relative price of its output is lower and it sells more to every consumer, including itself. Thus, ceteris paribus, a more productive country has worse terms of trade and purchases more from itself.[5]

Our primary focus, however, is how this covariance changes with the degree of spatial correlation in productivities. We will estimate this relationship empirically, but we first illustrate why we expect that $cov\left(\ln A_i^c, \ln \lambda_{ii}^c\right) < cov\left(\ln A_i^u, \ln \lambda_{ii}^u\right)$ and thus that $var\left(\ln\left(C_i^c/L_i\right)\right) > var\left(\ln\left(C_i^u/L_i\right)\right)$.

2.2 Spatial correlation and the covariance of productivity and gains from trade

This section illustrates how the spatial correlation of productivity influences the variance of welfare by shaping the covariance of productivity and gains from trade. The key is that bilateral trade costs increase with the physical distance between trading partners. Thus, when proximate countries have more similar productivity levels, more productive countries tend to enjoy greater gains from trade because their nearby trading partners are also more productive. Conversely, less productive countries experience lower gains from trade when productivity is more spatially correlated. To demonstrate this mechanism more formally, we start by examining the role of the spatial correlation of productivity in two settings in which countries are perfectly symmetric except for productivity differences. These stylized examples allows us to clearly illustrate our economic mechanism in isolation. We then examine how to identify this *ceteris paribus* prediction in asymmetric environments in which countries differ by other, potentially confounding, determinants of equilibrium trade flows. These more realistic examples inform how we empirically investigate our prediction.

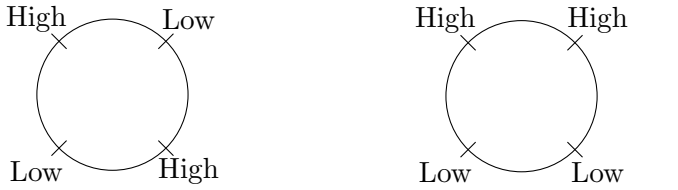
2.2.1 Stylized example 1: Four-country case

We start with the simplest possible environment in which one can demonstrate our result. The world is comprised of $N = 4$ countries of equal size, $L_i = L$ for $i = 1, \ldots, 4$. The four countries are evenly spaced on a symmetric geography such that each country is "near" two neighboring

[4] Typical estimates of the aggregate trade elasticity are between 4 and 8. Caliendo and Parro (2015) estimate that the trade elasticity for agricultural goods is between 8 and 17. Provided that $var\left(\ln \lambda_{ii}^c\right) - var\left(\ln \lambda_{ii}^u\right)$ is the same order of magnitude or smaller than $cov\left(\ln A_i^c, \ln \lambda_{ii}^c\right) - cov\left(\ln A_i^u, \ln \lambda_{ii}^u\right)$, this means that the second term on the right side of equation (4) is an order of magnitude smaller than the first term. Appendix A.1.3 shows that, if trade costs are symmetric ($\tau_{ij} = \tau_{ji}$) and countries equal sized ($L_i = L\ \forall i$), $var\left(\ln \lambda_{ii}^c\right) - var\left(\ln \lambda_{ii}^u\right) = \frac{\epsilon}{\epsilon+1}\left[cov(\ln A_i^c, \ln \lambda_{ii}^c) - cov(\ln A_i^u, \ln \lambda_{ii}^u)\right] + \frac{1+2\epsilon}{1+\epsilon}\left[cov(\ln \Phi_i^c, \ln \lambda_{ii}^c) - cov(\ln \Phi_i^u, \ln \lambda_{ii}^u)\right]$. Heuristically, the latter term is of smaller magnitude, since Φ_i is a price-index term that is a weighted sum of all other countries' prices. Thus, $var\left(\ln \lambda_{ii}^c\right) - var\left(\ln \lambda_{ii}^u\right)$ is the same order of magnitude as $cov\left(\ln A_i^c, \ln \lambda_{ii}^c\right) - cov\left(\ln A_i^u, \ln \lambda_{ii}^u\right)$.

[5] Under certain conditions, productivity increases can reduce the terms of trade so much that this growth is immiserizing (Bhagwati, 1958). The assumptions of standard quantitative trade models imply that increases in TFP do reduce the terms of trade but not so much as to lower welfare. Consider the free-trade equilibrium, $\tau_{ij} = 1\ \forall i, j$. In this case, there is a closed-form solution for equilibrium incomes ($Y_i = (A_i L_i)^{\frac{\epsilon}{\epsilon+1}}$) and we obtain the following comparative statics: $\frac{d \ln \lambda_{ii}}{d \ln A_i} = \frac{\epsilon}{\epsilon+1}\left(1 - \lambda_{ii}\right) > 0$ and $\frac{d \ln C_i}{d \ln A_i} = \frac{1}{\epsilon+1}\left(\epsilon + \lambda_{ii}\right) > 0$.

Figure 3: Four-country example: Productivity distributions



"Alternating" arrangement "Regional" arrangement

countries and farther from the remaining country. Thus, the trade cost matrix is

$$\tau \equiv \begin{bmatrix} 1 & d_1 & d_2 & d_1 \\ d_1 & 1 & d_1 & d_2 \\ d_2 & d_1 & 1 & d_1 \\ d_1 & d_2 & d_1 & 1 \end{bmatrix}, \quad 1 < d_1 < d_2 < d_1^2 \tag{5}$$

where the trade costs $d_2 > d_1$, a mnemonic for distance, obey the triangle inequality: $d_2 < d_1^2$.

For these four countries, consider a mirror-image productivity distribution in which two countries have high productivity and the other two countries have low productivity. Without loss of generality, normalize the lower productivity to one and denote the higher productivity level by $\tilde{a} > 1$. For this symmetric geography with four countries, these productivities might alternate – high, low, high, low – or the world may be divided into a high-productivity region and a low-productivity region. These two spatial arrangements are depicted in Figure 3. What are the consequences for trade and welfare?

Proposition 1 shows that the "regional" arrangement of productivities exhibits greater spatial correlation, as measured by Moran's I. As a result, the covariance of productivity and the domestic share of expenditure is lower when productivities are distributed this way. That makes the variance of welfare across countries greater. The mean of welfare across countries is lower. The proof of Proposition 1 appears in Appendix A.2.1.

Proposition 1 (Four-country case)**.** *Consider an economy in which $N = 4$, $L_i = L\ \forall i$, $\epsilon \geq 1$, and trade costs τ_{ij} are given by condition (5). Comparing the productivity distributions $A^c = (\tilde{a}, \tilde{a}, 1, 1)$ and $A^u = (\tilde{a}, 1, \tilde{a}, 1)$, where $\tilde{a} > 1$,*

- *A^c is more spatially correlated than A^u in the sense that the value of Moran's I for $\ln A^c$ is greater for any spatial weight matrix that is a one-to-one mapping between ω_{ij} and τ_{ij} and assigns a higher weight to the pairs with $\tau_{ij} = d_1$ than pairs with $\tau_{ij} = d_2$.*
- *Equilibrium income inequality, given by Y_1/Y_4, is greater for the more spatially correlated productivity distribution, A^c. Equivalently, the more productive economies' equilibrium double-factoral terms of trade are greater for the more spatially correlated productivity distribution.*

- *The covariance of productivity and the domestic share of expenditure is lower for the more spatially correlated productivity distribution:* $cov(\ln A_i^c, \ln \lambda_{ii}^c) < cov(\ln A_i^u, \ln \lambda_{ii}^u)$.
- *The variance of welfare across counties is greater for the more spatially correlated productivity distribution:* $var(\ln(C_i^c/L)) > var(\ln(C_i^u/L))$.
- *The mean of welfare across countries is lower for the more spatially correlated productivity distribution:* $\mathbb{E}(\ln(C_i^c/L)) < \mathbb{E}(\ln(C_i^u/L))$.

This four-country case establishes our prediction linking the spatial correlation of productivity to welfare inequality. Next, we illustrate this logic in a setting with an arbitrary number of countries that are perfectly symmetric except for productivity differences.

2.2.2 Stylized example 2: Circular geography with productivity sine wave

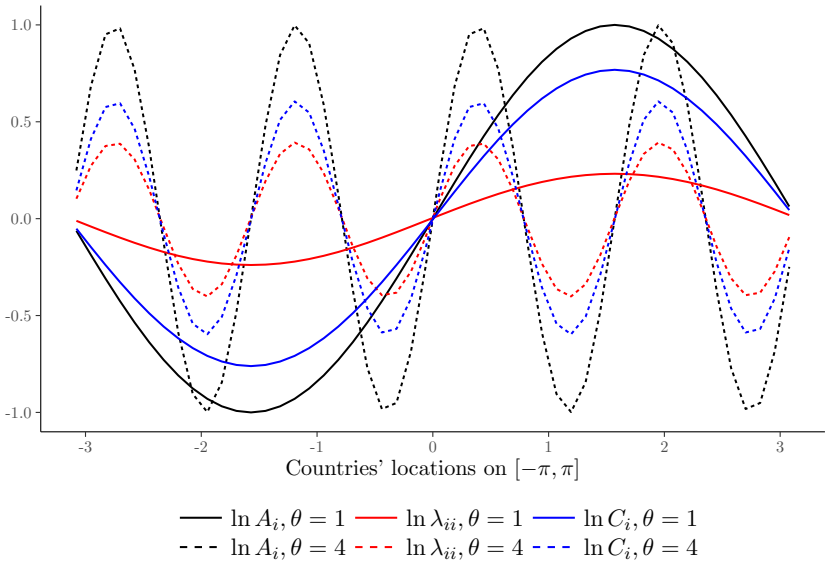
Our second stylized environment has productivity follow a sine wave over a one-dimensional space. There are N locations evenly spaced on the unit circle. These locations have equal population sizes, $L_i = 1\ \forall i$. Trade costs depend only on distance: the log trade cost between two locations is proportionate to the log distance between them. The trade elasticity is $\epsilon = 1$, so that welfare is simply $\ln A_i - \ln \lambda_{ii}$. Productivity $\ln A_i$ follows a sine-wave distribution, with an integer frequency of θ over the circle's circumference. This functional form has two convenient properties. First, the spatial correlation of productivity is governed by the frequency θ: lower frequencies exhibit greater spatial correlation. Second, the mean, variance, skewness, and kurtosis of the productivity distribution are independent of the frequency. Thus, we can explore the effect of spatial correlation by varying θ alone. While we do not have an analytical result, our numerical simulations deliver the same patterns for all parameter values we have examined.[6]

Figure 4 depicts the spatial distributions of productivities ($\ln A_i$), domestic shares of expenditure ($\ln \lambda_{ii}$), and welfare ($\ln C_i$) in this circular economy for the cases in which the sine wave has frequencies of $\theta = 1$ and $\theta = 4$. It is clear that the spatial correlation of productivity is greater in the $\theta = 1$ case, as location "zero" divides the circle into two contiguous regions with above-average and below-average productivity. In the $\theta = 4$ case, spatial correlation is lower because the distance between the productivity sine wave's peaks and troughs is shorter. Stated in terms of Moran's I, the spatial correlation statistic is 0.566 for $\theta = 1$ and 0.182 for $\theta = 4$.

The frequency of the exogenous productivity sine wave affects the amplitude of the endogenous welfare sine wave. In the case of higher spatial correlation, the equilibrium domestic share of expenditure series follows the productivity series less closely, as evident by the larger vertical gap between them. Thus, the smaller amplitude of the $\ln \lambda_{ii}$ series when productivity is more spatially correlated is accompanied by a lower value of $cov(\ln A_i, \ln \lambda_{ii})$. As a result, the amplitude of the welfare series is greater in the $\theta = 1$ case. Welfare dispersion is higher when productivity is more spatially correlated.

[6] Details of the parameters underlying Figure 4 are in Appendix A.2. By Theorem 1 of Allen, Arkolakis and Takahashi (2017), the equilibrium solution depicted for each parameter value is unique.

Figure 4: Circular geography with productivity sine wave



NOTES: This figure depicts an economy with a circular geography and a productivity distribution that follows a sine wave with frequency θ. There are $N = 50$ locations evenly spaced on the unit circle. Bilateral log trade costs are proportionate to the log length of the arc between two points on the circle. The (demeaned) distributions of productivities, equilibrium domestic shares of expenditure, and welfare are depicted for the cases of $\theta = 1$ and $\theta = 4$. See Appendix A.2.2 for parameterization details.

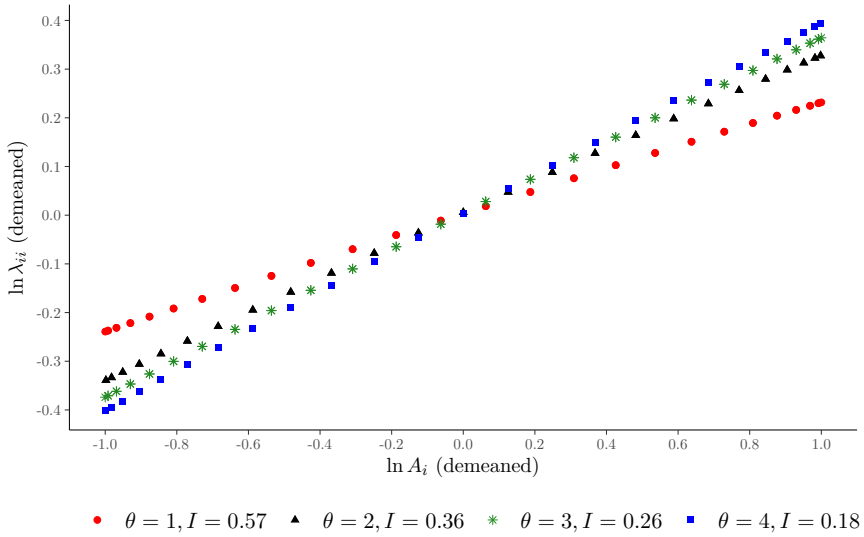
Figure 5 depicts the expenditure-productivity relationship in our sine-wave example for more values of the sine-wave frequency, θ. The scatter plot reveals an almost perfectly linear relationship between $\ln \lambda_{ii}$ and $\ln A_i$. The slope of this relationship, which is proportionate to $cov(\ln A_i, \ln \lambda_{ii})$, systematically varies with the spatial correlation of the sine wave. When the productivities are more spatially correlated, a location's domestic share of expenditure is less responsive to its own productivity level.

2.2.3 Asymmetric environments

Our stylized, many-country example in Section 2.2.2 demonstrates the consequence of spatial correlation of productivity for global welfare inequality in an ideal environment that holds fixed all other economic elements. Our empirical investigation must address the facts that there are other determinants of equilibrium trade flows and the distributions of trade costs and productivities are not symmetric. In this section, we use numerical simulations to motivate our empirical estimating equation that identifies our *ceteris paribus* prediction about the impact of spatial correlation in such settings.

First, economic characteristics other than productivity that influence domestic shares of expenditure complicate bivariate plots like Figure 5. A simple example is heterogeneity in country size L_i: all else equal, larger economies have a larger domestic share of expenditure. Variation in size

Figure 5: Circular geography with productivity sine wave: $cov(\ln \lambda_{ii}, \ln A_i)$



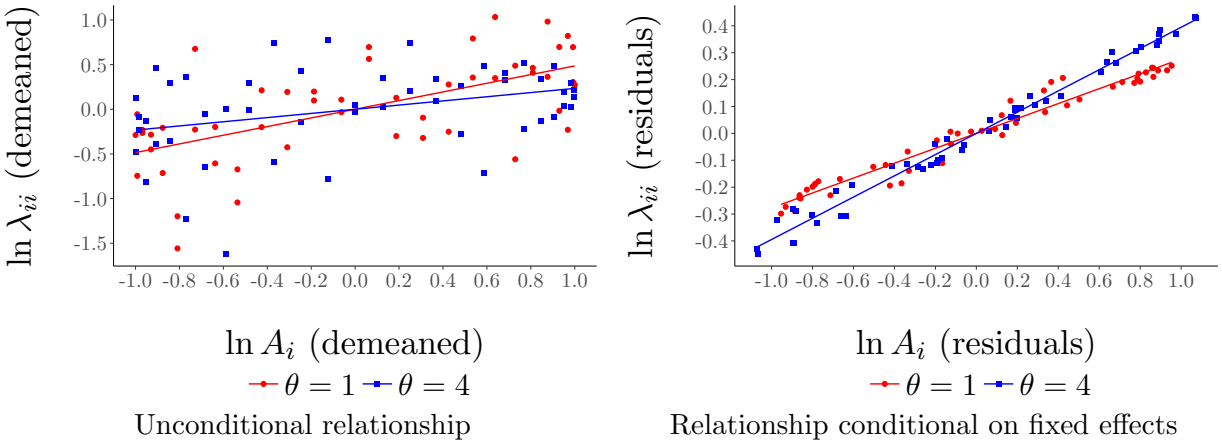
NOTES: This figure depicts the $\ln \lambda_{ii}$–$\ln A_i$ relationship for an economy with a circular geography and a productivity distribution that follows a sine wave with frequency θ. The legend reports the value of Moran's I for each sine wave. Geographic locations and trade costs are the same as in Figure 4. See Appendix A.2.2 for parameterization details.

orthogonal to productivity simply adds noise to the bivariate plot. However, variation in size correlated with productivity also introduces omitted variable bias. This can be empirically addressed by examining the covariance of the domestic share of expenditure and productivity conditional on size. More generally, any time-invariant country characteristics that influence the domestic share of expenditure and might be correlated with productivity can be absorbed by country fixed effects.

We illustrate this in Figure 6, which depicts the relationship between $\ln \lambda_{ii}$ and $\ln A_i$ in an environment that features, like the previous section, a circular geography and sine-wave productivity, and, unlike the previous section, heterogeneous country sizes. In particular, country size $\ln L_i$ is positively correlated with productivity $\ln A_i$ in the $\theta = 1$ state. The left panel depicts the covariance of $\ln \lambda_{ii}$ and $\ln A_i$ for the frequencies $\theta = 1$ and $\theta = 4$. The right panel depicts these covariances conditional on country fixed effects. While our *ceteris paribus* prediction is not evident in the left panel due to omitted variable bias, the right panel shows that the covariance of $\ln \lambda_{ii}$ and $\ln A_i$ is lower when θ is lower, controlling for heterogeneous country sizes.

Second, the real world features productivities and trade costs that do not exhibit the symmetry of a sine wave on a circle. Departing from the sine-wave distribution, Figure A.1 in Appendix A.2.2 depicts the expenditure-productivity relationship for the circular geography with equal-sized countries when we shuffle a productivity vector drawn from the normal distribution so as to vary its spatial correlation. There is a clear negative relationship: as Moran's I increases, the equilibrium domestic share of expenditure is less responsive to domestic productivity. Departing from the circular geography, Figure A.2 in Appendix A.2.3 plots the expenditure-productivity relationship

Figure 6: Circular geography with heterogeneous sizes and productivity sine wave



NOTES: This figure depicts the λ_{ii}–A_i relationship for an economy with a circular geography and a productivity distribution that follows a sine wave with frequency θ. Geographic locations and trade costs as in Figure 4. Country sizes L_i are positively correlated with A_i in the $\theta = 1$ state. See Appendix A.2.2 for parameterization details.

against Moran's I for an economy with countries randomly located on a two-dimensional space and random assignments of productivity levels that differ only in their spatial correlation. In such asymmetric geographies, some countries are more "remote" from economic activity and therefore exhibit a higher domestic share of expenditure, all else equal. This variation is absorbed by country fixed effects, since remoteness is a time-invariant characteristic. Conditional on these fixed effects, we find that greater spatial correlation reduces the covariance of the domestic share of expenditure and productivity.

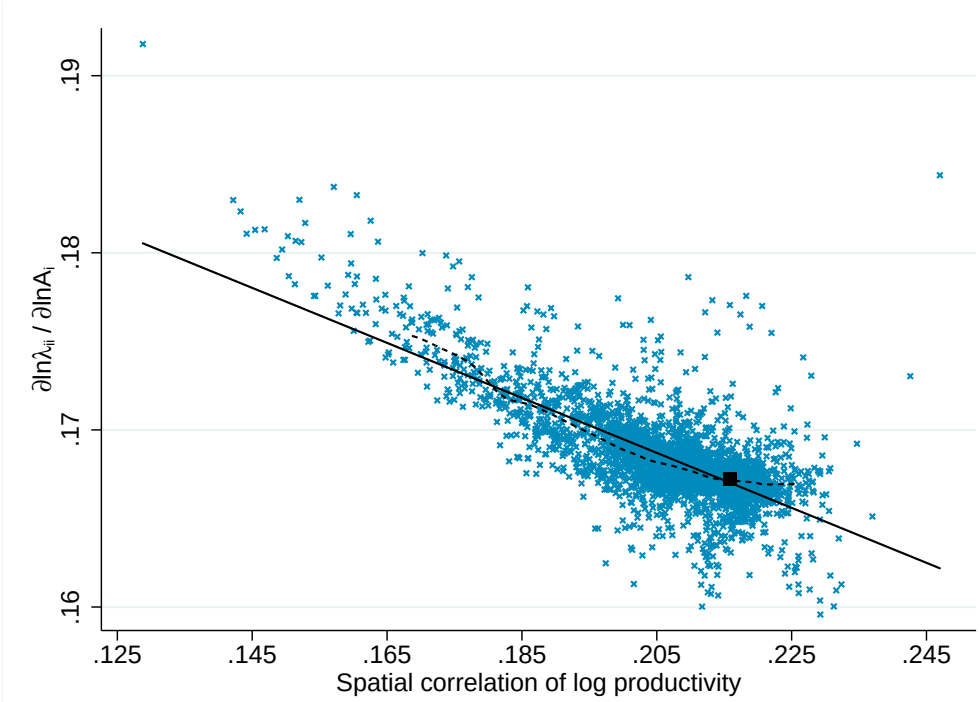
To examine our prediction with realistic productivities and trade costs, we simulate a global economy made up of 158 countries whose geographic coordinates, cereal yields, and crop areas are their 1961-2013 averages in our data. We impose distance-related trade costs and swap pairs of countries' productivity levels in order to vary spatial correlation without altering the mean or variance of the productivity distribution. We recover the covariance of expenditure and productivity in each equilibrium by regressing the domestic share of expenditure for country i at "time" t, where each t denotes an equilibrium associated with a different productivity distribution, on its own productivity and fixed effects:

$$\ln \lambda_{iit} = \beta_t \ln A_{it} + \pi_i^I + \pi_t^T + \mu_{it}. \tag{6}$$

As in the right panel of Figure 6, the country fixed effects π_i^I control for differences in countries' time-invariant determinants of the domestic share of expenditure, such as size and remoteness. The "year" fixed effects π_t^T control for differences in the average domestic shares of expenditure across different spatial distributions of productivity.

The coefficients β_t in equation (6) characterize the conditional covariance of $\ln \lambda_{ii}$ and $\ln A_i$ in each equilibrium. Since the equilibrium value of $\ln \lambda_{ii}$ depends on the entire vector of productivities

Figure 7: Real-world geography and bilateral productivity swaps



NOTES: Each observation is the estimated productivity elasticity of domestic expenditure share and spatial correlation of productivity for the equilibrium resulting from a bilateral swap of two countries' productivity levels. Countries' productivities and factor endowments are set equal to their long-run averages of cereal yield and log crop area, respectively. Bilateral trade costs are proportionate to bilateral distances between countries' crop centroids. The trade elasticity is set to 4 and the scale of trade costs is set so that the distance elasticity of trade is -1.5. Equilibria computed for 6499 bilateral swaps of productivities. Linear fit shown as solid line. Local polynomial fit for 1st through 99th percentiles of spatial correlation shown as dashed line. Equilibrium associated with long-run averages shown as square.

and not just $\ln A_i$, as shown by the gravity equation (1), this covariance differs across equilibria. Relating the general-equilibrium elasticity β_t to properties of the exogenous productivity vector shows how this covariance's contribution to welfare inequality depends on properties of the productivity vector. Figure 7 shows that this covariance exhibits a negative and roughly linear relationship with Moran's I, a statistic that summarizes the spatial correlation of productivity. On this realistic geography, when productivity is less spatially correlated, the equilibrium covariance of $\ln \lambda_{ii}$ and $\ln A_i$ is more positive and thus welfare inequality is lower.

While the line of best fit in Figure 7 is not perfect, the Moran's I statistic aptly summarizes how the spatial structure of productivity affects welfare inequality. In the model, the covariance of productivity and gains from trade is determined by the general-equilibrium solution of a system of non-linear equations. In Appendix Figure E.1, we show that relating this covariance to Moran's I for productivity captures changes in the variance of welfare per capita remarkably well. For each of the equilibria depicted in Figure 7, we compare the variance of welfare per capita in the model to that predicted by using the line of best fit. Regressing variance of welfare per capita in the model on

its predicted value yields an R^2 that exceeds .93. Further, in Appendix Figure E.2, we show that our linear approximation behaves well "out of sample" when we impose productivity vectors that exhibit far greater spatial correlation than those in Figure 7. Thus, Moran's I aptly captures how welfare inequality determined by the general-equilibrium model depends on the spatial structure of productivity. Our empirical investigation will therefore estimate the expenditure-productivity relationship using a linear regression and ENSO-driven variation in the spatial correlation of cereal productivity.[7]

2.3 Comparative advantage

We have obtained these predictions about the spatial correlation of absolute advantage A_i using a standard theoretical framework that makes two important assumptions about the pattern of comparative advantage. First, there is only one sector. Second, the pattern of comparative advantage across varieties within that sector is symmetric across countries.

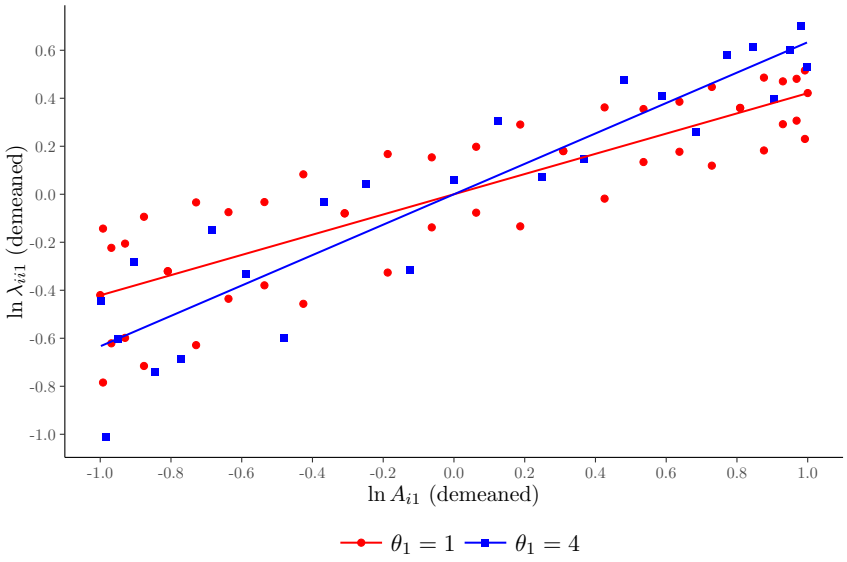
Our empirical investigation exploits exogenous variation in the spatial distribution of productivities in the agricultural sector, which constitutes a small share of global trade. What happens in an economy with multiple sectors? Appendix A.3 shows that our prediction linking the spatial correlation of productivity and the productivity-expenditure relationship holds for each sector in a multi-sector gravity model of trade. When consumers have Cobb-Douglas preferences over sectors and CES preferences over varieties within sectors, there are multi-sector analogues of equations (2), (3), and (4) that sum over sectors using their expenditure shares. Thus, the previous section's predictions about trade in one sector can be empirically investigated in a multi-sector world that introduces an additional dimension of comparative advantage.

Compared to a one-sector model, the opportunity to produce non-agricultural goods is an additional margin of adjustment that may dampen the magnitude of the welfare consequence of a given agricultural productivity shock. If agricultural and non-agricultural activities were positively correlated, there would be little scope for adjustment.[8] To illustrate the case in which these productivities are orthogonal, Figure 8 presents a multi-sector analogue of Figure 5 for an economy with two symmetric sectors that differ only in their sine-wave frequency. The idiosyncratic, orthogonal variation in the second sector's productivity adds noise to the relationship between the domestic share of agricultural expenditure and agricultural productivity, but it does not change the comparative static of interest. When the first sector's productivity is more spatially correlated, the covariance of its log productivity and log domestic share of expenditure is smaller. This raises

[7] An alternative strategy would be to calibrate the trade model to rationalize the observed data from one year and then evaluate how well the fitted model predicts the following year's outcomes when the spatial correlation of productivity differs. One could match the next year's observed productivities and compare observed expenditure shares to predicted expenditure shares or match expenditure shares and compare productivities. Since other shocks affect both variables, this alternative approach would still require the researcher to select the relevant exogenous variation and define a criterion for evaluating model fit. Our instrumental-variables approach employs standard statistical criteria to define appropriate exogenous variation and perform causal inference.

[8] Appendix A.3 shows that a multi-sector model with perfectly correlated productivities, proportionate bilateral trade costs, and equal trade elasticities delivers a welfare-difference expression exactly proportionate to the single-sector expression in equation (4).

Figure 8: Two-sector sine-wave economy: $cov(\ln \lambda_{ii1}, \ln A_{i1})$



NOTES: This figure depicts the λ_{iis}–A_{is} relationship for $s = 1$ in a two-sector economy in which sectoral productivity follows a sine wave with frequency θ_s. The two series depicted are frequencies $\theta_1 = 1$ and $\theta_1 = 4$ for the first sector. The second sector has frequency $\theta_2 = 10$ in both cases. The two sectors have identical trade costs τ_{ijs}, expenditure shares $\alpha_{i1} = \alpha_{i2} = \frac{1}{2}$, and trade elasticities $\epsilon_1 = \epsilon_2$. The two lines are the line of best fit for each series. When productivity is more spatially correlated (when θ_1 is lower), $cov(\ln \lambda_{ii1}, \ln A_{i1})$ is lower. See Table A.2 in Appendix A.3 for details of this example.

dispersion in welfare relative to the case in which the first sector's productivity is less spatially correlated.

Finally, these results concern the spatial correlation of absolute advantage A_i when comparative advantage is symmetric across countries. Standard quantitative trade models assume that the pattern of comparative advantage is symmetric across countries. In Appendix A.4, we examine how spatial correlation of comparative advantage may interact with the spatial correlation of absolute advantage. In short, when comparative advantage is sufficiently spatially correlated, an increase in neighboring countries' total factor productivity may reduce a country's gains from trade. When neighboring countries specialize in similar products, a neighbor's productivity improvement may actually worsen a country's terms of trade by increasing the world supply of that country's exports and thereby depressing its export price. Thus, if comparative advantage were sufficiently spatially correlated, it would imply that β_t in equation (6) would increase with the spatial correlation of A_i rather than decrease. Whether this is indeed the case is an empirical question.

2.4 From theory to empirics

Section 2.3 shows that our prediction linking the spatial correlation of productivity and the productivity-expenditure relationship holds for each sector in a multi-sector gravity model of trade. Examining this prediction requires an empirical setting that is suitable in a number of respects. First, the sector's bilateral trade flows should conform to the gravity equation that is at the heart of quan-

titative trade models and decrease with distance-related trade costs. Second, examining the role of the spatial correlation of productivity across a trade network requires a measure of productivity reported in comparable terms across the globe. Third, examining variation in global spatial correlation requires sufficient time-series variation to identify its effects. Finally, the variation in the spatial structure of productivity needs to be plausibly exogenous to support causal inference.

To satisfy these criteria, we study the cereals sector, which we define as the top eight cereals that account for more than 99 percent of global cereal production and trade.[9] With respect to the first criterion, trade flows of cereals are well characterized by the gravity equation, as reported in column 1 of Table C.1 in Appendix C.1. Cereals are often both exported to and imported from the same foreign trading partner, and cereal trade between countries that are farther apart is substantially lower. Cereals satisfy the second and third criteria because a standard measure of productivity, cereal yield (the output-land ratio), is available at the country-year level with nearly global coverage since 1961 from the United Nations Food and Agriculture Organization (FAO).

Finally, our examination of the cereals sector requires exogenous variation in productivity levels and the global spatial correlation of productivity. In an ideal experiment, a researcher could test our prediction by manipulating productivities around the world in a way that alters the global spatial correlation of productivities without changing the global mean or variance of productivities. Such an experiment is obviously not possible with international trade. However, because of the well-established sensitivity of cereal yields to environmental conditions (Schlenker and Roberts, 2009; Hsiang and Meng, 2015), we are able to approximate this ideal experiment by exploiting productivity variation attributable to temperature variation and a global climatic phenomenon known as the El Niño-Southern Oscillation (ENSO), described in the following section.

Our analysis, following convention in international economics, ignores countries' internal economic geography. This abstraction is motivated by our empirical application. While there is also annual variation in the within-country spatial correlation of cereal productivity, data constraints prevent us from measuring this variation and the relevant outcome variables within countries. Data on agricultural productivity, internal trade, and population counts for subnational spatial units on an annual basis have not been collected by most countries for most years. We therefore focus on international trade and the spatial correlation of productivity across countries.

3 The El Niño-Southern Oscillation

This section first summarizes the basic physics of ENSO and then empirically demonstrates that it drives annual changes in the global spatial correlation of cereal productivity.

[9] These cereals are barley, maize, millet, oats, rice, rye, sorghum, and wheat. According to the FAO, these eight cereals constituted 99.3% of global production (in metric tons) and 99.6% of global trade (in nominal USD) during 1961-2013. These cereals are not homogeneous goods. FAO data report quantities of wheat produced, but trade data distinguish durum and non-durum wheat. Trade data distinguish four types of rice, but the International Rice Genebank holds more than 125,000 rice varieties, which are differentiated by quality, appearance, and taste (Agcaoili-Sombilla and Rosegrant, 1994). Quantitative trade models make common predictions about trade flows while making different assumptions about the set of goods in the utility function. We study expenditure shares, so we need not map varietiess of cereal defined in our data sources to goods indexed by ω in the theoretical framework.

3.1 Background

The El Niño-Southern Oscillation is a naturally occurring, annual, climatic phenomenon characterized by mutually reinforcing circulation patterns between the atmosphere and the tropical Pacific ocean. While ENSO originates in the tropical Pacific, it is a major determinant of weather conditions around the world. Indeed, at an annual frequency, ENSO is often recovered as the first principal component of various local atmospheric or oceanographic variables across the planet (Sarachik and Cane, 2010).

ENSO is often colloquially described as consisting of one neutral state and two extreme states. These conditions are broadly characterized by the amount of heat that is released from the tropical Pacific ocean into the atmosphere (Cane and Zebiak, 1985). In typical "ENSO neutral" years, normal circulation patterns pushing westward contain a pool of warm water against Indonesia and other land masses in the South Pacific. An extreme "El Niño" state occurs when this circulation pattern weakens such that this pool of warm water spills eastward across a large area of the equatorial Pacific Ocean. With warm water exposed to the atmosphere over a greater sea surface area, El Niño years release more ocean heat into the atmosphere over a relatively short period. The opposite occurs during the "La Niña" state. During La Niña years, circulation patterns strengthen such that the same volume of warm water is pushed more firmly against the Indonesian landmass reducing sea-surface contact with the atmosphere and thus reducing heat released from the ocean.

These three distinct states are useful for broadly characterizing the ENSO phenomenon. However, in reality there is a continuum of ENSO conditions, with the amount of heat released into the tropical atmosphere each year somewhere in between La Niña and El Niño extremes. We henceforth refer to a positive ENSO event when conditions are between the neutral and El Niño states. Similarly, a negative ENSO event occurs when conditions are between the neutral and La Niña states.

ENSO conditions in the tropical Pacific affect the spatial pattern of weather conditions across the planet due to how heat travels when released in the tropics. Because there is almost no Coriolis effect near the equator (a result of the simple facts that the Earth is round and spins), atmospheric signals propagate rapidly throughout the tropics. During a positive ENSO event, the warm air initially released above the tropical Pacific Ocean is propagated throughout the tropics by a transport mechanism in the atmosphere known as an equatorial Kelvin wave that sweeps across the globe, altering weather conditions almost simultaneously throughout the tropics (Chiang and Sobel, 2002).[10] For this reason, it is often said that the tropical atmosphere is "teleconnected" during a positive ENSO event, as atmospheric conditions in locations distant from each other are linked through this mechanism. Because the equatorial Kelvin wave that connects local weather around the equator is constrained primarily to the tropics, where the Coriolis effect is weak, the weather conditions that prevail during a positive ENSO event does not generally extend to higher latitudes, which may in fact experience opposing weather conditions because of changes to atmospheric circulation.

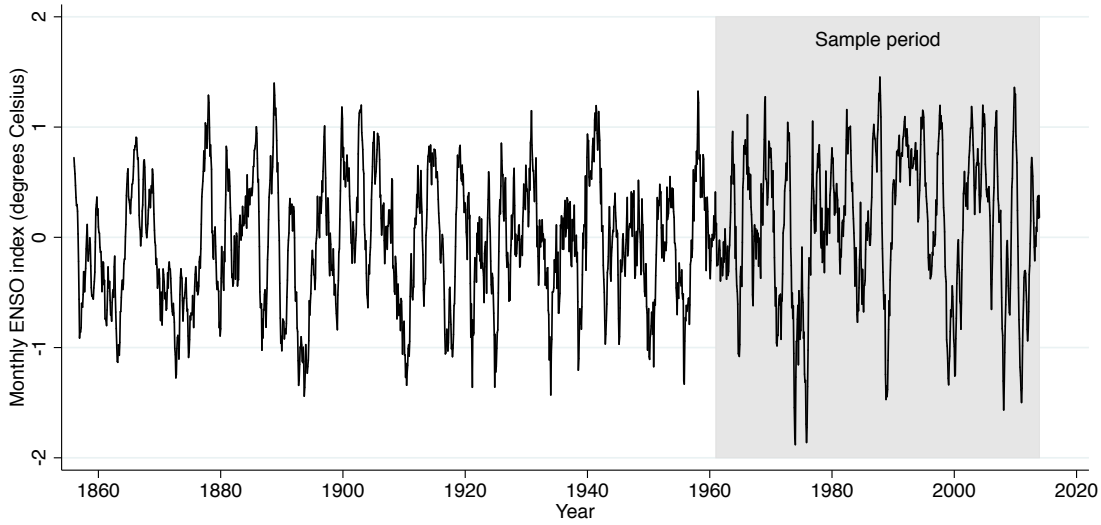
[10] This tropical phenomenon is described in Hsiang and Meng (2015). For a complete scientific treatment of ENSO physics, we refer interested readers to Sarachik and Cane (2010).

This physical mechanism allows ENSO to induce large areas of the planet to experience similar local temperature, precipitation, humidity, and other weather conditions. The spatial consequences of a positive ENSO event is perhaps best illustrated through temperature.[11] During a positive ENSO event, temperature conditions around the world are reorganized such that there is a spatially contiguous area of relatively warm temperature across the tropics and subtropics while almost simultaneously there is a spatially contiguous area of relatively cooler temperatures in higher-latitude locations. The opposite occurs during negative ENSO events. Less heat is released into the atmosphere and temperatures across the globe are less spatially organized.

ENSO conditions are typically summarized by the average sea-surface temperature over a fixed area in the tropical Pacific. In our main analysis, we employ the widely used NINO4 index, a statistic defined as average ocean temperature (in degrees Celsius) over a rectangular area bounded by 5°S - 5°N, 160°E - 150°W (see Figure E.3). Henceforth, we refer to the NINO4 index simply as the ENSO index. As shown later, choice of this particular ENSO measure is inessential for our results.

Figure 9 plots the monthly ENSO index for 1856-2013, which extends further back than our estimation sample period of 1961-2013. Observe that the index fluctuates between positive and negative ENSO values and appears stationary during this period. There are two important features of ENSO relevant for our empirical application: (i) the monthly timing of a typical ENSO event and (ii) how an ENSO event influences local temperatures around the planet both spatially and temporally.

Figure 9: Monthly ENSO index (1856-2013)



NOTES: Monthly ENSO index during 1856-2013. Shaded area shows our 1961-2013 sample period.

The timing of ENSO events, due to its tropical origins, is phase-shifted relative to the calendar year. An ENSO event generally begins during April-May of a given year and lasts until the following

[11] ENSO alters the spatial structure of other weather variables but these effects tend to be of smaller spatial scales. For example, during positive ENSO events there is typically flooding over the Pacific coast of South America while the Atlantic coast of South America primarily experiences droughts (Ropelewski and Halpert, 1987).

April-May, an interval known as the "tropical year." To illustrate the within-year evolution of ENSO events, Figure E.4 isolates the 10 most positive ENSO events during our 1961-2013 sample period and plots the monthly ENSO index 12 months before and after a given December. For each ENSO event, the ENSO index begins rising around April-May of a given year and dissipates by June of the following year. Because the ENSO index typically peaks in December, the cleanest annual measure of any ENSO event is simply the December value of the ENSO index. In all following empirical analyses, we use December values as our annualized measure of ENSO.[12]

There is a spatially and temporally distinct manner in which a typical ENSO event affects local temperatures around the planet. Figure 10 displays the canonical structure of warming that occurs when the ENSO index increases, month by month. Each map displays the time-series correlation of monthly temperatures for each pixel during the specified month and ENSO in month zero, defined as December. Yellow, orange, and red colors indicate locations that warm as the ENSO index increases; blues indicate locations that cool. In May before a December ENSO event (month -7), the east equatorial Pacific begins to warm. Regions throughout the tropics, both over land and the oceans, continue to warm for the next several months, peaking in the east Pacific in December (month 0) and over the rest of the tropics in March and April (months +3 and +4). This warming then dissipates across the tropics with little visible effect more than a year after the December peak. Higher latitudes experience some cooling through these months, though the effect is weaker. Figure 10 shows that the local impacts on temperatures around the planet from a single ENSO event straddles two calendar years. When using socio-economic data that is indexed by calendar years, this implies that one must examine how outcomes in a given year are influenced by both ENSO in that year and by ENSO in the previous year.

3.2 ENSO and the spatial correlation of cereal productivity

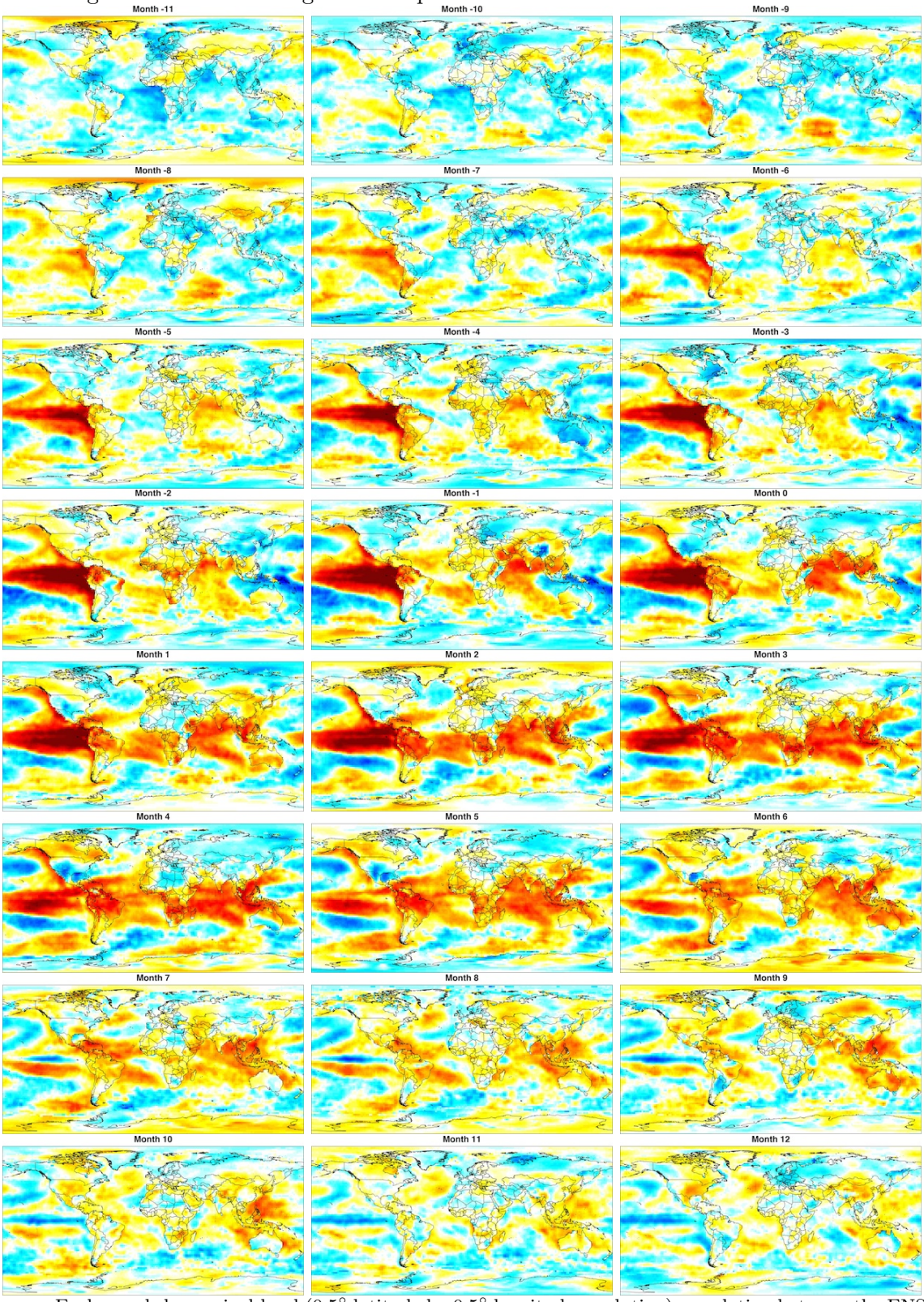
The spatial and temporal patterns shown in Figure 10 suggest that ENSO could drive global spatial correlation in cereal yields. To demonstrate this at an annual time scale, for which productivity and trade data is available, Figure 11 shows the country-level linear coefficients due to a 1-degree increase in the sum of contemporaneous and lagged December ENSO indices on crop-area weighted annual temperature (top panel) and log cereal yields (bottom panel).[13] ENSO fluctuations generate a clear spatial pattern in country-level temperatures and cereal yield. Consistent with the tropical climatic dynamics discussed above, increases in the ENSO index tend to raise temperatures and lower cereal productivities in countries closer to the equator and lower temperatures and raise cereal productivities in countries farther from the equator.

Figure 11 suggests that ENSO could drive global spatial correlation in cereal yields, but it

[12] We do not detect any statistically significant coefficients when estimating a time series regression of our annual December NINO4 measure of ENSO on a constant, a linear trend, and five lagged terms with optimal bandwidth Newey-West standard errors. A Dicky-Fuller test of our annual ENSO measure also strongly rejects the presence of a unit root in favor of stationarity (p=4.15e-21).

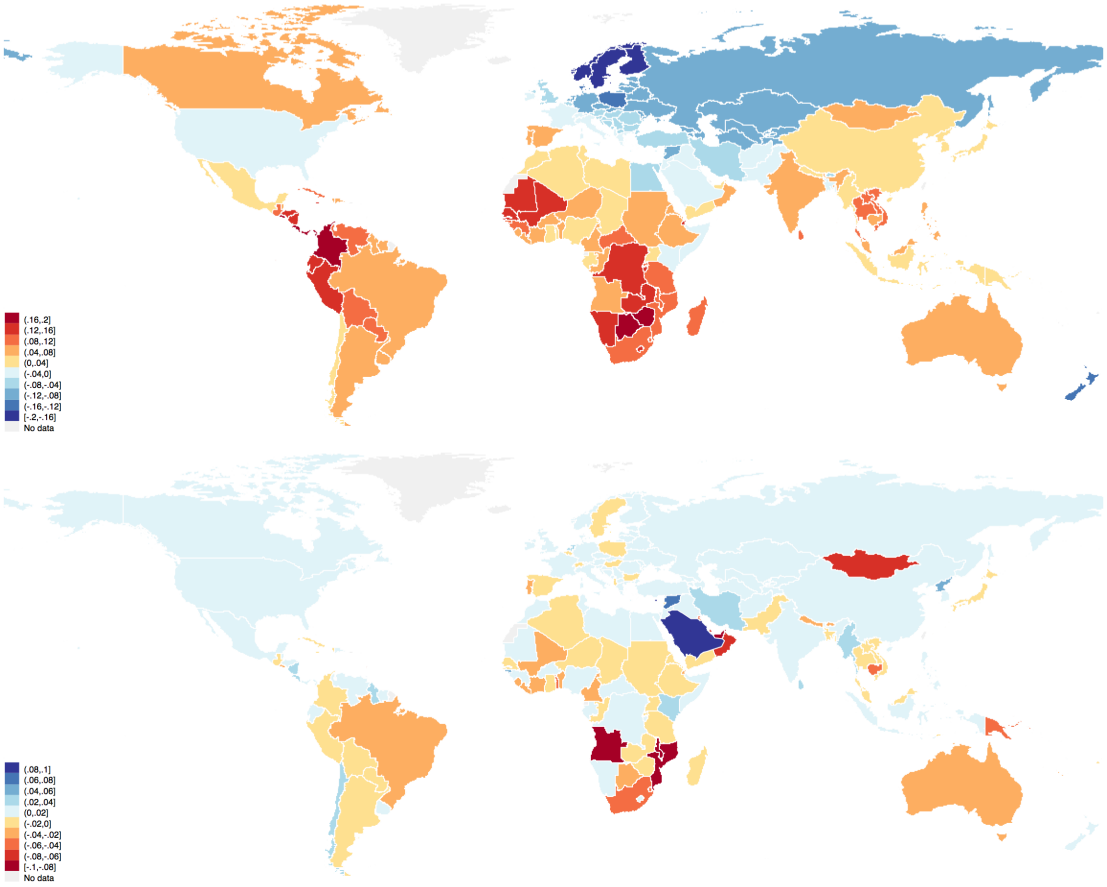
[13] Our country-by-year measure of aggregate cereal yield is the harvested area-weighted cereal-level yield across the eight major cereals.

Figure 10: Lead and lag local temperature correlation with December ENSO



NOTES: Each panel shows pixel-level (0.5° latitude by 0.5° longitude resolution) correlation between the ENSO index in December and pixel-level monthly temperatures for 11 months before (lead) and 12 months after (lag) December. Blue shows areas with negative correlation. Red shows areas with positive correlation.

Figure 11: ENSO's effects on temperatures and cereal yields



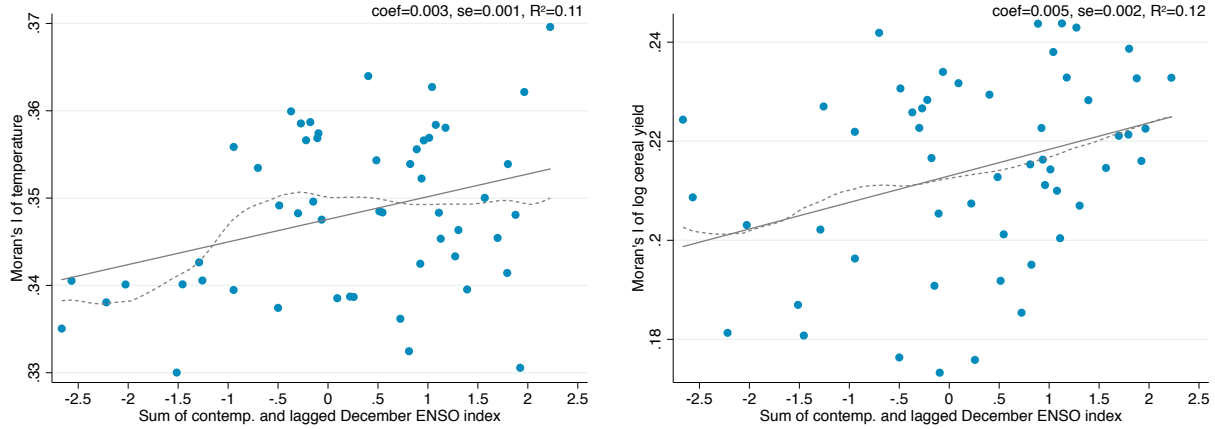
NOTES: Map shows the linear coefficient on the sum of contemporaneous and lagged ENSO for crop area-weighted temperature (top panel) and log cereal yields (bottom panel) for each country. Each country-specific time series model includes a constant and a linear time trend.

does not quantify the relationship. To calculate spatial correlation within each year, we turn to a standard measure, Moran's I. In particular, we construct an annual Moran's I statistic for both country-level temperature and log cereal yields.

Figure 12 shows a relationship between ENSO and the global spatial correlation in temperature (left panel) and cereal productivity (right panel). To characterize the ENSO phenomenon in terms of a scalar, we simplify the timing issues discussed above by plotting the sum of December ENSO indices in years t and $t-1$ on the horizontal axis and Moran's I in year t on the vertical axis. An increase in the ENSO index raises both the global spatial correlation in temperature and log cereal productivity. ENSO, in this simple bivariate model, explains 11% and 12% of annual variation in the global spatial correlations of temperature and cereal productivity, respectively.

To relax the timing simplification of Figure 12, Table 1 presents regressions of the annual Moran's I statistic for log cereal yields on flexible polynomial functions of December ENSO in year t and $t-1$. All models include a linear time trend and standard errors robust to serial correlation and heteroskedasticity. In column 1, we include only linear contemporaneous and lagged ENSO

Figure 12: Moran's I for temperatures and cereal yields and ENSO



NOTES: Left (right) panel shows the relationship between Moran's I of crop-weighted country-level temperature (log cereal yields) in year t and the sum of contemporaneous and lagged December ENSO. Linear fit shown as solid line. Local polynomial fit shown as dashed line.

terms. Column 2 augments column 1 by further including a linear interaction term and quadratic contemporaneous and lagged ENSO terms. Column 3 estimates the linear and quadratic effects for the sum of contemporaneous and lagged ENSO. This is a more parsimonious but restrictive version of column 2 by requiring a single coefficient for $ENSO_t$ and $ENSO_{t-1}$ and a single coefficient for $ENSO_t \times ENSO_{t-1}$, $ENSO_t^2$, and $ENSO_{t-1}^2$. Two results are evident. First, both contemporaneous and lagged ENSO affects the spatial correlation of cereal productivity but only after controlling for higher order terms, as shown in column 2. Second, compared with the model in column 2, column 3 produces a stronger fit, as summarized by a lower Bayesian Information Criterion (BIC) value. As a consequence, all empirics in Section 4 will use the functional form in column 3 to model the relationship between ENSO and the global spatial correlation of cereal productivity as it strikes a balance between allowing nonlinearity while limiting overfitting.

Columns 1-3 illustrate the overall effect of ENSO on the global spatial correlation of cereal productivity. It is natural to wonder whether one could simply drive global spatial correlation of cereal productivity using the global spatial correlation of temperature. This similarly exogenous alternative measure would possibly include an ENSO component as well as variation in local temperature due to other climatic factors. Column 4 shows that while annual Moran's I in temperature is correlated with annual Moran's I in cereal productivity, it has poorer predictive power than ENSO, as reflected by a higher BIC statistic. This is likely because cereal yields respond to various weather variables besides local temperature, all of which become more spatially correlated under a positive ENSO event. These other local weather channels are captured by ENSO in columns 1-3 and not by the global spatial correlation of just temperature in column 4. Indeed, in the following section, we show that using ENSO directly, rather than just local temperatures, to drive the global spatial correlation of cereal productivity, is essential for our empirical tests to be statistically precise.

Finally, consistent with our thought experiment in Section 2.1, ENSO appears to affect neither the global mean nor the variance of cereal productivity, as shown by the left and right panels of

Figure 13, respectively. Moreover, when we estimate a gravity model that relates bilateral trade flows to bilateral distances, Table C.1 shows that the distance elasticity is invariant to ENSO. This is consistent with the assumption, introduced in equation (4), that the trade elasticity is invariant to the spatial structure of productivity.

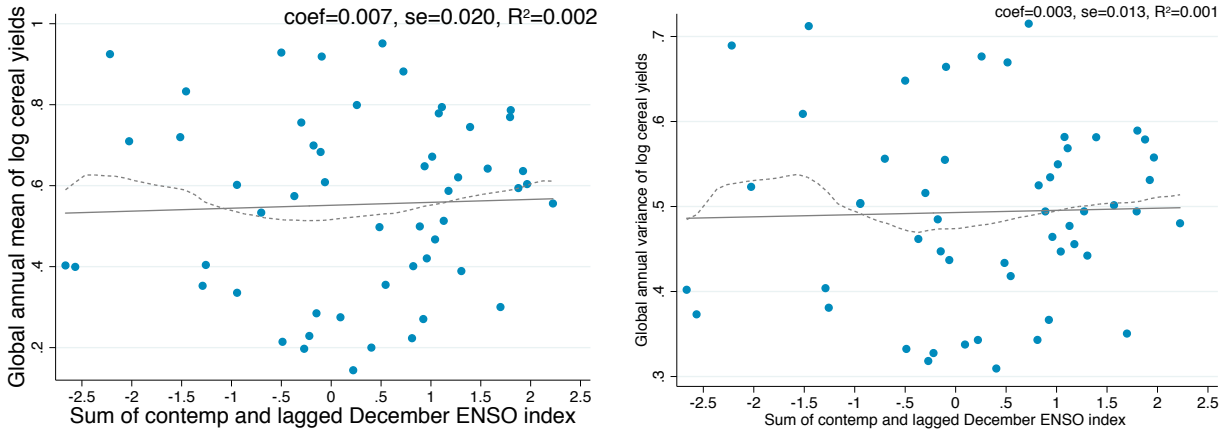
Table 1: Moran's I in cereal productivity and ENSO

Outcome is Moran-I in log cereal yields

	(1)	(2)	(3)	(4)
$ENSO_t$	0.008	0.008		
	(0.002)	(0.002)		
	[0.000]	[0.000]		
$ENSO_{t-1}$	0.003	0.005		
	(0.002)	(0.002)		
	[0.121]	[0.008]		
$ENSO_t$ x $ENSO_{t-1}$		0.004		
		(0.003)		
		[0.148]		
$ENSO_t^2$		-0.001		
		(0.002)		
		[0.639]		
$ENSO_{t-1}^2$		0.004		
		(0.003)		
		[0.197]		
$(ENSO_t + ENSO_{t-1})$			0.006	
			(0.001)	
			[0.000]	
$(ENSO_t + ENSO_{t-1})^2$			0.002	
			(0.001)	
			[0.070]	
$I_t(T_{it})$				0.541
				(0.163)
				[0.001]
BIC	-275.84	-267.21	-276.63	-272.95
Observations	53	53	53	53

NOTES: Time-series regressions of Moran's I in log cereal yields on nonlinear functions of contemporaneous and lagged December ENSO. All models include a linear time trend. Serial correlation and heteroskedasticity-robust Newey-West standard errors with optimal bandwidth in parentheses (Newey and West, 1987); p-values in brackets.

Figure 13: Global cross-sectional mean and variance in cereal productivity and ENSO



NOTES: Left (right) panel shows the relationship between the mean (variance) of cross-sectional country log cereal yields and the sum of contemporaneous and lagged December ENSO. Linear fit shown as solid line. Local polynomial fit shown as dashed line.

4 Empirical results

The theoretical results in Section 2 suggest that the covariance between agricultural productivity, $\ln A_i$, and the domestic share of expenditure, $\ln \lambda_{ii}$, should be lower when the spatial correlation of productivity across the entire trading network increases. This section examines this relationship empirically using exogenous temperature- and ENSO-driven changes in productivities and their global spatial correlation. We first describe our estimation strategy, then report our main finding and subject it to a series of robustness checks. Appendix B details our data sources.

4.1 Estimation strategy

We empirically estimate a variant of equation (6), used in Section 2.2.3 to theoretically demonstrate our prediction under the most realistic set of modeling assumptions. Specifically, for country i in year t during 1961-2013, we consider the following regression equation:

$$\ln \lambda_{iit} = \beta_0 \ln A_{it} + \beta_1 \ln A_{it} I_t + \Pi' \mathbb{Z}_{it} + \mu_{it} \tag{7}$$

where λ_{iit} is country i's domestic share of cereal expenditure in year t, constructed using FAO output and trade data (see Appendix B). A_{it} is cereal yield, also from the FAO. I_t is the Moran's I statistic capturing the spatial correlation of $\ln A_{it}$ for all countries in year t. All data used in constructing λ_{iit} and $\ln A_{it}$ for $\mathbb{Z}_{it}$ is a vector of semi-parametric controls. In Section 2.2.3, we discussed how time-invariant country characteristics such as size and remoteness could potentially generate omitted variable bias. We also noted that the average domestic share of expenditure may differ across equilibria. We empirically address these issues by including country and year fixed effects in $\mathbb{Z}_{it}$. In addition, $\mathbb{Z}_{it}$ includes country-specific time trends. μ_{it} is an error term.

β_0 and β_1 are our two reduced-form parameters of interest. β_0 captures the relationship between a country's gains from trade and productivity when productivity is spatially uncorrelated (when Moran's I is zero). β_1 captures the degree to which the global spatial correlation of productivities mediates this relationship between gains from trade and productivity.

$\widehat{\beta}_1$ connects the spatial correlation of productivity to the global variance of welfare. $\widehat{\beta}_1 < 0$ means that greater spatial correlation lowers the covariance of productivity and the domestic share of expenditure. Provided that the trade elasticity ϵ is unaltered by ENSO-driven variation in the spatial correlation of productivity, this implies a lower covariance of productivity $\ln A_i$ and the sufficient statistic for the gains from trade, $\frac{-1}{\epsilon} \ln \lambda_{ii}$. Greater spatial correlation of agricultural productivity causes more productive countries to experience greater gains from trade and less productive countries to experience lower gains from trade. Thus, all else equal, an increase in the spatial correlation of productivities increases global welfare dispersion.

Estimation of equation (7) by ordinary least squares (OLS) may be problematic if expenditure shares and productivity are simultaneously determined or if there are omitted determinants of expenditure shares that are correlated with productivity, even after conditioning on $\mathbb{Z}_{it}$. For example, demand shocks could affect expenditure shares and elicit supply responses that change average yields.[14] Similarly, if domestic cereal production employs imported intermediate goods, then unobserved trade-cost shocks could jointly affect domestic cereal yields and the domestic share of expenditure.

To address these potential sources of bias, we employ an instrumental-variables (IV) strategy that exploits plausibly exogenous variation in local yields and the global spatial correlation of yields. To drive local yields, we use country-level crop-area-weighted annual temperature, T_{it}, constructed from Legates and Willmott (1990*a*,*b*) (see Appendix B). Following the ENSO discussion in Section 3.1, global spatial correlation of yields is driven by contemporaneous and lagged ENSO.

Our second-stage equation (7) has two endogenous variables, $\ln A_{it}$ and $\ln A_{it} I_t$. We instrument for them using the following first-stage equations:

$$\ln A_{it} = \alpha_{11}' f(T_{it}) + \alpha_{12}' f(T_{it}) g(ENSO_t + ENSO_{t-1}) + \Gamma_1' \mathbb{Z}_{it} + \upsilon_{1it} \tag{8}$$

$$\ln A_{it} I_t = \alpha_{21}' f(T_{it}) + \alpha_{22}' f(T_{it}) g(ENSO_t + ENSO_{t-1}) + \Gamma_2' \mathbb{Z}_{it} + \upsilon_{2it} \tag{9}$$

where the vector of semi-parametric controls, $\mathbb{Z}_{it}$, includes the same variables as our second-stage equation (7). α_{11}', α_{12}', α_{21}', and α_{22}' are vectors of first-stage coefficients. $f()$ captures the relationship between local temperature and yield; nonlinearity in $f()$ is well documented around the world (Schlenker and Roberts, 2009; Schlenker and Lobell, 2010; Welch et al., 2010; Moore and Lobell, 2015). In particular, $f()$ is modeled as a restricted cubic spline of local temperature; the choice of the number of splines is detailed below. $g()$ captures the relationship between ENSO and the global spatial correlation of yields. Following the model selection results in Table 1, $g()$ is modeled

[14] Relatedly, Costinot, Donaldson and Komunjer (2012) show that, in a particular quantitative trade model, the endogenous determination of the varieties that are produced in equilibrium necessitates a selection correction to infer fundamental productivity from the *measured* productivity of varieties that are produced in equilibrium.

as linear and quadratic terms of $(ENSO_t + ENSO_{t-1})$. υ_{1it} and υ_{2it} are error terms.

Nonlinear functional forms for $f()$ and $g()$ are necessary to capture nonlinearities in our first-stage equations, but this means that we have more than two instruments for the two endogenous variables. Two-stage least squares (2SLS) estimation in such over-identified IV settings can exacerbate issues with biased point estimates and incorrectly sized inference. These issues worsen if the many instruments are also weak (Bound, Jaeger and Baker, 1995).

We address this concern using several weak-instrument diagnostics. First, we employ the limited information maximum likelihood (LIML) IV estimator, which is approximately median-unbiased for over-identified models (Mariano, 2001). Second, we conduct tests to detect weak instruments in our LIML estimator. Third, we conduct inference that is robust to the presence of weak instruments.

4.2 Main results

To begin, consider OLS estimates of β_0 and β_1 from equation (7), as shown in column 1 of Table 2. The estimate of β_0 is statistically precise and positive, but the OLS estimate of β_1 is noisy and in fact positive.

Columns 2 through 6 of Table 2 report IV estimates that address the potential bias of OLS estimates. Across columns, the number of spline terms in the temperature function $f()$ varies. Column 2 has 2 spline terms, the minimum needed to capture nonlinearity in $f()$. Each subsequent column adds an additional spline term in $f()$.[15] Because all models include a quadratic function of the sum of contemporaneous and lagged ENSO, this corresponds to 6, 9, 12, 15, and 18 instruments used jointly across the first-stage equations (8) and (9).[16] Panel A shows 2SLS estimates, while panel B shows LIML estimates. Because ENSO varies only in the time dimension, we cluster standard errors by year to allow arbitrary forms of spatial correlation and heteroskedasticity across countries within a given year. In robustness checks, we consider other error structures, including the Bekker (1994) adjustment that accounts for LIML standard errors being potentially too small in the presence of many weak instruments.

We first discuss our weak-instrument diagnostics. Across 2SLS estimates in columns 2 to 6 of panel A, we consistently find similar point estimates for $\widehat{\beta}_0 > 0$ and $\widehat{\beta}_1 < 0$. 2SLS estimates for both parameters are also statistically different from OLS estimates, suggesting that 2SLS estimates do not exhibit the same bias as OLS and thus are not the result of completely uninformative instruments. However, in over-identified IV settings, 2SLS estimates are still biased and incorrectly sized. This is evident as the Cragg-Donald joint F-statistic for both first-stage regressions across

[15] 2 to 6 spline terms correspond to 3 to 7 knots. Knots are placed between equally spaced percentiles of the temperature empirical distribution according to Harrell (2001).

[16] Columns 1-5 of Table F.2 show first-stage statistics for α'_{11} and α'_{12} from equation (8) and α'_{21} and α'_{22} from equation (9), corresponding to the IV specifications shown in columns 2-6 of Table 2. They show p-values from F-tests examining the joint significance of elements in each vector of first-stage coefficients. As expected, uninteracted local temperature is consistently a strong predictor of local cereal yields in first-stage equation (8). For the interaction between local yields and the global spatial correlation of yields in first-stage equation (9), both uninteracted local temperature (i.e. 0th order ENSO) and local temperature interacted with ENSO (i.e. 1st and 2nd order ENSO) are strong predictors.

Table 2: Domestic share of expenditure and spatial correlation of productivity

Outcome is log domestic share of expenditure						
	(1) OLS	(2) IV	(3) IV	(4) IV	(5) IV	(6) IV
				Panel A: 2SLS estimates		
$\ln A_{it}$ (β_0)	0.284	1.541	1.746	1.696	1.701	1.654
	(0.119)	(0.515)	(0.542)	(0.412)	(0.425)	(0.431)
	[0.021]	[0.004]	[0.002]	[0.000]	[0.000]	[0.000]
$\ln A_{it} \times I_t$ (β_1)	0.758	-3.321	-3.440	-3.391	-3.350	-3.290
	(0.487)	(2.071)	(2.148)	(1.476)	(1.493)	(1.555)
	[0.126]	[0.115]	[0.115]	[0.026]	[0.029]	[0.039]
Pct. change in welfare variance	-0.353	1.536	1.591	1.568	1.549	1.521
from 1 s.d. increase in I_t	(0.226)	(0.976)	(1.023)	(0.716)	(0.728)	(0.754)
	[0.119]	[0.116]	[0.120]	[0.029]	[0.033]	[0.044]
				Panel B: LIML estimates		
$\ln A_{it}$ (β_0)		2.110	2.380	2.114	2.196	2.308
		(0.837)	(0.847)	(0.604)	(0.669)	(0.771)
		[0.015]	[0.007]	[0.001]	[0.002]	[0.004]
$\ln A_{it} \times I_t$ (β_1)		-4.530	-4.907	-4.144	-4.218	-4.463
		(2.752)	(2.937)	(1.834)	(1.949)	(2.194)
		[0.106]	[0.101]	[0.028]	[0.035]	[0.047]
Pct. change in welfare variance		2.091	2.264	1.914	1.948	2.060
from 1 s.d. increase in I_t		(1.407)	(1.497)	(0.954)	(1.035)	(1.191)
		[0.137]	[0.131]	[0.045]	[0.060]	[0.084]
Number of temperature splines in $f()$		2	3	4	5	6
ENSO polynomial order in $g()$		2	2	2	2	2
Number of instruments		6	9	12	15	18
Cragg-Donald F-stat		7.052	5.832	5.174	4.324	3.801
Stock-Yogo crit. value: 10% max 2SLS bias		9.480	10.430	10.780	10.930	11.000
Stock-Yogo crit. value: 10% max 2SLS size		21.680	27.510	32.880	38.080	43.220
Stock-Yogo crit. value: 10% max LIML size		4.060	3.700	3.580	3.540	3.560
Kleibergen-Paap F-stat		6.100	5.664	3.963	3.332	3.069
Anderson-Rubin weak-id robust joint p-value		0.000	0.000	0.000	0.000	0.000
BIC for first stage equations		-30933.68	-30917.40	-31134.01	-31120.19	-31091.75
Observations	5452	5452	5452	5452	5452	5452

NOTES: This table reports estimates of β_0 and β_1 from equation (7). Column 1 shows OLS estimates. Columns 2-6 show IV estimates that vary by the number of temperature spline terms in $f()$. Panel A (B) shows 2SLS (LIML) IV estimates. All models include quadratic $ENSO_t + ENSO_{t-1}$ terms and incorporate country fixed effects, year fixed effects, and country-specific linear trends as included instruments. Percentage change shown in the variance of welfare for a one-standard-deviation increase in Moran's I relative to the historical mean, with standard errors calculated using the delta method. Standard errors clustered by year in parentheses; p-values in brackets.

columns 2 to 6 is well below the Stock-Yogo critical values for 10% maximal 2SLS bias and size (Cragg and Donald, 1993; Stock and Yogo, 2005).

To address these issues, columns 2 to 6 of panel B present LIML estimates. Again, we consistently find similar point estimates for $\widehat{\beta}_0 > 0$ and $\widehat{\beta}_1 < 0$. The LIML estimates are even farther away from the OLS estimates than the 2SLS estimates, suggesting that the LIML estimator mitigates bias in our 2SLS estimates.

LIML is an approximately median-unbiased estimator in over-identified settings, but standard errors may still be incorrectly sized in the presence of weak instruments. We show two tests to address whether weak instruments are a concern. First, across columns 2 to 6, the Cragg-Donald joint F-statistic for both first-stage regressions is above the Stock-Yogo critical values for 10% maximal LIML size, which rejects the presence of weak instruments. However, Stock-Yogo critical values are only valid for iid errors. While we also report the Kleiberg-Paap F-statistic, which is more appropriate given our clustered error structure (Kleibergen and Paap, 2006), there are no established critical values for non-iid errors. We therefore cannot entirely rule out the presence of weak instruments solely by looking at first-stage F-statistics. Thus, we turn to inference methods that are robust to the presence of weak instruments. For each IV model in columns 2 to 6, we present the p-value from the Anderson-Rubin test of the null hypothesis that β_0 and β_1 in equation (7) are jointly zero (Anderson and Rubin, 1949). This null hypothesis is strongly rejected. The combined evidence from these various diagnostics suggests that weak instruments are not a concern. This gives us confidence that our LIML estimates are unbiased and correctly sized.

Which number of spline terms in the temperature function $f()$ yields the most informative estimates of our parameters of interest? Note that this model selection is not crucial to our conclusions: across columns 2 through 6, the point estimates of β_0 and β_1 do not vary much. All the estimates of β_0 have p-values near or below 0.01, and the LIML estimates of β_1 have p-values ranging from 0.03 to 0.11. To select one specification, we employ the Bayesian Information Criterion (BIC) statistic from a joint seemingly unrelated regression of first-stage equations (8) and (9) to address the trade-off between capturing nonlinearities in $f()$ and having too many spline terms in $f()$. Table 2 shows that the BIC statistic is minimized with four temperature spline terms in column 4. This corresponds to the specification with the most precise LIML estimates of β_0 and β_1, with p-values of 0.001 and 0.03, respectively, and will serve as our benchmark model moving forward.

Our empirical estimates show that the spatial distribution of productivity affects a country's terms of trade, as revealed by its domestic share of expenditure. The positive relationship between its own productivity and domestic share of expenditure ($\hat{\beta}_0 > 0$) reveals that higher productivity worsens the terms of trade. This deterioration is dampened when productivity is more spatially correlated ($\hat{\beta}_1$), since higher productivity in neighboring countries improves a country's terms of trade.[17]

To quantify these estimates in welfare terms, suppose that the cross-sectional global spatial correlation of agricultural productivity were to increase by one standard deviation relative to the historical mean. Applying the expression for the variance of welfare in equation (3) to our benchmark LIML estimates in column 4, panel B of Table 2, we find that a one standard deviation increase in the spatial correlation of productivity leads to a statistically significant 2% increase in the global variance of welfare (see Appendix D.1 for details).[18]

[17] At empirically observed levels of spatial correlation, this does not reverse the positive relationship between $\ln A_{it}$ and $\ln \lambda_{iit}$. As shown in Figure 12, the spatial correlation of cereal yields lies between 0.17 and 0.25 in our estimation sample. Thus, $\hat{\beta}_0 + \hat{\beta}_1 \times I_t > 0$ at all historical values of I_t for the estimates reported in Table 2.

[18] As a point of comparison, Kopczuk, Saez and Song (2010) find that the annual variance of log earnings across

4.3 Additional robustness checks

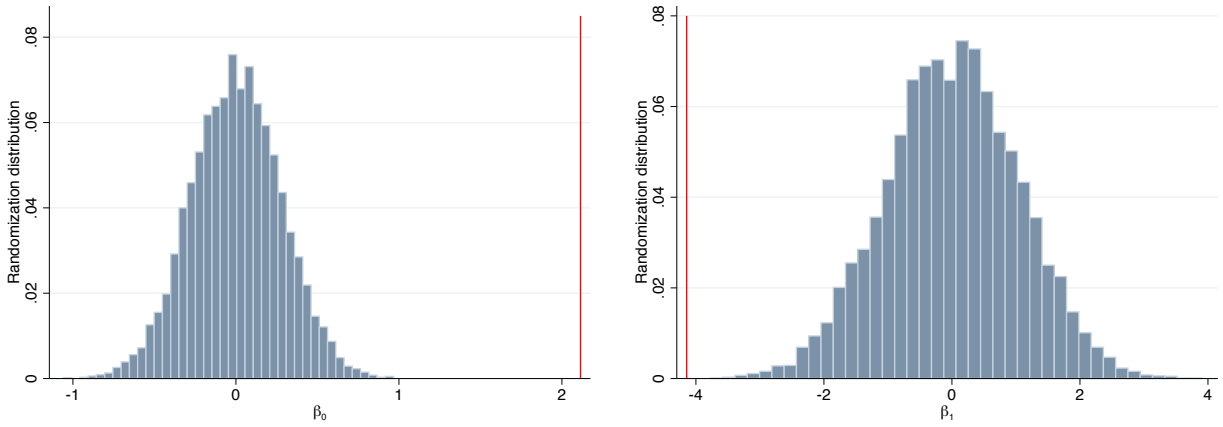
This section presents several robustness checks of our main empirical result. They are designed to test the validity of our statistical assumptions, the interpretation of our results, and the consequences of our data-construction choices. Our benchmark model throughout is that shown in column 4, panel B of Table 2.

Randomization inference Our main source of identifying variation is global time-series fluctuations in the ENSO cycle, as shown in Figure 9. While it is plausible that ENSO is uncorrelated with unobserved determinants of domestic shares of expenditure over a large sample of years, spurious correlations could occur within a 53-year sample period.

To examine the relevance of this concern, we conduct a placebo test by randomly reshuffling years in our panel data, breaking the time-series link between domestic shares of expenditure and ENSO-driven changes in country-level cereal yields and the global spatial correlation in yields. This allows us to obtain an empirical distribution of our estimated reduced-form coefficients, $\widehat{\beta}_0$ and $\widehat{\beta}_1$, under placebo conditions and compute the probability of observing our benchmark estimates if years were randomly assigned.

The left and right panels of Figure 14 show the empirical distribution for $\widehat{\beta}_0$ and $\widehat{\beta}_1$, respectively, for 10,000 randomly reshuffled years without replacement. The vertical line shows the location of our estimated $\widehat{\beta}_0$ and $\widehat{\beta}_1$ from the observed data. We find that it is highly unlikely that our main result is due to small-sample bias.

Figure 14: Randomization inference



NOTES: Empirical distributions of $\widehat{\beta}_0$ (left panel) and $\widehat{\beta}_1$ (right panel) from 10,000 random assignments of years. Vertical lines show $\widehat{\beta}_0$ and $\widehat{\beta}_1$ from observed data estimated using benchmark model in column 4, panel B of Table 2.

Standard errors Standard errors are clustered by year in our benchmark model because ENSO treatment occurs at the global time-series level. Table F.3 considers alternative error structures. Column 1 reproduces our benchmark results. To account for serial correlation, column 2 allows

U.S. workers increased on average by 2% per year between 1970-2003.

year-level clustering and common serial correlation across countries within a 10-year rolling window following Driscoll and Kraay (1998). Column 3 allows differential serial correlation and heteroskedasticity across countries over our entire sample period by clustering standard errors by both year and country. Allowing both forms of serial correlation has little effect on standard errors. Finally, if instruments are weak, standard errors from the LIML estimator may be too small (Hansen, Hausman and Newey, 2008). Column 4 applies the Bekker (1994) adjustment to our benchmark LIML estimates. This only slightly inflates our standard errors, which is unsurprising given that the various tests in Table 2 do not suggest our instruments are weak.

Controlling for time-varying trade costs Our IV model correctly identifies β_0 and β_1 when ENSO conditions influence a country's domestic share of cereal expenditure only through its effects on local yields and the global spatial correlation in yields.[19] While it is unlikely that ENSO, as a naturally occurring climatic phenomenon, is affected by economic activity, the exclusion restriction could be violated if ENSO affects domestic cereal expenditure outside of its influence on cereal yields. For example, as noted above, a violation would occur if ENSO were to directly affect trade costs.

To address this potential violation of the exclusion restriction, Table 3 augments our benchmark model with additional controls designed to capture time-and-country-varying trade costs. Column 1 replicates our benchmark result. In column 2, we add a country-year-varying proxy for trade costs by interacting the global annual crude oil price with the country's average log domestic share of expenditure over our sample period. Column 3 uses an alternative measure of cross-sectional trade openness by interacting the global oil price with a country's centrality, measured as the average of its inverse distance to every other country weighted by that trading partner's long-run average log agricultural output. In both cases, these proxies for trade costs do not meaningfully alter our estimates of β_0 and β_1. Columns 4 and 5 provide more flexible specifications by interacting year fixed effects with the two cross-sectional measures of trade openness used in columns 2 and 3. Again, our coefficients of interest are relatively unaffected by the inclusion of these controls, suggesting that unobserved shocks to trade costs are not correlated with our ENSO-driven instruments. Cereals may be subject to export restrictions that are imposed in response to productivity shocks. In column 6, we include a dummy variable that indicates if a country imposed a new export restriction on cereals that year, using data from the UNCTAD TRAINS database. Controlling for such export restrictions does not alter our result. Finally, ENSO also alters local precipitation. If precipitation

[19] For example, Hsiang, Meng and Cane (2011) show that warmer ENSO conditions increase the likelihood of civil conflicts in the tropics over the same period. This relationship, however, need not imply an exclusion-restriction violation. Suppose ENSO increases civil conflicts in the tropics only through lowered cereal yields. In that scenario, civil conflict would serve as a "bad control" in our IV specification, potentially biasing our coefficients of interest (see Angrist and Pischke 2009, p. 64-68). Our exclusion-restriction assumption is invalid only if ENSO increases civil conflicts partially through non-agricultural channels and if civil conflicts affect domestic share of expenditure by, for example, raising international trade costs relative to internal trade costs. Because the current climate-conflict literature currently supports both agricultural and non-agricultural channels (Hsiang, Burke and Miguel, 2013), the inclusion of conflict as a control would not deliver a unique interpretation: it either jeopardizes a valid identification strategy or show that our instrumental-variable strategy is invalid.

Table 3: Controlling for time-varying trade costs
Outcome is log domestic share of expenditure

	(1)	(2)	(3)	(4)	(5)	(6)	(7)
$\ln A_{it}$ (β_0)	2.114	2.178	2.163	2.492	2.297	2.115	2.270
	(0.604)	(0.612)	(0.593)	(0.737)	(0.641)	(0.604)	(0.796)
	[0.001]	[0.001]	[0.001]	[0.001]	[0.001]	[0.001]	[0.006]
$\ln A_{it} \times I_t$ (β_1)	-4.144	-4.254	-4.189	-4.748	-4.227	-4.145	-4.281
	(1.834)	(1.865)	(1.825)	(2.095)	(1.844)	(1.833)	(1.985)
	[0.028]	[0.027]	[0.026]	[0.028]	[0.026]	[0.028]	[0.036]
ln oil price × average ln λ_{ii}		Yes					
ln oil price × centrality			Yes				
Year FE × average ln λ_{ii}				Yes			
Year FE × centrality					Yes		
Export restrictions						Yes	
Precipitation							Yes
Observations	5452	5452	5452	5452	5452	5452	5452

NOTES: Estimates of β_0 and β_1 from equation (7). Column 1 replicates benchmark model from column 4, panel B, of Table 2. Column 2 (3) controls for the interaction of global log oil price and cross-sectional average log domestic share of expenditure (output-weighted inverse distance averaged across all other countries). Column 4 (5) controls for the interaction of year fixed effects and cross-sectional average log domestic share of expenditure (output-weighted inverse distance averaged across all other countries). Column 6 controls for introductions of export restrictions. Column 7 controls for quadratic precipitation terms. Standard errors clustered by year in parentheses; p-values in brackets.

is also a determinant of trade costs, there may be an exclusion restriction violation. In column 7, we include quadratic terms for total annual precipitation for each country and find that it does not alter our main estimates.

Large economies Our estimate of $\hat{\beta}_0 > 0$ implies that a positive productivity shock worsens an economy's terms of trade. This is at odds with the small-open-economy assumption that terms of trade are exogenous to local conditions. Of course, some economies must influence world prices, but since our estimating equation treats each country as an informative observation without weighting by size, our results suggest that the "typical" economy is not small. To address this more explicitly, column 2 of Table F.4 excludes the ten largest economies that account for more than half of world cereal production from our estimation sample. The resulting estimates of $\hat{\beta}_0$ and $\hat{\beta}_1$ are very similar to our benchmark estimates in column 1 of Table F.4. This finding is consistent with the idea that trade costs make all markets "local", so that no exporter is a price taker.

Sample split Table F.4 further examines whether β_0 and β_1 varies over our sample period. Column 3 shows estimates using the years 1961-1987, the first half of our sample period. Column 4 restricts the years to 1988-2013, the second half of our sample period. While estimates from the second half of our sample period are smaller in absolute magnitude than those from the first half,

the differences are not statistically significant.

Dynamic effects Table 4 empirically estimates dynamic responses that the static model presented in Section 2 necessarily omits. Column 1 replicates our benchmark contemporaneous-productivity specification for a sample in which t is restricted to 1962-2012, the sample period that allows for both lead and lagged yields.

Improvements since the 1980s in the forecasting of strong ENSO events (Chen et al., 2004; Shrader, 2017) could allow the domestic share of expenditure to respond to future ENSO-driven cereal yields. To examine whether agricultural trade anticipates future ENSO events, column 2 tests for the effects of lead log yields, as instrumented by ENSO in years $t+1$ and t. Future ENSO-driven yields do not influence the domestic share of expenditure.

Past yields might influence the domestic share of expenditure if past productivity affects contemporary productivity through intertemporal channels such as depletion of soil nutrients or if past output is stored to facilitate current consumption. Cereal storage, in particular, has been shown to facilitate consumption smoothing in many settings (Williams and Wright, 2005; Roberts and Schlenker, 2013). We address this in two ways. Column 3 examines the effects of lagged log yields generally, as instrumented by ENSO in years $t-1$ and $t-2$. We find that past ENSO-driven yields do not influence the domestic share of expenditure. Our standard measure of domestic expenditure is contemporaneous output minus exports; this includes potential changes in stored cereal inventories. In column 4, we use a measure of domestic expenditure that removes changes in cereal inventory using cereal storage data from the FAO.[20] The estimated coefficients are smaller in absolute magnitude than our benchmark estimates; however, they are not statistically different.

ENSO and local temperature definitions Table F.5 considers alternative definitions of ENSO and country-level local temperatures. Column 1, panel A reproduces our benchmark results using the NINO4 measure as our ENSO index and crop-area-weighted country-level temperatures. In columns 2, 3 and 4, we use NINO3, NINO34, and NINO12, alternative measures of ENSO that differ by the spatial area over which average sea-surface temperature is calculated (see Figure E.3). In panel B, we construct country-level temperature from pixel-level temperature data by taking the pixel average across the total area of a country rather than weight by growing crop area.[21] Our results are largely unaffected by these two data-construction choices.

Our identification strategy need not require ENSO per se. Rather, one needs an exogenous driver of the global spatial correlation of cereal yields that exhibits a sufficiently strong first stage. In Table F.6, we report estimates produced by replacing $g(ENSO_t + ENSO_{t-1})$ in equations (8) and (9) with the annual global spatial correlation of temperature, $I_t(T_{it})$. While the point estimates

[20] This measure is contemporaneous output minus exports minus change in cereal inventory, where the latter is defined as the difference in stored cereals in year t minus stored cereals in year $t-1$. This implicitly assumes that all stored cereals are domestically produced. The sample is smaller due to observations with missing storage data.

[21] Our sample of countries increases slightly when using total-area-weighted temperature compared with using crop-area-weighted temperature because a handful of small-sized countries have no agricultural activity in the Ramankutty et al. (2008) dataset.

Table 4: Dynamic effects
Outcome is log domestic share of expenditure

	(1)	(2)	(3)	(4)
$\ln A_{it}$	2.217			1.326
	(0.651)			(0.634)
	[0.001]			[0.041]
$\ln A_{it} \times I_t$	-4.152			-3.233
	(1.874)			(1.590)
	[0.031]			[0.047]
$\ln A_{it+1}$		0.724		
		(0.503)		
		[0.156]		
$\ln A_{it+1} \times I_{t+1}$		-0.830		
		(1.642)		
		[0.615]		
$\ln A_{it-1}$			0.851	
			(0.526)	
			[0.112]	
$\ln A_{it-1} \times I_{t-1}$			-2.039	
			(1.354)	
			[0.138]	
2nd stage sample period	1962-2012	1962-2012	1962-2012	1961-2013
Remove storage behavior?	No	No	No	Yes
Observations	5237	5236	5235	5191

NOTES: Estimates of β_0 and β_1 from equation (7). Column 1 reproduces benchmark model using log yields in year t instrumented by December ENSO in years t and $t-1$. Column 2 uses log yields in year $t+1$, instrumented by December ENSO conditions in years $t+1$ and t. Column 3 uses log yields in year $t-1$, instrumented by December ENSO conditions in years $t-1$ and $t-2$. Column 4 uses log yields in year t to examine effects on a measure of domestic share of expenditure that includes stored cereals. Sample period for 2nd stage equation is 1962-2012 for columns 1-3 and 1961-2013 for column 4. Standard errors clustered by year in parentheses; p-values in brackets.

in Table F.6 do not differ drastically from the corresponding estimates in panel B of Table 2, the first stages are weaker than when ENSO is used as the source of exogenous variation. As already suggested by Table 1, $I_t(T_{it})$ does not predict the global spatial correlation of cereal yields as strongly as ENSO. In particular, the Kleibergen-Papp F-stat is below the Stock-Yogo critical values for 10% maximal LIML size in all columns of Table F.6. In short, ENSO is preferred to the spatial correlation of an intermediate local weather variable as the source of exogenous variation in the global spatial correlation of cereal yields on the basis of the strength of the first-stage relationship.

Domestic expenditure share construction As detailed in Appendix B, we do not observe cereal prices for all cereal-country-year observations with positive cereal output. Our benchmark

measure of domestic share of expenditure imputes missing cereal-level prices using the average export-volume-weighted cereal export unit value for that country and year. While this imputation increases the number of observations in our estimation sample, this procedure could bias our estimates if it introduces measurement error into our outcome variable that is correlated with our instrumented regressors.

Table F.7 considers alternative approximations for the domestic expenditure share. Column 1 reproduces our benchmark result. Columns 2 through 4 consider alternative price imputations. Column 2 imputes missing export unit values using producer prices.[22] Columns 3 and 4 impute missing cereal prices using the lowest and highest observed export unit values, rather than the average, for a given country and year. All three alternative imputation methods yield estimates of β_0 and β_1 that are statistically indistinguishable from the benchmark estimate in column 1. To see if our benchmark result is sensitive to the source of trade data, domestic expenditure share in Column 5 uses bilateral trade data from Comtrade instead of FAO trade data. Our results are unaffected.

5 Application: Inequality under future climate change

In this section, we demonstrate how to incorporate our general-equilibrium mechanism into reduced-form analyses of economic outcomes when the global spatial structure of productivity changes. Recent reviews of the reduced-form climate change impact literature emphasize the need to consider general-equilibrium effects in projections of economic outcomes under climate change (Dell, Jones and Olken, 2014; Hsiang, 2016). To that end, we take an otherwise standard reduced-form approach to projecting climate impacts that hold spatial correlation fixed and show what happens to projections of future welfare inequality when one incorporate changes in the spatial correlation of productivities due to climate change.[23] Including spatial correlation is one means of accounting for the role of international trade without imposing the full structure of quantitative trade models, similar to a proposal by Monte, Redding and Rossi-Hansberg (2018) to use observables to account for heterogeneous local employment elasticities implied by a quantitative model of commuting flows.

Because our exercise serves only to highlight the implications of incorporating this particular general-equilibrium mechanism, let us also emphasize the other potential general-equilibrium effects that are omitted. First, with the exception of changes in agricultural productivity due to climate-driven changes in local temperature over the 21st century, we hold all other variables fixed at recent historical values. Thus, we do not take into account important trends such as technological change. Second, we apply estimates based on past exogenous annual changes in agricultural productivity to future long-term productivity changes due to climate change. This implies that we omit possible adaptations in anticipation of future climate change (Deschênes and Greenstone, 2007; Hsiang,

[22] See discussion in Appendix B regarding concerns with using FAO's producer prices.

[23] There is currently no scientific consensus on how ENSO will be affected by anthropogenic climate change (Stocker et al., 2013). Our projection exercise therefore assumes ENSO is stationary over the 21st century and does not contribute to long-run changes in the global spatial correlation of agricultural productivities.

2016). Third, we do not consider other potential adjustments such as factor reallocation across sectors and across crops within the agricultural sector. All three practices are standard in reduced-form analyses of climate impacts and may ultimately result in different realized climate impacts than what we project. Our objective is merely to demonstrate how spatial correlation can be incorporated into reduced-form approaches to climate projection; readers interested in climate impact projections that incorporate these other mechanisms should turn to Costinot, Donaldson and Smith (2016), Desmet and Rossi-Hansberg (2015), and Krusell and Smith (2016).

We first report climate change's anticipated effects on the global variance and spatial correlation of agricultural productivity. We then show how incorporating these changes in the spatial correlation of productivities affects welfare projections.

5.1 Agricultural productivity under climate change

To examine how climate change will affect agricultural productivity, we estimate a nonlinear log cereal yield response function using historical variation in annual temperatures across countries and years. Specifically, for the period 1961-2013, we estimate:

$$\ln A_{it} = k(T_{it}) + \mathbb{X}_{it}\Psi + \nu_{it} \tag{10}$$

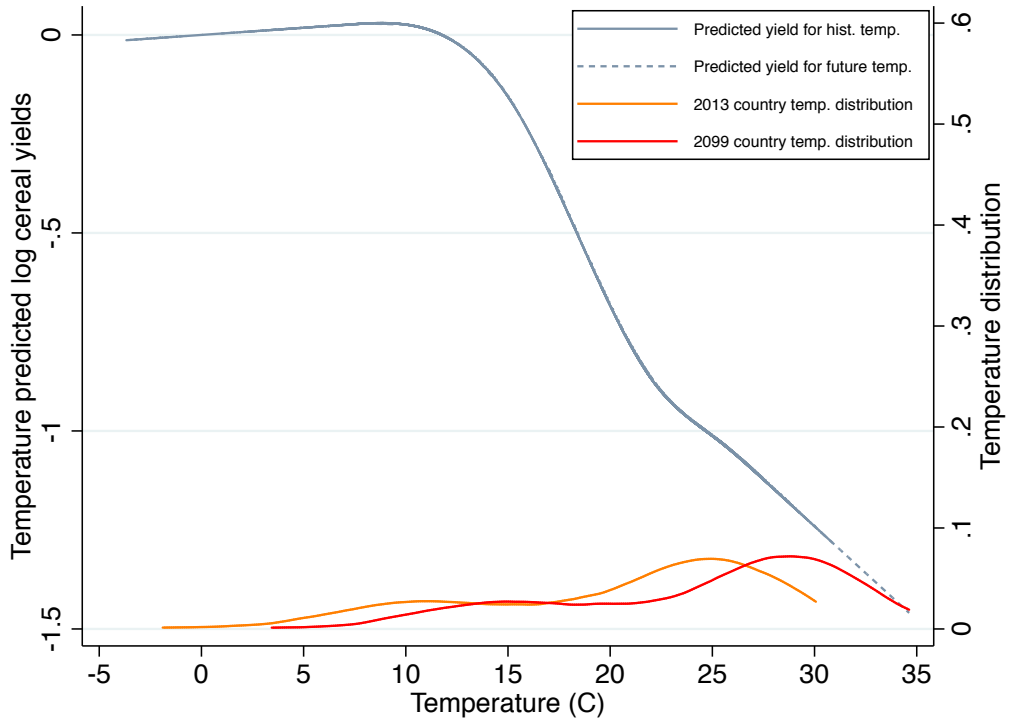
where $k()$ is a restricted cubic spline function and the benchmark set of controls in $\mathbb{X}_{it}$ include country fixed effects, year fixed effects, and country-specific quadratic trends. Figure 15 shows the estimated cubic spline response function, $k()$, using four temperature spline terms. It also shows two cross-sectional temperature distributions: observed temperatures in 2013 and the forecast for 2099 under a business-as-usual (Representative Concentration Pathway 8.5) climate scenario obtained from the Coupled Model Intercomparison Project (CMIP5) multi-model ensemble mean.[24] Column 1 of Table F.8 shows that the coefficients of $k()$ shown in Figure 15 are jointly statistically significant with a productivity-maximizing temperature around 9°C. Table F.8 also indicates that the predicted optimal temperature is relatively insensitive to the number of knots in the spline function and to the inclusion of precipitation controls.

Next, we combine the estimated coefficients in equation (10) with local temperature projections under a business-as-usual climate scenario to project log cereal yields in the 2014-2099 period. All other variables in equation (10) are fixed at 2013 levels (see Appendix D.2 for details). Figure 16 maps the projected change in country-level log cereal yields under climate change between 2013-2099. Consistent with the nonlinear yield response function shown in Figure 15, climate change lowers agricultural productivities across much of the world with the exception of a few upper-latitude countries that experience modest gains.

Climate change alters two important moments of the cross-country agricultural productivity

[24] The Coupled Model Intercomparison Project is a coordinated effort by the climate-science community to harmonize model runs across various climate models. The average climate projection across CMIP models is known as the multi-model ensemble mean. CMIP5 was used to inform the Fifth Assessment Report of the Intergovernmental Panel on Climate Change (see Taylor, Stouffer and Meehl (2012) for details).

Figure 15: Estimated temperature response function for log cereal yields



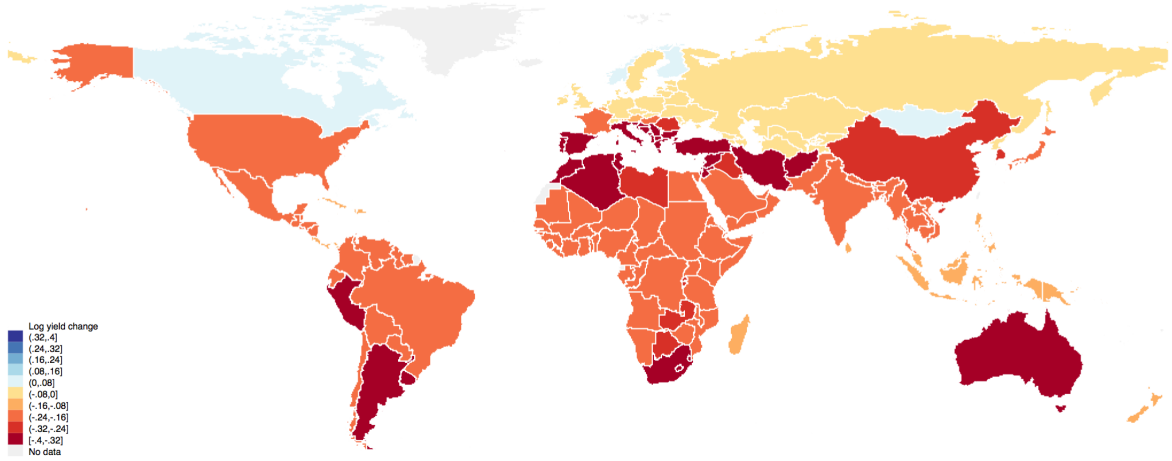
NOTES: Gray solid line shows $k()$ in equation (10), the predicted relationship between crop-area-weighted country-level temperature and log cereal yields, estimated during 1961-2013. Restricted cubic spline function is estimated using four spline terms with knots placed along the temperature support according to Harrell (2001). Gray dashed line shows additional predicted log cereal yields using extrapolated temperature in 2099. Estimated model corresponds to column 1 of Table F.8. Orange line shows the distribution of observed country-level temperature in 2013. Red line shows country-level projected temperature in 2099 from CMIP5 ensemble mean under a business-as-usual (RCP 8.5) scenario.

distribution. First, the variance of agricultural productivity increases. In 2013, of the 12 countries with temperatures below the global productivity-maximizing temperature, 10 had productivities above the cross-sectional mean (see Figure E.5).[25] As temperatures increase under climate change, these countries with high relative productivity will gain further by moving towards the productivity-maximizing temperature shown in Figure 15. Concurrently nearly all other countries will experience productivity losses as they move away from the optimal temperature. Because the gains from climate change are experienced almost exclusively by relatively high productivity countries, there is a resulting increase in the cross-country variance of productivity, depicted by the gray line in Figure 17.

Second, as temperatures increase across the planet, the spatial correlation of agricultural pro-

[25] Figure E.5 shows that the unconditional relationship between log productivity and temperature is very similar to the conditional relationship depicted in Figure 14, $k(T_{it})$. Thus, we can describe how climate change alters the variance and spatial correlation of productivity in terms of the nonlinear shape of $k(T_{it})$, even though productivity incorporates other determinants contained in controls $\mathbb{X}_{it}\Psi$ and residual ν_{it} from equation (10).

Figure 16: Change in log cereal yields under climate change (2013-2099)



NOTES: Map shows the projected change in country-level log cereal yields under climate change between 2013-2099. Projected change in log yields obtained after estimating equation (10) with four spline terms as shown in column 1 of Table F.8. Climate projections from CMIP5 ensemble mean under a business-as-usual (RCP 8.5) scenario.

Figure 17: Variance and spatial correlation of agriculture productivity under climate change



NOTES: Gray (blue) series shows the change in the global variance (Moran's I) of log cereal yields over the 21st century under climate change. Climate projections from CMIP5 ensemble mean under a business-as-usual (RCP 8.5) scenario.

ductivities increases. This is again due to the non-monotone yield response function shown in Figure 15 and the fact that surface temperatures are generally decreasing in distance to the equator. Absent climate change, mid-latitude locations experience the productivity-maximizing temperature. Locations closer to and farther from the equator both generally exhibit lower yields.

As climate change increases temperatures across the globe, latitudes closer to the poles now experience the productivity-maximizing temperature, with less productive locations becoming more bunched around the equator. This bifurcation of global agriculture into high-productivity poles and a low-productivity band around the equator increases the spatial correlation of agricultural productivity.[26] The resulting increase in Moran's I for agricultural productivity under climate change is indicated by the blue series in Figure 17.

5.2 Welfare projections and changes in spatial structure

The change in the spatial correlation of agricultural productivity due to climate change is consequential for global welfare inequality. To demonstrate this, we combine projected local agricultural productivity under climate change with our estimates of $\widehat{\beta}_0$ and $\widehat{\beta}_1$ in Section 4 to project future domestic shares of expenditure via equation (7) and welfare variance via equation (3) (see Appendix D.2 for details). We consider two scenarios with different terms-of-trade effects.[27] In the first scenario, we fix the spatial correlation of temperature-predicted agricultural productivities to its 2013 value. In the second scenario, we allow climate change to increase the spatial correlation of productivities as depicted in Figure 17.

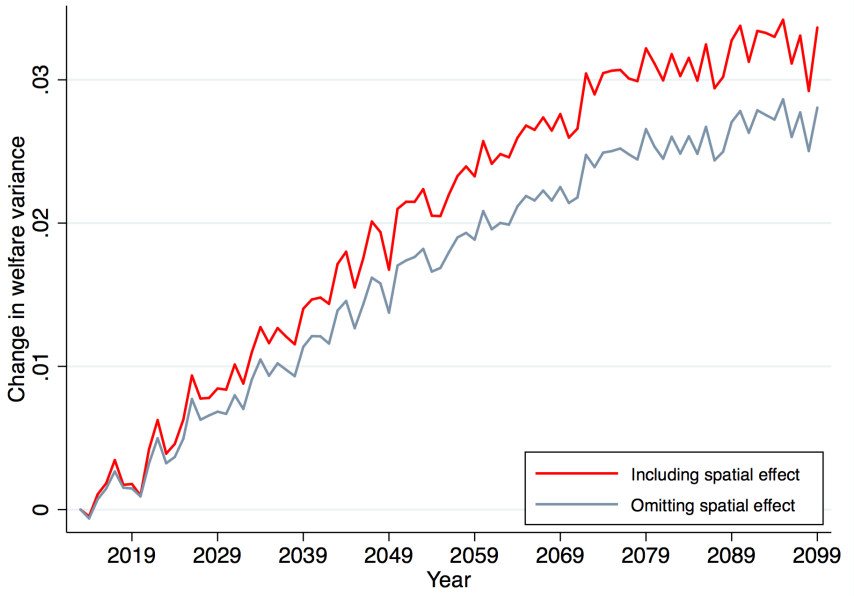
The projected change in the variance of welfare over the 21st century is shown in Figure 18. The gray line shows the projection that omits changes in spatial correlation and the red line shows the projection that include such changes. Omitting changes in spatial correlation, the projected increase in the variance of agricultural productivity generates a projected increase in the variance of welfare. The projection that incorporates increases in the spatial correlation of agricultural productivity due to climate change predicts a 20% greater increase in welfare inequality between 2013-2099 compared to the projection that holds spatial correlation fixed.

Figure 18 shows how incorporating changes in spatial correlation affects projections of welfare inequality in an otherwise standard reduced-form projection that does not include any general-equilibrium changes under climate change. One can also ask the following inverted question: how much of the variance of welfare implied by the trade model considered in Section 2.2.3 is explained by our reduced-form approach to incorporating changes in spatial correlation? Figure E.2 compares structural and reduced-form predictions of welfare variance when using predicted climate change-driven log cereal productivities from equation (10) for the years 2013 and 2099. As with the simulations shown in Figure E.1, our reduced-form predictions incorporating changes in spatial correlation match welfare variance from our trade model remarkably well.

[26] Additionally, the country-specific shift in temperature due to climate change is not spatially uniform. Because of surface albedo changes due to polar ice melt, there is higher warming in the poles relative to lower latitude areas. However, this latitude-dependent gradient is relatively small compared to the average global temperature change and thus plays a second-order role in determining changes in the spatial correlation of productivity. For example, the projected temperature change over the 21st century for Gabon, the country located closest to the equator, is 3.4°C. For Finland, the country located closest to the north pole, the projected temperature change is 2.9°C.

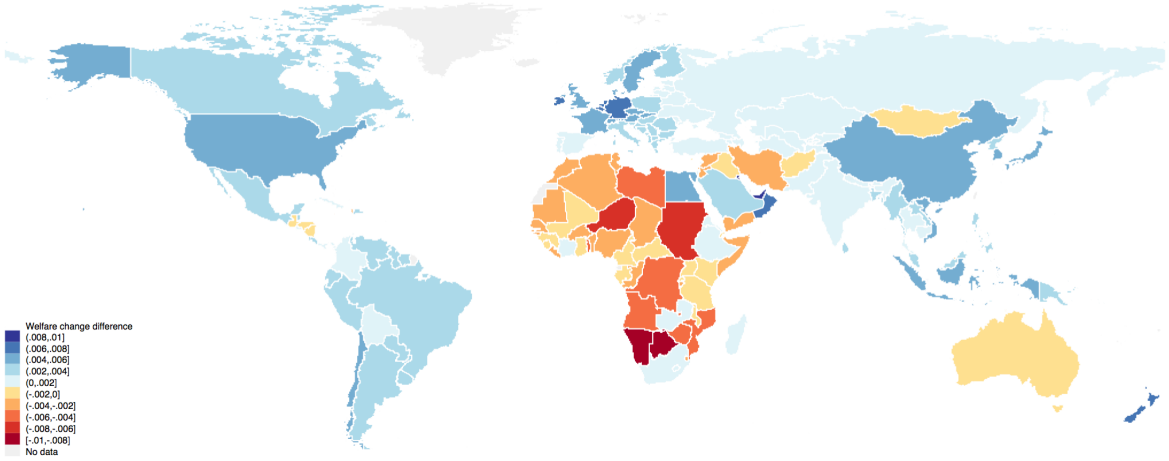
[27] In autarky, the variance of welfare would be proportionate to the variance of productivity. Since a productivity increase is associated with worse terms of trade, an increase in the variance of productivity causes a smaller increase in the variance of welfare when there is international trade.

Figure 18: Variance in climate-driven welfare over the 21st century



NOTES: Gray (red) line shows the change in the variance of welfare when omitting (including) changes in the spatial correlation of log cereal yields over the 21st century under climate change. Climate projections from CMIP5 ensemble mean under a business-as-usual (RCP 8.5) scenario.

Figure 19: Differences in projected welfare changes due to change in spatial correlation (2013-2099)



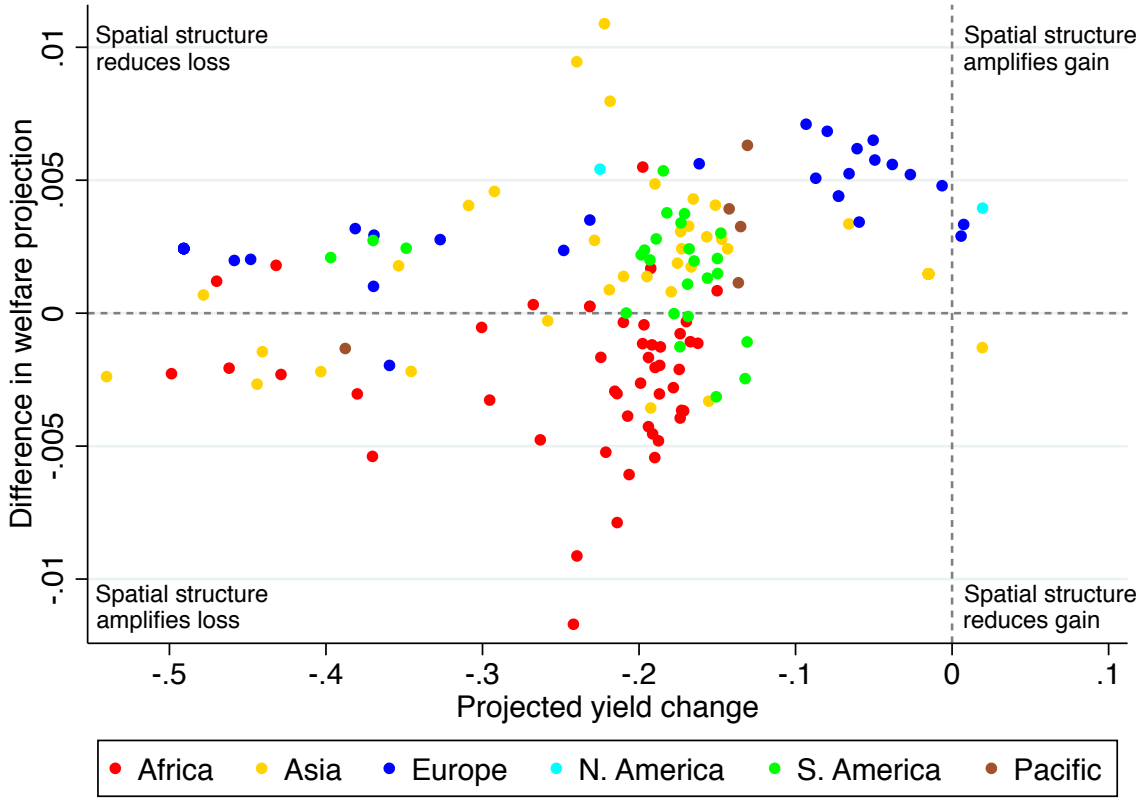
NOTES: Map shows the difference in projected country-level welfare change over 2013-2099 between projections that include (Figure D.2) and omit (Figure D.1) changes in spatial correlation. Climate projections from CMIP5 ensemble mean under a business-as-usual (RCP 8.5) scenario.

How do the projections differ across countries? Figure 19 maps the difference between the two projections.[28] Including an increase in the spatial correlation of productivity causes the gains from trade to be lower in less productive countries and higher in more productive countries than in a

[28] See equation (D.14) at the end of Appendix D.3.

projection that holds spatial correlation fixed. In particular, Figure 19 shows that most countries in Africa, and a few in Asia and South America have lower gains from trade in the projection that incorporates changes in spatial correlation. This is because the relatively high local temperatures that drive yield losses in these countries is compounded by similar temperatures simultaneously experienced by neighboring countries. In the simplest terms, a key feature of climate change is that it makes Ethiopia and Kenya less productive at the same time, lowering the gains from trade compared to a scenario in which each country warms independently. By the same logic, parts of Europe and North American have higher gains from trade when the projection includes increases in spatial correlation. The relatively milder temperatures experienced by these countries is accompanied by similar temperatures over neighboring locations.

Figure 20: Differences in welfare projections due to change in spatial correlation and projected yield changes



NOTES: Scatter shows the difference in projected country-level welfare change between projections that include and omit changes in spatial correlation (from Figure 19) plotted against change in log cereal yields (from Figure 16) over 2013-2099 under climate change. Countries are color-coded by continent.

Figure 20 depicts climate-change forecasts for each country in terms of the predicted change in agricultural productivity from Figure 16 on the horizontal axis and the difference in projected welfare from omitting the change in spatial correlation shown in Figure 19 on the vertical axis. The vast majority of countries suffer a decrease in agricultural productivity as a result of increased

temperature, as already shown in Figure 16. As in Figure 19, the strongest contrast in Figure 20 is between outcomes for African and European economies.[29] While there is substantial heterogeneity in the productivity declines across countries within each continent, most economies in Africa, and a few in South America and Asia, experience productivity losses that would be considerably amplified by changes in spatial correlation. By contrast, most European economies have reduced projected welfare losses when changing spatial correlation is considered. For the few economies with increased productivity under climate change, the differences across projections are close to zero.

6 Conclusion

This paper studies how the spatial structure of the global productivity distribution shapes the distribution of welfare across countries. In particular, we use a standard trade model with distance-related trade costs to show that, holding the unconditional moments of the productivity distribution fixed, greater spatial correlation of productivity can increase welfare inequality. The increase in spatial correlation causes high-productivity locations to enjoy larger gains from trade than they would if productivity were spatially uncorrelated. In settings in which welfare differences are arbitraged away by mobile factors of production, greater spatial correlation of productivity would make population density, rather than welfare per capita, more unequal across locations.[30]

To empirically investigate this relationship, we exploit a global natural experiment that is well-suited for identifying general-equilibrium effects following a change in the spatial structure of the international trade network. Specifically, we use the El Niño-Southern Oscillation, a naturally occurring global climatic phenomenon, which exogenously alters the annual spatial correlation of cereal productivity around the planet. We examine how the spatial correlation of cereal productivity governs the response of the domestic share of expenditure, a sufficient statistic for the gains from trade in a broad class of trade models, to local productivity. Using data from the past five decades of cereal trade, we find that high-productivity locations enjoy larger gains from trade when cereal productivity is more spatially correlated, as predicted. More broadly, our empirical approach advances the use of causal inference techniques to validate general-equilibrium predictions. Such estimates can increase our confidence in the application of structural models.

In our application, we demonstrate that incorporating changes in the spatial correlation of productivities substantially alters predictions about global welfare inequality when forecasting the consequences of anthropogenic climate change. This interplay between the spatial structure of productivity and welfare inequality is potentially important in many other domains. Many determinants of productivity - such as natural endowments, political institutions, and demographics - tend to exhibit substantial spatial correlation. For natural endowments in particular, spatial correlation may change following the relocation of existing endowments (e.g., migrating wildlife stocks), the discovery of new uses for them (e.g., solar and wind availability), or the discovery of

[29] See Figure E.6 for the same plot with country identifiers.

[30] Appendix A.5 proves that this is the case for a symmetric geography with four locations.

new endowments (e.g., fossil fuel deposits). This paper provides a framework for analyzing the general-equilibrium welfare consequences of such widespread productivity changes.

References

Acemoglu, Daron, and Jaume Ventura. 2002. "The World Income Distribution." *The Quarterly Journal of Economics*, 117(2): 659–694.

Agcaoili-Sombilla, Mercedita C, and Mark W Rosegrant. 1994. "International trade in a differentiated good: Trade elasticities in the world rice market." *Agricultural Economics*, 10(3): 257–267.

Allen, Treb, and Costas Arkolakis. 2014. "Trade and the Topography of the Spatial Economy." *The Quarterly Journal of Economics*, 129(3): 1085–1140.

Allen, Treb, Costas Arkolakis, and Yuta Takahashi. 2017. "Universal Gravity."

Anderson, James E., and Eric van Wincoop. 2003. "Gravity with Gravitas: A Solution to the Border Puzzle." *American Economic Review*, 93(1): 170–192.

Anderson, T. W., and Herman Rubin. 1949. "Estimation of the Parameters of a Single Equation in a Complete System of Stochastic Equations." *The Annals of Mathematical Statistics*, 20(1): 46–63.

Angrist, Joshua D., and Jörn-Steffen Pischke. 2009. *Mostly Harmless Econometrics: An Empiricist's Companion.* Princeton University Press.

Arkolakis, Costas, Arnaud Costinot, and Andrés Rodríguez-Clare. 2012. "New Trade Models, Same Old Gains?" *American Economic Review*, 102(1): 94–130.

Barro, Robert J. 1991. "Economic Growth in a Cross Section of Countries." *The Quarterly Journal of Economics*, 106(2): 407–443.

Bekker, Paul A. 1994. "Alternative Approximations to the Distributions of Instrumental Variable Estimators." *Econometrica*, 62(3): 657–681.

Bhagwati, Jagdish. 1958. "Immiserizing Growth: A Geometrical Note." *The Review of Economic Studies*, 25(3): 201–205.

Bleakley, Hoyt. 2007. "Disease and Development: Evidence from Hookworm Eradication in the American South." *The Quarterly Journal of Economics*, 122(1): 73–117.

Bound, John, David A. Jaeger, and Regina M. Baker. 1995. "Problems with Instrumental Variables Estimation When the Correlation Between the Instruments and the Endogeneous Explanatory Variable is Weak." *Journal of the American Statistical Association*, 90(430): 443–450.

Brock, William, Gustav Engström, and Anastasios Xepapadeas. 2014. "Spatial climate-economic models in the design of optimal climate policies across locations." *European Economic Review*, 69: 78 – 103.

Burke, Marshall, Solomon M. Hsiang, and Edward Miguel. 2015. "Global non-linear effect of temperature on economic production." *Nature*, 527(7577): 235–239.

Caliendo, Lorenzo, and Fernando Parro. 2015. "Estimates of the Trade and Welfare Effects of NAFTA." *The Review of Economic Studies*, 82(1): 1–44.

Cane, Mark A., and Stephen E. Zebiak. 1985. "A Theory for El Niño and the Southern Oscillation." *Science*, 228(4703): 1085–1087.

Caselli, Francesco. 2005. "Accounting for Cross-Country Income Differences." In *Handbook of Economic Growth.* , ed. Philippe Aghion and Steven N. Durlauf, 679 – 741. Elsevier.

Chen, Dake, Mark A. Cane, Alexey Kaplan, Stephen E. Zebiak, and Daji Huang. 2004. "Predictability of El Nino over the past 148 years." *Nature*, 428(6984): 733—736.

Chiang, John C.H., and Adam H. Sobel. 2002. "Tropical Tropospheric Temperature Variations Caused by ENSO and Their Influence on the Remote Tropical Climate." *Journal of Climate*, 15(18): 2616–2631.

Costinot, Arnaud, and Andrés Rodríguez-Clare. 2014. "Trade Theory with Numbers: Quantifying the Consequences of Globalization." Vol. 4 of *Handbook of International Economics*, Chapter 4, 197–261. Elsevier.

Costinot, Arnaud, Dave Donaldson, and Cory Smith. 2016. "Evolving Comparative Advantage and the Impact of Climate Change in Agricultural Markets: Evidence from 1.7 Million Fields around the World." *Journal of Political Economy*, 124(1): 205–248.

Costinot, Arnaud, Dave Donaldson, and Ivana Komunjer. 2012. "What Goods Do Countries Trade? A Quantitative Exploration of Ricardo's Ideas." *The Review of Economic Studies*, 79(2): 581–608.

Cragg, John G., and Stephen G. Donald. 1993. "Testing Identifiability and Specification in Instrumental Variable Models." *Econometric Theory*, 9(2): 222–240.

Debaere, Peter, and Hongshik Lee. 2003. "The Real-Side Determinants of Countries' Terms of Trade." unpublished.

Dell, Melissa, Benjamin F. Jones, and Benjamin A. Olken. 2012. "Temperature Shocks and Economic Growth: Evidence from the Last Half Century." *American Economic Journal: Macroeconomics*, 4(3): 66–95.

Dell, Melissa, Benjamin F. Jones, and Benjamin A. Olken. 2014. "What Do We Learn from the Weather? The New Climate-Economy Literature." *Journal of Economic Literature*, 52(3): 740–98.

Deschênes, Olivier, and Michael Greenstone. 2007. "The Economic Impacts of Climate Change: Evidence from Agricultural Output and Random Fluctuations in Weather." *American Economic Review*, 97(1): 354–385.

Desmet, Klaus, and Esteban Rossi-Hansberg. 2015. "On the spatial economic impact of global warming." *Journal of Urban Economics*, 88: 16 – 37.

Disdier, Anne-Célia, and Keith Head. 2008. "The Puzzling Persistence of the Distance Effect on Bilateral Trade." *The Review of Economics and Statistics*, 90(1): 37–48.

Driscoll, John C., and Aart C. Kraay. 1998. "Consistent Covariance Matrix Estimation with Spatially Dependent Panel Data." *The Review of Economics and Statistics*, 80(4): 549–560.

Easterly, William, and Ross Levine. 2003. "Tropics, Germs, and Crops: How Endowments Influence Economic Development." *Journal of Monetary Economics*, 50(1): 3–39.

Eaton, Jonathan, and Samuel Kortum. 2002. "Technology, Geography, and Trade." *Econometrica*, 70(5): 1741–1779.

Feenstra, Robert C., Robert Inklaar, and Marcel P. Timmer. 2015. "The Next Generation of the Penn World Table." *American Economic Review*, 105(10): 3150–82.

Gallup, John Luke, Jeffrey D. Sachs, and Andrew D. Mellinger. 1999. "Geography and Economic Development." *International Regional Science Review*, 22(2): 179–232.

Hansen, Christian, Jerry Hausman, and Whitney Newey. 2008. "Estimation With Many Instrumental Variables." *Journal of Business & Economic Statistics*, 26(4): 398–422.

Harrell, Frank. 2001. *Regression Modeling Strategies: With Applications to Linear Models, Logistic Regression, and Survival Analysis.* Springer.

Head, Keith, and Thierry Mayer. 2004. "The Empirics of Agglomeration and Trade." , ed. J. V. Henderson and J. F. Thisse Vol. 4 of *Handbook of Regional and Urban Economics*, Chapter 59, 2609–2669. Elsevier.

Head, Keith, and Thierry Mayer. 2014. "Gravity Equations: Workhorse,Toolkit, and Cookbook." Vol. 4 of *Handbook of International Economics*, Chapter 3, 131–195. Elsevier.

Hornbeck, Richard. 2012. "Nature versus Nurture: The Environment's Persistent Influence through the Modernization of American Agriculture." *American Economic Review Papers and Proceedings*, 102(3): 245–249.

Hsiang, Solomon. 2016. "Climate Econometrics." *Annual Review of Resource Economics*, 8(1): 43–75.

Hsiang, Solomon M., and Kyle C. Meng. 2015. "Tropical Economics." *American Economic Review: Papers and Proceedings*, 105(5): 257–61.

Hsiang, Solomon M, Kyle C Meng, and Mark A Cane. 2011. "Civil conflicts are associated with the global climate." *Nature*, 476(7361): 438–441.

Hsiang, Solomon M., Marshall Burke, and Edward Miguel. 2013. "Quantifying the Influence of Climate on Human Conflict." *Science*, 341(6151).

Jameson, G. J. O. 2006. "Counting Zeros of Generalised Polynomials: Descartes' Rule of Signs and Laguerre's Extensions." *The Mathematical Gazette*, 90(518): 223–234.

Johnson, Paul, and Chris Papageorgiou. 2018. "What Remains of Cross-Country Convergence?" University Library of Munich, Germany MPRA Paper 89355.

Kaplan, A., M. Cane, Y. Kushnir, A. Clement, M. Blumenthal, and B. Rajagopalan. 1998. "Analyses of global sea surface temperature 1856-1991." *Journal of Geophysical Research*, 103: 18,567–18,589.

Kleibergen, Frank, and Richard Paap. 2006. "Generalized reduced rank tests using the singular value decomposition." *Journal of Econometrics*, 133(1): 97 – 126.

Klenow, Peter J., and Andrés Rodríguez-Clare. 1997. "The Neoclassical Revival in Growth Economics: Has It Gone Too Far?" *NBER Macroeconomics Annual*, 12: 73–103.

Kopczuk, Wojciech, Emmanuel Saez, and Jae Song. 2010. "Earnings inequality and mobility in the United States: evidence from social security data since 1937." *The Quarterly Journal of Economics*, 125(1): 91–128.

Krugman, Paul. 1980. "Scale Economies, Product Differentiation, and the Pattern of Trade." *American Economic Review*, 70(5): 950–59.

Krusell, Per, and Anthony A. Smith. 2016. "Climate Change around the World." *mimeo.*

Legates, D. R., and C. J. Willmott. 1990*a*. "Mean Seasonal and Spatial Variability Global Surface Air Temperature." *Theoretical and Applied Climatology*, 41: 11–21.

Legates, D. R., and C. J. Willmott. 1990*b*. "Mean Seasonal and Spatial Variability in Gauge-Corrected, Global Precipitation." *International Journal of Climatology*, 10: 111–127.

Lind, Nelson, and Natalia Ramondo. 2018. "Trade with Correlation." National Bureau of Economic Research Working Paper 24380.

Lucas, Robert E. 1988. "On the mechanics of economic development." *Journal of Monetary Economics*, 22(1): 3 – 42.

Mariano, Roberto S. 2001. "Simultaneous Equation Model Estimators: Statistical Properties and Practical implications." *A Companion to Theoretical Econometrics*, , ed. B. Baltagi, 122–143. Blackwell: Oxford, UK.

Monte, Ferdinando, Stephen J. Redding, and Esteban Rossi-Hansberg. 2018. "Commuting, Migration, and Local Employment Elasticities."

Moore, Frances C., and David B. Lobell. 2015. "The fingerprint of climate trends on European crop yields." *Proceedings of the National Academy of Sciences*, 112(9): 2670–2675.

Newey, Whitney K., and Kenneth D. West. 1987. "A Simple, Positive Semi-Definite, Heteroskedasticity and Autocorrelation Consistent Covariance Matrix." *Econometrica*, 55(3): 703–708.

Nordhaus, William D. 2006. "Geography and macroeconomics: New data and new findings." *Proceedings of the National Academy of Sciences of the United States of America*, 103(10): 3510–3517.

Nunn, Nathan, and Diego Puga. 2012. "Ruggedness: The Blessing of Bad Geography in Africa." *Review of Economics and Statistics*, 94(1): 20–36.

Ramankutty, Navin, Amato T. Evan, Chad Monfreda, and Jonathan A. Foley. 2008. "Farming the planet: 1. Geographic distribution of global agricultural lands in the year 2000." *Global Biogeochemical Cycles*, 22.

Redding, Stephen, and Anthony J. Venables. 2004. "Economic geography and international inequality." *Journal of International Economics*, 62(1): 53–82.

Roberts, Michael J., and Wolfram Schlenker. 2013. "Identifying Supply and Demand Elasticities of Agricultural Commodities: Implications for the US Ethanol Mandate." *American Economic Review*, 103(6): 2265–95.

Ropelewski, C. F., and M. S. Halpert. 1987. "Global and Regional Scale Precipitation Patterns Associated with the El Niño/Southern Oscillation." *Monthly Weather Review*, 115(8): 1606–1626.

Sachs, Jeffrey D, and Andrew M Warner. 1997. "Fundamental Sources of Long-Run Growth." *American Economic Review*, 87(2): 184–188.

Sarachik, Edward S., and Mark A. Cane. 2010. *The El Niño-Southern Oscillation Phenomenon.* Cambridge University Press.

Schlenker, Wolfram, and David B Lobell. 2010. "Robust negative impacts of climate change on African agriculture." *Environmental Research Letters*, 5(1): 014010.

Schlenker, Wolfram, and Michael J Roberts. 2009. "Nonlinear temperature effects indicate severe damages to U.S. crop yields under climate change." *Proceedings from the National Academy of Science*, 106(37): 15594–8.

Shrader, Jeffrey. 2017. "Expectations and adaptation to environmental risks." *mimeo.*

Stock, James, and Motohiro Yogo. 2005. "Testing for Weak Instruments in Linear IV Regression." *Identification and Inference for Econometric Models*, , ed. Donald W.K. Andrews, 80–108. New York:Cambridge University Press.

Stocker, T.F., D. Qin, G.-K. Plattner, L.V. Alexander, S.K. Allen, N.L. Bindoff, F.-M. Bréon, J.A. Church, U. Cubasch, S. Emori, P. Forster, P. Friedlingstein, N. Gillett, J.M. Gregory, D.L. Hartmann, E. Jansen, B. Kirtman, R. Knutti, K. Krishna Kumar, P. Lemke, J. Marotzke, V. Masson-Delmotte, G.A. Meehl, I.I. Mokhov, S. Piao, V. Ramaswamy, D. Randall, M. Rhein, M. Rojas, C. Sabine, D. Shindell, L.D. Talley, D.G. Vaughan, and S.-P. Xie. 2013. "Technical Summary." *Climate Change 2013: The Physical Science Basis. Contribution of Working Group I to the Fifth Assessment Report of the Intergovernmental Panel on Climate Change*, , ed. T.F. Stocker, D. Qin, G.-K. Plattner, M. Tignor, S.K. Allen, J. Boschung, A. Nauels, Y. Xia, V. Bex and P.M. Midgley, Chapter TS, 33–115. Cambridge, United Kingdom and New York, NY, USA:Cambridge University Press.

Taylor, Karl E., Ronald J. Stouffer, and Gerald A. Meehl. 2012. "An Overview of CMIP5 and the Experiment Design." *Bulletin of the American Meteorological Society*, 93(4): 485–498.

Welch, Jarrod R., Jeffrey R. Vincent, Maximilian Auffhammer, Piedad F. Moya, Achim Dobermann, and David Dawe. 2010. "Rice yields in tropical/subtropical Asia exhibit large but opposing sensitivities to minimum and maximum temperatures." *Proceedings of the National Academy of Sciences*, 107(33): 14562–14567.

Williams, Jeffrey C, and Brian D Wright. 2005. *Storage and Commodity Markets.* Cambridge University Press.

Appendix

A Theory appendix

A.1 General economic environment

This appendix section provides details of perfect-competition results presented in Section 2 and extends them to the Krugman (1980) model of monopolistic competition.

A.1.1 Perfect-competition microfoundations

Production function. In the Armington model, each country i produces a distinct variety using a linear production technology such that one unit of labor yields A_i units of output. Under perfect competition, its price is w_i/A_i and thus the Dixit-Stigliz price index is $P_j = \left(\sum_{i=1}^{N} \left(w_i \tau_{ij}/A_i\right)^{1-\sigma}\right)^{1/(1-\sigma)}$. In the Eaton and Kortum (2002) model, there is a continuum of varieties, and each country's efficiency in producing them follows a Fréchet distribution with location parameter T_i and dispersion parameter ϑ.

Gravity equation. Written in terms of expenditure shares, the gravity equation is

$$\lambda_{ij} = \frac{\chi_i \left(\tau_{ij} w_i\right)^{-\epsilon}}{\sum_{l=1}^{N} \chi_l \left(\tau_{lj} w_l\right)^{-\epsilon}}$$

In the Armington model, $\epsilon = \sigma - 1$ and $\chi_i = A_i^{\epsilon}$. In the Eaton-Kortum model without intermediate inputs, $\epsilon = \vartheta$ and $\chi_i = T_i$. Thus, the equilibrium trade flows associated with a productivity distribution $\{A_i\}_i$ and trade elasticity ϵ in the Armington model are equal to the equilibrium trade flows for an Eaton-Kortum model in which efficiency distributions have location parameters $T_i = A_i^{\epsilon}$.

Welfare. Equation (2) is an immediate consequence of the main result in Arkolakis, Costinot and Rodríguez-Clare (2012). They show that, in a broad class of models, the gains from trade relative to autarky are equal to $-\frac{1}{\epsilon} \ln \lambda_{ii}$. In our theoretical environment, autarky welfare is equal to $\ln A_i + \gamma$, as implied by equation (2). γ is a function of structural parameters. In the Armington model with symmetric preferences, γ is zero. In the Eaton and Kortum (2002) model, $\gamma = \left[\Gamma\left(1 + \frac{1-\sigma}{\theta}\right)\right]^{1/(1-\sigma)}$ where Γ is the gamma function.

A.1.2 Krugman (1980) microfoundations

We now discuss the case of monopolistic competition with homogeneous firms, in which the measure of varieties available in equilibrium is endogenously determined. Consider a many-country version of the Krugman (1980) model in which fixed costs f_j and marginal costs c_j may vary across countries. Denote the equilibrium number of homogeneous firms producing in country j by n_j.

Gravity equation. In the free-entry equilibrium, $\epsilon = \sigma - 1$, $n_i = L_i/\left(\sigma f_i\right)$, and $\chi_i = n_i c_i^{-\epsilon}$.

Welfare. In this setting, real per capita consumption is

$$\ln\left(C_i/L_i\right) = \frac{1}{\epsilon}\ln n_i - \ln c_i + \ln\left(\frac{\sigma-1}{\sigma}\right) - \frac{1}{\epsilon}\ln\lambda_{ii}$$

If population size L_i and fixed costs f_i are country-invariant ($n_i = n\ \forall j$) and we interpret productivity as shifting marginal costs, $A_i = c_i^{-1}$, then this is equivalent to equation (2) with $\gamma = \frac{1}{\epsilon}\ln n + \ln\left(\frac{\sigma-1}{\sigma}\right)$. If population size L_i and marginal costs c_i are country-invariant and we interpret productivity as shifting fixed costs, $A_i = f_i^{-1/\epsilon}$, then this is equivalent to equation (2) with $\gamma = \frac{1}{\epsilon}\ln\left(L/\sigma\right) + \ln\left(\frac{\sigma-1}{\sigma c}\right)$.

In the case of countries with heterogeneous population sizes, equation (2) must be extended to replace γ with a location-specific γ_i that depends on structural parameters other than productivity. For example, if productivity shifts marginal costs, $A_i = c_i^{-1}$, then we obtain

$$\ln\left(\frac{C_i}{L_i}\right) = \ln A_i + \gamma_i - \frac{1}{\epsilon}\ln\lambda_{ii}, \tag{2'}$$

where $\gamma_i = \frac{1}{\epsilon}\ln n_i + \ln\left(\frac{\sigma-1}{\sigma}\right)$. If we assume that $cov(\ln A_i^u, \gamma_i) = cov(\ln A_i^c, \gamma_i)$, we obtain an extension of equation (4):

$$\begin{aligned} var\left(\ln C_i^c/L_i\right) - var\left(\ln C_i^u/L_i\right) = &-\frac{2}{\epsilon}\left[cov\left(\ln A_i^c, \ln\lambda_{ii}^c\right) - cov\left(\ln A_i^u, \ln\lambda_{ii}^u\right)\right] \\ &-\frac{2}{\epsilon}\left[cov\left(\gamma_i, \ln\lambda_{ii}^c\right) - cov\left(\gamma_i, \ln\lambda_{ii}^u\right)\right] \\ &+\frac{1}{\epsilon^2}\left[var\left(\ln\lambda_{ii}^c\right) - var\left(\ln\lambda_{ii}^u\right)\right]. \end{aligned} \tag{4'}$$

A.1.3 The case of symmetric trade costs

Starting from the equilibrium system of equations and using the assumption of symmetric trade costs ($\tau_{ij} = \tau_{ji}$):

$$\begin{aligned} Y_i = w_i L_i &= \sum_j \left(\frac{w_i}{A_i}\right)^{-\epsilon} \tau_{ij}^{-\epsilon}\frac{w_j L_j}{\Phi_j} = \left(\frac{w_i}{A_i}\right)^{-\epsilon}\Omega_i \\ \Rightarrow \frac{w_i}{A_i} &= \left(\frac{\Omega_i}{A_i L_i}\right)^{\frac{1}{\epsilon+1}} \\ \Rightarrow \Phi_i &= \sum_j \tau_{ji}^{-\epsilon}\left(\frac{w_j}{A_j}\right)^{-\epsilon} = \sum_j \tau_{ji}^{-\epsilon}\left(A_j L_j/\Omega_j\right)^{\frac{\epsilon}{\epsilon+1}} \\ &= \sum_j \tau_{ji}^{-\epsilon}\left(A_j L_j/\Phi_j\right)^{\frac{\epsilon}{\epsilon+1}} \end{aligned}$$

The last equality exploits the fact that we can normalize incomes such that $\Phi_i = \Omega_i$ when trade is balanced and $\tau_{ij}^{-\epsilon}$ is symmetric, as established in Anderson and van Wincoop (2003) and Head and Mayer (2014).

Combining $\lambda_{ii} = \frac{(w_i/A_i)^{-\epsilon}}{\Phi_i}$, the above expression for w_i/A_i, and the assumption of symmetric trade costs yields the result that

$$\lambda_{ii} = \frac{(\Omega_i/(A_i L_i))^{\frac{-\epsilon}{\epsilon+1}}}{\Phi_i} = (A_i L_i)^{\frac{\epsilon}{\epsilon+1}} \Phi_i^{-\frac{2\epsilon+1}{\epsilon+1}}$$

Thus, in the case in which $L_i = L \ \forall i$, $var(\ln \lambda_{ii}) = \frac{\epsilon}{\epsilon+1} cov(\ln A_i, \ln \lambda_{ii}) - \frac{1+2\epsilon}{1+\epsilon} cov(\ln \Phi_i, \ln \lambda_{ii})$. Comparing these outcomes for productivity distributions A^c and A^u in the case in which $L_i = L \ \forall i$,

$$\begin{aligned} var(\ln \lambda_{ii}^c) - var(\ln \lambda_{ii}^u) = & \frac{\epsilon}{\epsilon+1}\Big[cov(\ln A_i^c, \ln \lambda_{ii}^c) - cov(\ln A_i^u, \ln \lambda_{ii}^u)\Big] \\ & - \frac{1+2\epsilon}{1+\epsilon}\Big[cov(\ln \Phi_i^c, \ln \lambda_{ii}^c) - cov(\ln \Phi_i^u, \ln \lambda_{ii}^u)\Big]. \end{aligned}$$

A.2 Spatial correlation and the covariance of productivity and gains from trade

This appendix section contains the proof of the four-country case presented in Section 2.2.1 and details the construction and parameterization of the illustrative examples presented in Section 2.2.

A.2.1 Four-country case

The proof of Proposition 1 follows.

A^c is more spatially correlated than A^u

Proof. Recall that Moran's I is given by:

$$I(\ln A, W) = \frac{N}{\sum_i \sum_j \omega_{ij}} \frac{\sum_i \left(\ln A_i - \overline{\ln A}\right) \sum_j \omega_{ij} \left(\ln A_j - \overline{\ln A}\right)}{\sum_i \left(\ln A_i - \overline{\ln A}\right)^2}$$

where ω_{ij} are spatial weights. Define the spatial weight matrix

$$\{\omega_{ij}\} = \begin{bmatrix} \omega_0 & \omega_1 & \omega_2 & \omega_1 \\ \omega_1 & \omega_0 & \omega_1 & \omega_2 \\ \omega_2 & \omega_1 & \omega_0 & \omega_1 \\ \omega_1 & \omega_2 & \omega_1 & \omega_0 \end{bmatrix}$$

Thus, there is a one-to-one mapping between ω_{ij} and τ_{ij}. ω_1 is the spatial weight associated with trade cost d_1; ω_2 is the spatial weight associated with trade cost d_2.

The average log productivity is given by $\overline{\ln A} = \frac{1}{2}\ln \tilde{a}$. For the correlated state, $\ln A^c = (\ln \tilde{a}, \ln \tilde{a}, 0, 0)$, so the demeaned log productivity vector is equal to $\widehat{\ln A^c} = (\frac{1}{2}\ln \tilde{a}, \frac{1}{2}\ln \tilde{a}, -\frac{1}{2}\ln \tilde{a}, -\frac{1}{2}\ln \tilde{a})$. For the uncorrelated state, $\ln A^u = (\ln \tilde{a}, 0, \ln \tilde{a}, 0)$ and $\widehat{\ln A^u} = (\frac{1}{2}\ln \tilde{a}, -\frac{1}{2}\ln \tilde{a}, \frac{1}{2}\ln \tilde{a}, -\frac{1}{2}\ln \tilde{a})$.

$\ln A^c$ is more spatially correlated than $\ln A^u$ if and only if $I(\ln A^c, W) > I(\ln A^u, W) \iff \sum_i \widehat{\ln A_i^c} \sum_j \omega_{ij} \widehat{\ln A_j^c} > \sum_i \widehat{\ln A_i^u} \sum_j \omega_{ij} \widehat{\ln A_j^u}$.

The relevant terms are as follows:

$$\sum_j \omega_{ij}\widehat{\ln A_j^c} = \begin{cases} \frac{1}{2}(\omega_0-\omega_2)\ln\tilde{a} & \text{for } i=1,2 \\ -\frac{1}{2}(\omega_0-\omega_2)\ln\tilde{a} & \text{for } i=3,4 \end{cases}$$

$$\sum_i \widehat{\ln A_i^c}\sum_j \omega_{ij}\widehat{\ln A_j^c} = (\omega_0-\omega_2)(\ln\tilde{a})^2$$

$$\sum_j \omega_{ij}\widehat{\ln A_j^u} = \begin{cases} \frac{1}{2}(\omega_0-2\omega_1+\omega_2)\ln\tilde{a} & \text{for } i=1,3 \\ -\frac{1}{2}(\omega_0-2\omega_1+\omega_2)\ln\tilde{a} & \text{for } i=2,4 \end{cases}$$

$$\sum_i \widehat{\ln A_i^u}\sum_j \omega_{ij}\widehat{\ln A_j^u} = (\omega_0-2\omega_1+\omega_2)(\ln\tilde{a})^2$$

$I(\ln A^c, W) > I(\ln A^u, W) \iff \omega_0-\omega_2 > \omega_0-2\omega_1+\omega_2 \iff \omega_1 > \omega_2.$ □

Equilibrium for the correlated state: $A^c = (\tilde{a}, \tilde{a}, 1, 1)$

By symmetry, the equilibrium incomes and market access of countries 1 and 2 are identical, $Y_1 = Y_2$ and $\Phi_1 = \Phi_2$. Similarly, countries 3 and 4 have identical outcomes: $Y_3 = Y_4$ and $\Phi_3 = \Phi_4$. As a result, the equilibrium incomes that solve $Y_i = \sum_{j=1}^N \lambda_{ij}Y_j$ can without loss of generality be characterized by the scalar $x \equiv Y_1/Y_4$, the relative income levels.

$$Y_1 = \lambda_{11}Y_1 + \lambda_{12}Y_2 + \lambda_{13}Y_3 + \lambda_{14}Y_4 \Rightarrow x = \frac{\lambda_{13}+\lambda_{14}}{1-\lambda_{11}-\lambda_{12}}$$

Equilibrium expenditure shares can be expressed as $\lambda_{ij} = A_i^\epsilon Y_i^{-\epsilon}\tau_{ij}^{-\epsilon}/\Phi_j$. Thus $\lambda_{ij}A_i^{-\epsilon}Y_i^\epsilon = \tau_{ij}^{-\epsilon}/\Phi_j$ and

$$x = \frac{\tau_{13}^{-\epsilon}/\Phi_3 + \tau_{14}^{-\epsilon}/\Phi_4}{\tilde{a}^{-\epsilon}Y_1^\epsilon - \tau_{11}^{-\epsilon}/\Phi_1 - \tau_{12}^{-\epsilon}/\Phi_2}.$$

Using the facts that $\Phi_1 = \Phi_2 = Y_1^{-\epsilon}\tilde{a}^\epsilon(1+d_1^{-\epsilon}) + Y_3^{-\epsilon}(d_2^{-\epsilon}+d_1^{-\epsilon})$ and $\Phi_3 = \Phi_4 = Y_1^{-\epsilon}\tilde{a}^\epsilon(d_2^{-\epsilon}+d_1^{-\epsilon}) + Y_3^{-\epsilon}(1+d_1^{-\epsilon})$, it can be shown that the equilibrium value of x is the solution to the equation

$$x^{2\epsilon+1} + \underbrace{\frac{d_2^{-\epsilon}+d_1^{-\epsilon}}{1+d_1^{-\epsilon}}}_{\equiv r^c}\tilde{a}^\epsilon\left(x^{\epsilon+1}-x^\epsilon\right) - \tilde{a}^{2\epsilon} = 0. \tag{A.1}$$

Equilibrium for the uncorrelated state: $A^u = (\tilde{a}, 1, \tilde{a}, 1)$

Analogous to the correlated state, this case can be solved by exploiting the facts that countries 1 and 3 have identical outcomes, $Y_1 = Y_3$ and $\Phi_1 = \Phi_3$, and countries 2 and 4 have identical outcomes: $Y_2 = Y_4$ and $\Phi_2 = \Phi_4$. The equation that characterizes equilibrium relative income x is

$$x^{2\epsilon+1} + \underbrace{\frac{d_1^{-\epsilon}+d_1^{-\epsilon}}{1+d_2^{-\epsilon}}}_{\equiv r^u}\tilde{a}^\epsilon\left(x^{\epsilon+1}-x^\epsilon\right) - \tilde{a}^{2\epsilon} = 0. \tag{A.2}$$

Note that $0 < r^c < r^u < 1$ since $d_1^2 > d_2 > d_1 > 0$.

Comparing equilibria

Equations (A.1) and (A.2) show that relative income in each equilibrium is given by the zeros of the following generalized polynomial

$$R(x;r) = x^{2\epsilon+1} + r\tilde{a}^{\epsilon}\left(x^{\epsilon+1} - x^{\epsilon}\right) - \tilde{a}^{2\epsilon}$$

when $r > 0$ is evaluated at r^c and r^u, respectively. By Descartes' rule of signs, $R(x;r)$ has exactly one real positive zero (for a given value of r) (Jameson, 2006).[31] Denote this zero of $R(x;r)$ by $x^*(r)$.

We prove that $x^*(r)$ is decreasing by contradiction. Let $r_1 < r_2$ and denote by x_1^* and x_2^* their respective unique positive zeros. Suppose that $x_1^* < x_2^*$. Consider the function $F(x) = R(x;r_2) - R(x;r_1) = (r_2 - r_1)\tilde{a}^{\epsilon}x^{\epsilon}(x-1)$. It is evident that $F(0) = F(1) = 0$, $F(x) < 0\ \forall x \in (0,1)$, and $F(x) > 0\ \forall x > 1$. When evaluated at x_1^*, $F(x_1^*) = R(x_1^*;r_2) - R(x_1^*;r_1) = R(x_1^*;r_2)$, since x_1^* is a zero of $R(x;r_1)$.

Note that $R(x;r)$ is continuous in x and that $R(0;r) < 0$. Therefore, $R(x;r_2) < 0\ \forall x \in (0,x_2^*)$. Since $x_1^* \in (0,x_2^*)$ by assumption, $F(x_1^*) = R(x_1^*;r_2) < 0$. Since $F(x) > 0\ \forall x > 1$, we conclude that $x_1^* \in (0,1)$. We also know that $\forall x > x_1^*, R(x;r_1) > 0$ since $R(x_1^*;r_1) = 0$ and $\lim_{x\to+\infty} R(x;r_1) = +\infty$. Together, these results imply that $R(1;r_1) > 0$. Yet, $R(1;r_1) = 1 - \tilde{a}^{2\epsilon} < 0$ as $\tilde{a} > 1$. Thus, we have a contradiction. We conclude that $r_1 < r_2 \Rightarrow x_1^* > x_2^*$.

Denote the equilibrium relative incomes by x_c and x_u. Since $r^u > r^c$, $x_u < x_c$. The ratio of equilibrium incomes is greater in the correlated case. Since the countries are of equal size, the ratio of equilibrium incomes x is also the more productive economy's "double-factoral terms of trade". Thus, the more productive economies' double-factoral terms of trade are greater in the correlated case.

$cov(\ln A_i, \ln \lambda_{ii})$ is lower in the spatially correlated case

Proof. Equilibrium domestic shares of expenditure can be expressed as $\lambda_{ii} = A_i^{\epsilon}Y_i^{-\epsilon}/\Phi_i$. For the correlated state A^c, $\Phi_1 = \Phi_2 = Y_1^{-\epsilon}\tilde{a}^{\epsilon}(1 + d_1^{-\epsilon}) + Y_3^{-\epsilon}(d_2^{-\epsilon} + d_1^{-\epsilon})$ and $\Phi_3 = \Phi_4 = Y_1^{-\epsilon}\tilde{a}^{\epsilon}(d_2^{-\epsilon} + d_1^{-\epsilon}) + Y_3^{-\epsilon}(1 + d_1^{-\epsilon})$, so

$$\lambda_{11}^c = \lambda_{22}^c = A_1^{\epsilon}Y_1^{-\epsilon}/\Phi_1 = \frac{1}{1 + d_1^{-\epsilon} + \tilde{a}^{-\epsilon}x_c^{\epsilon}(d_2^{-\epsilon} + d_1^{-\epsilon})} = \frac{1}{(1 + d_1^{-\epsilon})(1 + \tilde{a}^{-\epsilon}x_c^{\epsilon}r^c)}$$
$$\lambda_{33}^c = \lambda_{44}^c = A_3^{\epsilon}Y_3^{-\epsilon}/\Phi_3 = \frac{1}{1 + d_1^{-\epsilon} + \tilde{a}^{\epsilon}x_c^{-\epsilon}(d_2^{-\epsilon} + d_1^{-\epsilon})} = \frac{1}{(1 + d_1^{-\epsilon})(1 + \tilde{a}^{\epsilon}x_c^{-\epsilon}r^c)}$$

For the uncorrelated state A^u, $\Phi_1 = \Phi_3 = Y_1^{-\epsilon}\tilde{a}^{\epsilon}(1 + d_2^{-\epsilon}) + 2Y_2^{-\epsilon}d_1^{-\epsilon}$ and $\Phi_2 = \Phi_4 = Y_2^{-\epsilon}(1 +$

[31] It also has either 0 or 2 negative zeros that are obviously not of interest.

$d_2^{-\epsilon}) + 2Y_1^{-\epsilon}\tilde{a}^{\epsilon}d_1^{-\epsilon}$, so

$$\lambda_{11}^u = \lambda_{33}^u = A_1^{\epsilon}Y_1^{-\epsilon}/\Phi_1 = \frac{1}{1 + d_2^{-\epsilon} + 2\tilde{a}^{-\epsilon}x_u^{\epsilon}d_1^{-\epsilon}} = \frac{1}{(1 + d_2^{-\epsilon})(1 + \tilde{a}^{-\epsilon}x_u^{\epsilon}r^u)}$$
$$\lambda_{22}^u = \lambda_{44}^u = A_2^{\epsilon}Y_2^{-\epsilon}/\Phi_2 = \frac{1}{1 + d_2^{-\epsilon} + 2\tilde{a}^{\epsilon}x_u^{-\epsilon}d_1^{-\epsilon}} = \frac{1}{(1 + d_2^{-\epsilon})(1 + \tilde{a}^{\epsilon}x_u^{-\epsilon}r^u)}$$

Thus, we obtain the following demeaned values of the log domestic shares of expenditure

$$\begin{aligned}\widehat{\ln \lambda_{11}} &= -\tfrac{1}{2}\left[\ln\left(1 + x^{\epsilon}\tilde{a}^{-\epsilon}r\right) - \ln\left(1 + \tilde{a}^{\epsilon}x^{-\epsilon}r\right)\right] \\ \widehat{\ln \lambda_{44}} &= -\widehat{\ln \lambda_{11}}\end{aligned}$$

when evaluated at (r^c, x_c) and (r^u, x_u) for the two respective equilibria.

The covariance of productivity and the domestic share of expenditure is therefore

$$cov(\ln A_i, \ln \lambda_{ii}) = \frac{-1}{4}\ln \tilde{a}\left[\ln\left(1 + x^{\epsilon}\tilde{a}^{-\epsilon}r\right) - \ln\left(1 + \tilde{a}^{\epsilon}x^{-\epsilon}r\right)\right]$$

Recall that ϵ and $\tilde{a}$ are fixed parameters while x is a function of r. This covariance is positive because $\tilde{a} > x$.[32]

It can be shown that $cov(\ln A_i, \ln \lambda_{ii})$ is increasing in r.

$$\frac{\mathrm{d}cov(\ln A_i, \ln \lambda_{ii})}{\mathrm{d}r} \propto -\frac{\mathrm{d}\ln\left(\frac{1+x^{\epsilon}\tilde{a}^{-\epsilon}r}{1+\tilde{a}^{\epsilon}x^{-\epsilon}r}\right)}{\mathrm{d}r} \propto \underbrace{\left(\frac{\tilde{a}}{x}\right)^{\epsilon} - \left(\frac{x}{\tilde{a}}\right)^{\epsilon}}_{>0} - \underbrace{\frac{r\epsilon}{x}\left[2 + x^{\epsilon}\tilde{a}^{-\epsilon} + x^{-\epsilon}\tilde{a}^{\epsilon}\right]}_{>0}\underbrace{\frac{\mathrm{d}x}{\mathrm{d}r}}_{<0} > 0$$

Since $r^u > r^c$, the covariance of productivity and the domestic share of expenditure is lower for A^c than A^u. Thus, the covariance of productivity and the equilibrium gains from trade, $cov(\ln A_i, \frac{-1}{\epsilon}\ln \lambda_{ii})$, is greater for A^c than A^u.

□

$var(\ln(C_i/L))$ is greater in the spatially correlated case

Proof. In both equilibria,

$$var(\ln \lambda_{ii}) = \frac{2}{4}\left(\widehat{\ln \lambda_{11}}\right)^2 + \frac{2}{4}\left(\widehat{\ln \lambda_{44}}\right)^2 = \left(\widehat{\ln \lambda_{11}}\right)^2 = \frac{4\epsilon^2}{(\ln \tilde{a})^2}\left(cov(\ln A_i, -\frac{1}{\epsilon}\ln \lambda_{ii})\right)^2.$$

Therefore

$$\begin{aligned}var(\ln(C_i/L)) &= var(A_i) + 2cov(\ln A_i, \frac{-1}{\epsilon}\ln \lambda_{ii}) + \frac{1}{\epsilon^2}var(\ln \lambda_{ii}) \\ &= var(A_i) + 2cov(\ln A_i, \frac{-1}{\epsilon}\ln \lambda_{ii}) + \frac{4}{(\ln \tilde{a})^2}\left(cov(\ln A_i, -\frac{1}{\epsilon}\ln \lambda_{ii})\right)^2\end{aligned}$$

[32] $\tilde{a} > x$ because x is the largest positive zero of $R(x; r)$, $R(x'; r) < 0\ \forall x' \in (0, x)$, and $R(\tilde{a}; r) = (1+r)(\tilde{a}-1)\tilde{a}^{2\epsilon} > 0$.

This is increasing in $cov(\ln A_i, \frac{-1}{\epsilon}\ln\lambda_{ii})$ if and only if

$$2+\frac{8}{(\ln\tilde{a})^2}cov(\ln A_i, -\frac{1}{\epsilon}\ln\lambda_{ii})>0 \iff \ln\tilde{a}>\frac{1}{\epsilon}\ln\left(\frac{1+\tilde{a}^{\epsilon}x^{-\epsilon}r}{1+x^{\epsilon}\tilde{a}^{-\epsilon}r}\right)$$

This inequality is true. The triangle inequality for trade costs, $d_2 < d_1^2$, implies that $r^u < 1$. If $r<1$ and $\epsilon \geq 1$, then $R(\sqrt{\tilde{a}};r)\leq 0$.[33] Thus, $x^*(r)\geq\sqrt{\tilde{a}}\ \forall r\in(0,1)$. That implies the following inequality:

$$\frac{1+\tilde{a}^{\epsilon}x^{-\epsilon}r}{1+x^{\epsilon}\tilde{a}^{-\epsilon}r}\leq\frac{\tilde{a}^{\epsilon}x^{-\epsilon}(1+r)}{x^{\epsilon}\tilde{a}^{-\epsilon}(1+r)}=\left(\frac{\tilde{a}}{x}\right)^{2\epsilon}\leq\left(\frac{\tilde{a}}{\sqrt{\tilde{a}}}\right)^{2\epsilon}=\tilde{a}^{\epsilon}$$

Thus, $var(\ln(C_i/L))$ is increasing in $cov(\ln A_i, \frac{-1}{\epsilon}\ln\lambda_{ii})$.

□

$\mathbb{E}(\ln(C_i/L))$ is lower in the spatially correlated case

Proof. By equation (2), the difference in average welfare between the uncorrelated and correlated states is

$$\mathbb{E}(\ln(C_i^u/L))-\mathbb{E}(\ln(C_i^c/L))=-\frac{1}{4\epsilon}\sum_{i=1}^{4}[\ln\lambda_{ii}^u-\ln\lambda_{ii}^c]=\frac{1}{4\epsilon}\ln\left(\prod_{i=1}^{4}\frac{\lambda_{ii}^c}{\lambda_{ii}^u}\right).$$

Due to the symmetry of the problem, $\lambda_{11}^c=\lambda_{22}^c$, $\lambda_{33}^c=\lambda_{44}^c$, $\lambda_{11}^u=\lambda_{33}^u$ and $\lambda_{22}^u=\lambda_{44}^u$. Consequently,

$$\mathbb{E}(\ln(C_i^u/L))-\mathbb{E}(\ln(C_i^c/L))=\frac{1}{2\epsilon}\ln\left(\frac{\lambda_{11}^c\lambda_{44}^c}{\lambda_{11}^u\lambda_{44}^u}\right)$$

The following results were obtained in proving that $cov(\ln A_i, \ln\lambda_{ii})$ is lower in the spatially correlated case:

$$\frac{\lambda_{11}^c}{\lambda_{11}^u}=\frac{1+d_2^{-\epsilon}}{1+d_1^{-\epsilon}}\frac{1+\left(\frac{x_u}{\tilde{a}}\right)^{\epsilon}r^u}{1+\left(\frac{x_c}{\tilde{a}}\right)^{\epsilon}r^c}\qquad\frac{\lambda_{44}^c}{\lambda_{44}^u}=\frac{1+d_2^{-\epsilon}}{1+d_1^{-\epsilon}}\frac{1+\left(\frac{x_u}{\tilde{a}}\right)^{-\epsilon}r^u}{1+\left(\frac{x_c}{\tilde{a}}\right)^{-\epsilon}r^c}$$

Recall that $r^c=\frac{d_1^{-\epsilon}+d_2^{-\epsilon}}{1+d_1^{-\epsilon}}$ and $r^u=\frac{d_1^{-\epsilon}+d_1^{-\epsilon}}{1+d_2^{-\epsilon}}$. It follows that $\frac{1+r^c}{1+r^u}=\frac{1+d_2^{-\epsilon}}{1+d_1^{-\epsilon}}$ and therefore

$$\frac{\lambda_{11}^c}{\lambda_{11}^u}=\frac{1+r^c}{1+r^u}\frac{1+\left(\frac{x_u}{\tilde{a}}\right)^{\epsilon}r^u}{1+\left(\frac{x_c}{\tilde{a}}\right)^{\epsilon}r^c}\qquad\frac{\lambda_{44}^c}{\lambda_{44}^u}=\frac{1+r^c}{1+r^u}\frac{1+\left(\frac{x_u}{\tilde{a}}\right)^{-\epsilon}r^u}{1+\left(\frac{x_c}{\tilde{a}}\right)^{-\epsilon}r^c}$$

[33]

$$\begin{aligned}R(\sqrt{\tilde{a}};r)&=\tilde{a}^{\frac{2\epsilon+1}{2}}+r\tilde{a}^{\epsilon}(\tilde{a}^{\frac{\epsilon+1}{2}}-\tilde{a}^{\frac{\epsilon}{2}})-\tilde{a}^{2\epsilon}=\tilde{a}^{\epsilon}\left(\tilde{a}^{\frac{1}{2}}+r\tilde{a}^{\frac{\epsilon}{2}}(\tilde{a}^{\frac{1}{2}}-1)-\tilde{a}^{\epsilon}\right)\\&\leq\tilde{a}^{\epsilon}\left(\tilde{a}^{\frac{1}{2}}+\tilde{a}^{\frac{\epsilon}{2}}(\tilde{a}^{\frac{1}{2}}-1)-\tilde{a}^{\epsilon}\right)=-\tilde{a}^{\epsilon}\left(\tilde{a}^{\frac{\epsilon}{2}}-\tilde{a}^{\frac{1}{2}}\right)\left(1+\tilde{a}^{\frac{\epsilon}{2}}\right)\leq 0\end{aligned}$$

Combining the above expressions yields

$$\frac{\lambda_{11}^c \lambda_{44}^c}{\lambda_{11}^u \lambda_{44}^u} = \left(\frac{1+r^c}{1+r^u}\right)^2 \frac{1 + r^u V\left(\left(\frac{x_u}{\tilde{a}}\right)^\epsilon\right) + (r^u)^2}{1 + r^c V\left(\left(\frac{x_c}{\tilde{a}}\right)^\epsilon\right) + (r^c)^2}$$

where $V(\cdot)$ denotes the function $V(x) = x + x^{-1}$, which for $x \in (0,1)$ is greater than 2 and decreasing. From proofs above, we know that $1 > r^u > r^c > 0$ and $\tilde{a} > x_c > x_u > 1$. Therefore $1 > (x_c/\tilde{a})^\epsilon > (x_u/\tilde{a})^\epsilon > 0$ and $V\left((x_u/\tilde{a})^\epsilon\right) > V\left((x_c/\tilde{a})^\epsilon\right) > 2$. Now consider the ratio

$$Q(r) = \frac{1 + rV\left(\left(\frac{x^*(r)}{\tilde{a}}\right)^\epsilon\right) + r^2}{(1+r)^2} = 1 + \frac{r}{1+r}\left(V\left(\left(\frac{x^*(r)}{\tilde{a}}\right)^\epsilon\right) - 2\right).$$

Since $r^u > r^c > 0$, we have $\frac{r^u}{1+r^u} > \frac{r^c}{1+r^c}$. Combining this result with the fact that $V\left(\left(\frac{x_u}{\tilde{a}}\right)^\epsilon\right) - 2 > V\left(\left(\frac{x_c}{\tilde{a}}\right)^\epsilon\right) - 2 > 0$ leads to $Q(r^u) > Q(r^c)$. As a consequence:

$$\frac{\lambda_{11}^c \lambda_{44}^c}{\lambda_{11}^u \lambda_{44}^u} = \frac{Q(r^u)}{Q(r^c)} > 1 \Rightarrow \ln\left(\frac{\lambda_{11}^c \lambda_{44}^c}{\lambda_{11}^u \lambda_{44}^u}\right) > 0 \Rightarrow \mathbb{E}(\ln(C_i^u/L)) > \mathbb{E}(\ln(C_i^c/L))$$

□

A.2.2 Circular geography

Figures 4 and 5 present an illustrative example in which we parameterize A_i and τ_{ij} on a circular geography. As stated in the main text, $N = 50$, $\epsilon = 1$, and $L_i = 1$ $\forall i$. Countries have locations given by $l_i = \frac{\pi}{N}(2i - 1 - N)$ for $i = 1, \ldots, N$. Productivity $\ln A_i$ has a mean value of 10 and follows a sine wave with amplitude 1 and frequency θ.[34] Bilateral trade costs are given by $\ln \tau_{ij} = .8 \ln(1 + \|l_i - l_j\|)$, where $\|l_i - l_j\|$ is the distance between locations i and j on the circle.

Figures 4 and 5 depict demeaned distributions. Table A.1 reports the means and variances of countries' welfare per capita under autarky and trade.

Table A.1: Outcomes for one-sector sine-wave economy

Frequency of $\ln A$ sine wave (θ)	1	2	3	4
Autarky welfare ($\ln A$) mean	10	10	10	10
Autarky welfare ($\ln A$) variance	0.510204	0.510204	0.510204	0.510204
Trading-equilbrium welfare ($\ln C/L$) mean	12.2654	12.2769	12.2807	12.2836
Trading-equilbrium welfare ($\ln C/L$) variance	0.298203	0.226274	0.203006	0.184882

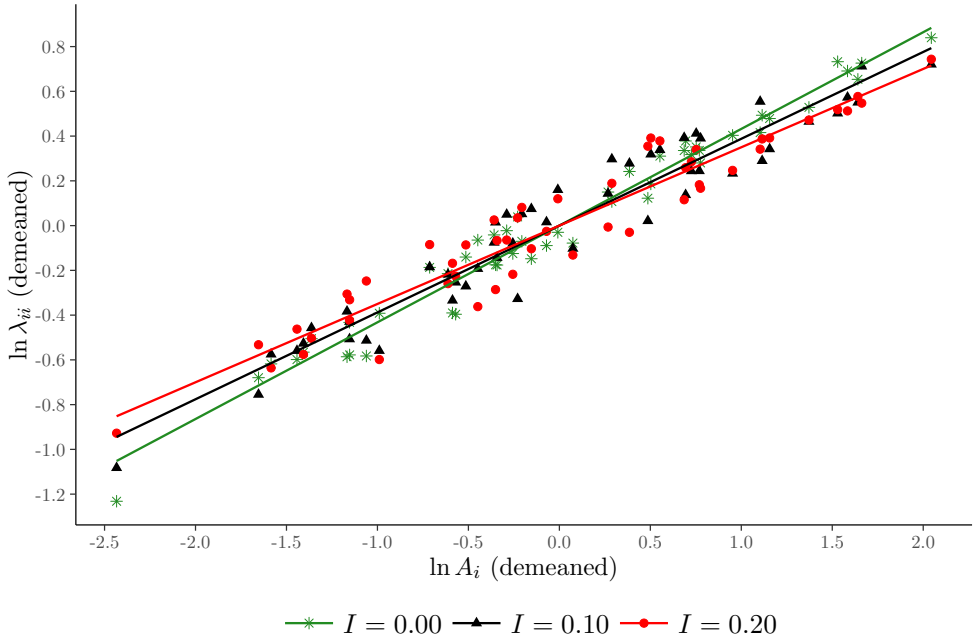
Figure 6 introduces heterogeneous sizes to the parameterization used in Figures 4 and 5. Size $\ln L_i$ is the sum of a sine wave with mean value 10, amplitude 1, and frequency $\theta_L = 1$ and Gaussian

[34] The standard deviation of a sine wave is proportional to its amplitude and independent of its frequency. This is true for both the function and our N-point discretization.

noise $\sim \mathcal{N}(0,1)$.

Figure A.1 depicts the expenditure-productivity relationship in a circular geography with equal-sized countries for three selected productivity vectors. These otherwise arbitrary productivity distributions differ only in their spatial correlation. They were generated by shuffling a vector $\ln A_0$ that was drawn from $\mathcal{N}(0,1)$.

Figure A.1: Circular geography with equal-sized countries and arbitrary productivities



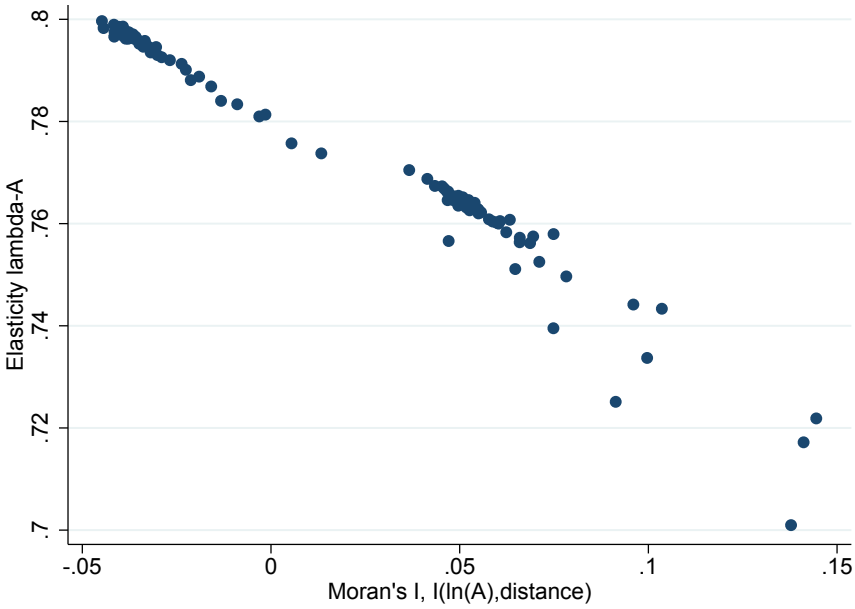
NOTES: This figure depicts the λ_{ii}-A_i relationship in an economy with a circular geography for three randomly generated productivity distributions. Geography, equal-sized locations, and trade costs are the same as in Figure 4.

A.2.3 Randomly generated geography

In Figure A.2, we examine how the relationship between productivity and domestic share of expenditure depends on the spatial correlation of productivity in a randomly generated geography. We draw $N = 50$ locations' coordinates on a plane $l_j \in \mathbb{R}^2$ from a standard normal distribution. We generate bilateral, distance-related trade costs using $\ln \tau_{ij} = \tau \ln(1 + d_{ij})$, where distance $d_{ij} = \|l_i - l_j\|$ is the Euclidean norm on $\mathbb{R}^2$ and τ is a positive scaling factor. Countries are of equal size, $L_j = 1\ \forall j$. The trade elasticity $\epsilon = 4$.

To construct M productivity distributions that have identical first and second moments and different spatial covariances, we employ a procedure that makes use of the eigenvectors of a transformation of the spatial weight matrix. Let I denote the identity matrix and consider $J = ee^\intercal$, where e is the constant vector of ones. The object of interest is the matrix $\Pi = CWC$ where C corresponds to the centering matrix: $C = I - \frac{1}{N}J$ and W is our spatial weight matrix. It can be shown

Figure A.2: Random-geography economy



NOTES: This figure depicts how $cov(\ln \lambda_{ii}, \ln A_i)$ varies with the spatial correlation of productivity, as measured by Moran's I, over a randomly generated geography. We vary the spatial distribution of productivity while holding the first and second moments fixed. The elasticity of λ_{ii} with respect to A_i is $\hat{\beta}_t$ estimated from $\ln \lambda_{iit} = \beta_t \ln A_{it} + \pi_i^I + \pi_t^T + \epsilon_{it}$, as described in the text. See Appendix A.2.3 for parameterization details.

that the upper and lower bounds of Moran's I are given by: $\lambda_{max} \frac{N}{W_0}$ and $\lambda_{min} \frac{N}{W_0}$ where λ_{max} and λ_{min} denote the largest and the smallest eigenvalues of Π respectively and $W_0 = \sum_{i=1}^N \sum_{j=1}^N W_{ij}$. More generally, Moran's I will be equal to $\lambda_i \frac{N}{W_0}$ when evaluated at the ith eigenvector. It can also be shown that the non-constant eigenvectors of Π are centered and have identical second moments.

With these eigenvectors in hand, we apply a translation $T_c : v \to v + c$ with $c \in \mathbb{R}_+^2$ to the non-constant eigenvectors of Π. We employ linear combinations of the strictly positive vectors produced by this transformation to produce a set of M productivity distributions denoted $(A_1, \ldots, A_M)$. By construction, these productivity distributions have identical first and second moments but vary in their spatial covariance as measured by Moran's I.

A.3 Multiple-sector case

This appendix section provides details of the multi-sector economic environment summarized in Section 2.3.

Preferences. Individuals in country i have preferences that are Cobb-Douglas over sectors $s = 1, \ldots, S$ and constant elasticity of substitution (CES) within sectors. Thus, the relevant price

indices are

$$P_i = \prod_{s=1}^{S} P_{is}^{\alpha_{is}} \text{ and } P_{is} = \left(\int_{\omega_s} p_i(\omega_s)^{1-\sigma_s} d\omega_s \right)^{1/(1-\sigma_s)},$$

where $\alpha_{is} \geq 0$ are expenditure shares ($\sum_{s=1}^{S} \alpha_{is} = 1$) and σ_s are sectoral elasticities of substitution across varieties.

Production. Productivity in country j in sector s is A_{is}.

Trade costs. Selling one unit to j from i in sector s requires producing $\tau_{ijs} \geq 1$ units, with $\tau_{iis} = 1$.

Gravity equation. Denote sales from i to j in sector s by X_{ijs} and j's total expenditure by $X_j \equiv \sum_{i=1}^{N} \sum_{s=1}^{S} X_{ijs}$. Across sectors, Cobb-Douglas preferences cause optimizing consumers to spend α_{js} of their total expenditure in sector s, $X_{js} = \alpha_{js} X_j$. Within each sector, CES preferences result in the share of expenditure by j on goods from i in sector s taking the form of a gravity equation:

$$\lambda_{ijs} = \frac{X_{ijs}}{X_{js}} = \frac{\chi_{is} \left(\tau_{ijs} w_i\right)^{-\epsilon_s}}{\sum_{l=1}^{N} \chi_{ls} \left(\tau_{ljs} w_l\right)^{-\epsilon_s}} = \frac{\chi_{is} \left(\tau_{ijs} w_i\right)^{-\epsilon_s}}{\Phi_{js}}.$$

Equilibrium. In a competitive equilibrium, labor-market clearing, goods-market clearing, and budget constraints are satisfied such that total income $Y_i = w_i L_i$ and sectoral income $Y_{is} = w_i L_{is}$ satisfy $Y_{is} = \sum_{j=1}^{N} X_{ijs}$, $Y_i = \sum_{s=1}^{S} Y_{is}$, and $X_{is} = \alpha_{is} Y_i$ for all countries. The equilibrium system of equations is

$$Y_{is} = \sum_{j=1}^{N} \lambda_{ijs} \alpha_{js} \sum_{s'=1}^{S} Y_{js'}.$$

In this environment, real consumption per capita is

$$\ln\left(\frac{C_i}{L_i}\right) = \sum_{s=1}^{S} \alpha_{is} \left(\ln A_{is} + \gamma_s - \frac{1}{\epsilon_s} \ln \lambda_{iis} \right).$$

The first two terms, $\sum_{s=1}^{S} \alpha_{is} \left(\ln A_{is} + \gamma_s\right)$, are per capita welfare in autarky, and the final term, $-\sum_{s=1}^{S} \frac{\alpha_{is}}{\epsilon_s} \ln \lambda_{iis}$, summarizes the gains from trade.

Dispersion in per capita welfare across countries thus depends on the exogenous variation in productivities A_{is} and the endogenous variation in domestic shares of expenditure λ_{iis}. For the sake of expositional brevity, assume that expenditures shares are common across countries, $\alpha_{is} = \alpha_s \ \forall i$ In that case, the variance of per capita welfare is

$$var\left(\ln\left(\frac{C_i}{L_i}\right)\right) = var\left(\sum_{s=1}^{S} \alpha_{is} \ln A_{is}\right) + var\left(\sum_{s=1}^{S} \frac{\alpha_{is}}{\epsilon_s} \ln \lambda_{iis}\right) - 2 \sum_{s=1}^{S} \sum_{s'=1}^{S} \frac{\alpha_s \alpha_{s'}}{\epsilon_{s'}} cov\left(\ln A_{is}, \ln \lambda_{iis'}\right)$$

To examine the role of spatial correlation, consider two productivity distributions – a correlated state c and an uncorrelated state u. Assume that unconditional variance of the productivity distributions is the same, $var\left(\sum_{s=1}^{S} \alpha_{is} \ln A_{is}^c\right) = var\left(\sum_{s=1}^{S} \alpha_{is} \ln A_{is}^u\right)$. The difference in welfare dispersion then depends on the covariance of productivities and domestic shares of expenditure,

both within and across sectors, and between domestic shares of expenditure.

$$var\left(\ln\left(C_i^c L_i\right)\right) - var\left(\ln\left(C_i^u / L_i\right)\right) = 2\sum_{s=1}^{S}\sum_{s'=1}^{S}\frac{\alpha_s\alpha_{s'}}{\epsilon_{s'}}\left\{cov\left(\ln A_{is}^u, \ln\lambda_{iis'}^u\right) - cov\left(\ln A_{is}^c, \ln\lambda_{iis'}^c\right)\right\}$$
$$-\sum_{s=1}^{S}\sum_{s'=1}^{S}\frac{\alpha_s\alpha_{s'}}{\epsilon_s\epsilon_{s'}}\left\{cov\left(\ln\lambda_{iis}^u, \ln\lambda_{iis'}^u\right) - cov\left(\ln\lambda_{iis}^c, \ln\lambda_{iis'}^c\right)\right\} \tag{A.3}$$

Just as in the single-sector case, for typical values of the sectoral trade elasticities, $2\frac{\alpha_s\alpha_{s'}}{\epsilon_{s'}}$ is an order of magnitude larger than $\frac{\alpha_s\alpha_{s'}}{\epsilon_s\epsilon_{s'}}$. Thus, the difference in welfare dispersion is governed by the $cov\left(\ln A_{is}, \ln\lambda_{iis'}\right)$ terms, provided that the block of $cov\left(\ln A_{is}, \ln\lambda_{iis'}\right)$ terms is the same order of magnitude as the block of $cov\left(\ln\lambda_{iis}, \ln\lambda_{iis'}\right)$ terms.

Under what circumstances is studying differences in $cov\left(\ln A_{is}, \ln\lambda_{iis}\right)$ in one sector alone informative about welfare dispersion? For simplicity, consider the two-sector case and three possible relationships between the two sectors: perfectly correlated productivities, perfectly anti-correlated productivities, and orthogonal productivities.

In the perfectly correlated case, there is little scope for adjustment across sectors, and thus outcomes are similar to those obtained in the one-sector environment. In fact, if all sectors have perfectly correlated productivities ($A_{is} \propto A_i\ \forall s$), perfectly correlated spatial linkages ($\tau_{ijs} \propto \tau_{ij}\ \forall s$), and equal trade elasticities ($\epsilon_s = \epsilon\ \forall s$), then expenditure shares are equal across sectors, $\lambda_{ijs} = \lambda_{ij}$, and the difference in welfare dispersion in equation (A.3) is exactly proportionate to the single-sector expression in equation (4).

If sectoral productivities are perfectly anti-correlated, then outcomes in one sector may be exactly offset by outcomes in another, leaving welfare unchanged. That is, it is possible to construct circumstances in which the sum of covariances of productivities and domestic shares of expenditure within sectors is exactly the opposite of the sum of cross-sector covariances. Consider the two-sector case with equal expenditure shares $\alpha_1 = \alpha_2 = \frac{1}{2}\ \forall j$ and equal trade elasticities $\epsilon_1 = \epsilon_2 = \epsilon$. If the two sectors' productivities are perfectly anti-correlated, such that $\ln A_{i1} + \ln A_{i2}$ is a constant, then it can be shown that $\sum_{s=1}^{S}\sum_{s'=1}^{S}\frac{\alpha_s\alpha_{s'}}{\epsilon_{s'}}cov\left(\ln A_{is}, \ln\lambda_{iis'}\right) = 0$. Thus, our predictions about trade flows are valid, but the welfare consequences of these changes are fully offset by the non-agricultural sector's anti-correlated changes.

What about the orthogonal case? Figure 8 depicts a two-sector sine-wave economy with two symmetric sectors that differ only in their sine-wave frequency. Table A.2 reports the means and variances of countries' welfare per capita under autarky and trade. Compared to Table A.1, the variance of autarky welfare is lower because autarky welfare is the simple average of two sectors' (orthogonal) productivities with the same mean and variance. The mean trading-equilibrium welfare is higher (the gains from trade are larger) in the multi-sector case due to gains from specialization according to comparative advantage. This additional margin of adjustment also dampens the de-

Table A.2: Outcomes for two-sector sine-wave economy

Frequency of $\ln A_1$ sine wave (θ_1)	1	2	3	4
Autarky welfare ($\frac{1}{2}\ln A_1 + \frac{1}{2}\ln A_2$) mean	10	10	10	10
Autarky welfare ($\frac{1}{2}\ln A_1 + \frac{1}{2}\ln A_2$) variance	0.255102	0.255102	0.255102	0.255102
Trading-equilbrium welfare ($\ln C/L$) mean	12.3610	12.3699	12.3721	12.3736
Trading-equilbrium welfare ($\ln C/L$) variance	0.114255	0.097649	0.092189	0.087935

gree to which greater spatial correlation of productivity in one of the two sectors affects the variance of welfare in the trading equilibrium, but our main prediction still holds in this multi-sector setting with orthogonal productivities.

A.4 Spatial correlation of comparative advantage

This appendix section addresses how the spatial correlation of comparative advantage interacts with the spatial correlation of absolute advantage.

To consider the role of spatially correlated patterns of comparative advantage, we extend the Eaton and Kortum (2002) model, in which comparative advantage is symmetric across countries, to have "continents" of countries with correlated relative productivities. The world economy consists of N countries partitioned across $k = 1, \ldots, K$ continents. Country i belongs to continent $k(i)$ and its productivity in good ω is $z_i(\omega)$. We depart from Eaton and Kortum (2002) by assuming that the vector of productivities $(Z_1, \ldots, Z_N)$ is drawn from a multivariate nested Fréchet distribution:

$$F(z_1, \ldots, z_n) = \exp\left\{ -\sum_{k=1}^{K} \left(\sum_{i:k(i)=k} (T_i z_i^{-\vartheta})^{\frac{1}{\rho_k}} \right)^{\rho_k} \right\},$$

where the location parameter T_i governs the absolute advantage of country i and the dispersion parameter ϑ is common across countries. Parameters $(\rho_1, \ldots, \rho_k)$ govern the degree of within-continent correlation in productivities, which is decreasing in ρ_k. When $\rho_k = 1\ \forall k$, these productivities are independent, as in Eaton and Kortum (2002).

After considerable algebraic manipulations, it can be shown that the gravity equation for this generalized productivity distribution is

$$\lambda_{ij} = \frac{(T_i (w_i \tau_{ij})^{-\vartheta})^{\frac{1}{\rho_{k(i)}}}}{\sum_{m:k(m)=k(i)} (T_m (w_m \tau_{mj})^{-\vartheta})^{\frac{1}{\rho_{k(i)}}}} \frac{\Phi_{k(i)j}}{\Phi_j},$$

where $\Phi_{kj} = \left(\sum_{i:k(i)=k} (T_i (w_i \tau_{ij})^{-\vartheta})^{\frac{1}{\rho_k}} \right)^{\rho_k}$ and $\Phi_j = \sum_{k=1}^{K} \Phi_{kj}$.

To study the interaction of the spatial correlation of comparative advantage and the spatial correlation of absolute advantage, we simulate a world economy with a symmetric geography and a

Table A.3: Estimates of β_1 and within-continent correlation $1-\rho$

	Within-continent correlation $1-\rho$									
K	0	0.1	0.2	0.3	0.4	0.5	0.6	0.7	0.8	0.9
2	-0.101	-0.100	-0.097	-0.092	-0.083	-0.067	-0.046	-0.021	0.001	0.013
3	-0.101	-0.099	-0.096	-0.090	-0.080	-0.065	-0.045	-0.019	0.004	0.016
4	-0.101	-0.097	-0.092	-0.085	-0.074	-0.058	-0.037	-0.012	0.013	0.027

NOTES: This table reports estimates of β_1 obtained from the regression $\ln \lambda_{iit} = \beta_0 \ln A_{it} + \beta_1 \ln A_{it} I_t + \pi_i^I + \pi_t^T + \mu_{it}$ on equilibrium outcomes from a simulated global economy with 50 countries as described in the text of Appendix A.4. The correlation parameter $\rho_k = \rho \; \forall k$, the dispersion parameter is $\vartheta = 8.28$ (Eaton and Kortum, 2002), and the level parameter $\ln T_i$ follows a sine wave, as in Section 2.2.2, with $\theta = 1, \ldots, 8$. In the standard model, $1 - \rho = 0$.

sine-wave productivity distribution, as in Section 2.2.2. We divide the 50 countries into two, three, or four continents with $\rho_k = \rho \; \forall k$. As we increase within-continent correlation in comparative advantage by lowering ρ from 1.0 to 0.1 in steps of size 0.1, we find that the effect of spatial correlation in absolute advantage is initially dampened and then reversed. As reported in Table A.3, for the highest values of $1-\rho$, the estimated β_1 is positive. That is, for sufficiently high within-continent correlation of comparative advantage, the $cov(\ln \lambda_{ii}, \ln A_i)$ relationship depicted in Figure 5 becomes steeper with greater spatial correlation of A_i, not flatter.

Thus, our empirical estimate of β_1 in equation (7) captures the effect of spatial correlation in absolute advantage as mediated by the existing spatial correlation in comparative advantage. Standard quantitative trade models have symmetric patterns of comparative advantage, in which case β_1 should be negative. If patterns of comparative advantage within cereals are very spatially correlated, β_1 could be positive.

A.5 Mobile labor

In an economic-geography model in which welfare differences are arbitraged away by mobile factors of production (e.g., Allen and Arkolakis 2014), greater spatial correlation of productivity makes population density, rather than welfare per capita, more unequal across locations. We demonstrate this using a symmetric geography with four locations, akin to the first stylized example of Section 2.2.1, in which the population of each location is endogenously determined. Locations' productivities vary exogenously, and their amenities are identical.

Given four locations with trade costs given by equation (5), total population L, and an elasticity of substitution σ, the endogenous populations $\{L_i\}_{i=1}^4$ and welfare level W must satisfy two equations:

$$L_i^{\tilde{\sigma}} = A_i^{\tilde{\sigma}(\sigma-1)} W^{1-\sigma} \sum_{j=1}^{4} \tau_{ji}^{1-\sigma} A_j^{(1-\tilde{\sigma})(\sigma-1)} L_j^{\tilde{\sigma}} \qquad \text{and} \qquad L = \sum_{j=1}^{4} L_j,$$

where $\tilde{\sigma} \equiv \frac{\sigma-1}{2\sigma-1}$. Let $\mathbf{L}$ denote the vector containing $L_1, \ldots, L_4$, let $\mathbf{T}$ denote the (symmetric)

matrix of trade costs raised (element-wise) to the power $\frac{1}{1-\sigma}$, and let $\mathbf{A}$ denote the 4-by-4 diagonal matrix with $\{A_1, \ldots, A_4\}$ on the diagonal.

The equilibrium equation of interest can then be written as

$$\left(\mathbf{I} - \frac{1}{W^{\sigma-1}}\mathbf{A}^{\tilde{\sigma}(\sigma-1)}\mathbf{T}\mathbf{A}^{(1-\tilde{\sigma})(\sigma-1)}\right)\mathbf{L}^{\tilde{\sigma}} = 0.$$

$W^{\sigma-1}$ is the eigenvalue and $\mathbf{L}^{\tilde{\sigma}}$ is the eigenvector of the matrix $\mathbf{A}^{\tilde{\sigma}(\sigma-1)}\mathbf{T}\mathbf{A}^{(1-\tilde{\sigma})(\sigma-1)}$.

Let $\mathbf{A}_c$ and $\mathbf{A}_u$ denote diagonal matrices whose diagonal elements are $(\tilde{a}, \tilde{a}, 1, 1)$ and $(\tilde{a}, 1, \tilde{a}, 1)$, respectively, with $\tilde{a} > 1$. Also, let $\bar{a} \equiv \tilde{a}^{\sigma-1} > 1$, $\bar{d}_1 \equiv d_1^{1-\sigma}$, and $\bar{d}_2 \equiv d_2^{1-\sigma}$.

Consider the eigenvalue $\lambda_c = W_c^{\sigma-1}$ and eigenvector $\mathbf{L}_c^{\tilde{\sigma}}$ associated with $\mathbf{A}_c^{\tilde{\sigma}(\sigma-1)}\mathbf{T}\mathbf{A}_c^{(1-\tilde{\sigma})(\sigma-1)}$. We can verify that the eigenvector $\mathbf{L}_c^{\tilde{\sigma}} = (x_c, x_c, 1, 1)$ and the eigenvalue $\lambda_c = \bar{a}^{1-\tilde{\sigma}}(d_1^{1-\sigma} + d_2^{1-\sigma})x_c + d_1^{1-\sigma} + 1$ satisfy the equation of interest. This implies that the equilibrium value of x_c is given by

$$\bar{a}^{1-\tilde{\sigma}}(\bar{d}_1 + \bar{d}_2)x_1^2 - (\bar{a} - \bar{d}_1 - 1 + \bar{a}\bar{d}_1)x_1 - (\bar{d}_1 + \bar{d}_2)\bar{a}^{\tilde{\sigma}} = 0. \tag{A.4}$$

Similarly, in the case of $\mathbf{A}_u$, consider the eigenvalue $\lambda_u = W_u^{\sigma-1}$ and the eigenvector $\mathbf{L}_u^{\tilde{\sigma}}$ associated with $\mathbf{A}_u^{\tilde{\sigma}(\sigma-1)}\mathbf{T}\mathbf{A}_u^{(1-\tilde{\sigma})(\sigma-1)}$. We can verify that the eigenvector $\mathbf{L}_u^{\tilde{\sigma}} = (x_u, 1, x_u, 1)$ and the eigenvalue $\lambda_u = 2\bar{a}^{1-\tilde{\sigma}}\bar{d}_1 x_2 + \bar{d}_2 + 1$ satisfy the equation of interest. This implies that the equilibrium value of x_u is given by

$$2\bar{a}^{1-\tilde{\sigma}}\bar{d}_1 x_u^2 - (\bar{a} - \bar{d}_2 - 1 + \bar{a}\bar{d}_2)x_u - 2\bar{a}^{\tilde{\sigma}}\bar{d}_1 = 0. \tag{A.5}$$

The quadratic equations (A.4) and (A.5) each have one positive and one negative root. Restricting attention to the positive roots, we can compare the relative sizes of x_c and x_u. It can be shown that $x_c > x_u$.

The equilibrium values of $\mathbf{L}_c$ and $\mathbf{L}_c$ are

$$\mathbf{L}_c = \frac{L}{2x_c^{\frac{1}{\tilde{\sigma}}} + 2}\begin{bmatrix} x_c^{\frac{1}{\tilde{\sigma}}} \\ x_c^{\frac{1}{\tilde{\sigma}}} \\ 1 \\ 1 \end{bmatrix} \quad \text{and} \quad \mathbf{L}_u = \frac{L}{2x_u^{\frac{1}{\tilde{\sigma}}} + 2}\begin{bmatrix} x_u^{\frac{1}{\tilde{\sigma}}} \\ 1 \\ x_u^{\frac{1}{\tilde{\sigma}}} \\ 1 \end{bmatrix}.$$

It can then be shown that $cov(\ln A_i, \ln L_i)$ is greater for $\mathbf{A}_c$ than $\mathbf{A}_u$ because $x_c > x_u$. Thus, with welfare equalized across locations, the productivity-population relationship is more positive when productivity is more spatially correlated.

B Data sources and construction

Agricultural data Our cereal data cover barley, maize, millet, oats, rice, rye, sorghum, and wheat. We use cereal-level measures of output (in metric tons, 1961-2013), yield (in metric tons per

harvested hectare, 1961-2013), trade quantity (in metric tons, 1961-2013), trade value (in nominal USD, 1961-2013), producer prices (in nominal local currency, 1966-2013), and change in storage (in metric tons, 1961-2013) for each country and year obtained from the FAO.[35] The gravity analysis in Table C.1 uses bilateral values of cereal trade flows (exporter-importer-year value in current USD) for 1962-2013 obtained from Comtrade.[36]

Domestic share of expenditure aggregated across cereals $c = 1, \ldots, C$ for country i in year t is

$$\lambda_{iit} = \frac{\sum_{c=1}^{C} X_{ciit}}{\sum_{c=1}^{C} X_{ciit} + \sum_{j \neq i} \sum_{c=1}^{C} X_{cjit}}$$

where X_{cjit} is the value of cereal c sold to i by j in year t. We observe X_{cjit} for $j \neq i$. We must construct X_{ciit} using data on output quantities, export quantities, and prices. $X_{ciit} = (q_{cit} - \text{exports}_{cit}) \cdot p_{cit}$, where q_{cit} is domestic output quantity, exports_{cit} is export quantity, and p_{cit} is domestic price.

There are two potential data sources for price p_{cit}, neither of which are ideal. The first data source is export unit values, $\frac{\sum_{j \neq i} X_{cijt}}{\text{exports}_{cit}}$, which are observed when a country exports a cereal. Unfortunately, only 53% of the cereal-country-year observations in our sample with positive output quantities have positive export quantities. The second price measure, producer prices in nominal local currency, presents two challenges. First, producer prices are available for only 59% of the cereal-country-year observations with positive cereal output. Second, due to resource constraints at the time, the FAO did not standardize the collection of 1966-1990 producer prices as it did for prices since 1991. As such, FAO warns against the combined use of the full 1966-2013 panel and notes that the FAO is "not in a position to give any explanation for the existing differences" between 1966-1990 and 1991-2013 producer prices.[37] Thus, despite extensive efforts to convert 1966-1990 FAO producer prices into nominal US dollars, use of producer prices raises concerns.

In light of these limitations and to ensure sufficient statistical power in our estimation, we elect to approximate domestic expenditure $\sum_{c=1}^{C} X_{ciit}$ by domestic quantity times average export unit value, $\left(\sum_{c=1}^{C} (q_{cit} - \text{exports}_{cit})\right) \left(\frac{\sum_{c=1}^{C} \sum_{j \neq i} X_{cijt}}{\sum_{c=1}^{C} \text{exports}_{cit}}\right)$. This measure is available for every year that a country exports at least one cereal, yielding a sizable estimation sample. This approximation of domestic expenditure $\sum_{c=1}^{C} X_{ciit}$ makes our outcome variable a noisy measure of the domestic share of expenditure. Table F.7 presents results for alternative approximations of the domestic share of expenditure. Our measure of cereal yield in country i and year t is harvested area-weighted cereal-level yield.

Finally, for several robustness checks, we also use bilateral trade data from the U.N. Comtrade database.[38] Comtrade data has the disadvantage of using cereal codes that differ from that used by

[35] Available at http://www.fao.org/faostat/en/#data.

[36] Bilateral trade value for cereals is only available starting in 1986 from FAO. We are furthermore unable to use Comtrade data to construct cereal own expenditure share because Comtrade does not provide export quantities over our sample period.

[37] See here: http://fenixservices.fao.org/faostat/static/documents/PA/PA_e.pdf

[38] Available at https://comtrade.un.org

the FAO. As such, despite careful matching of cereal categories across the two datasets, we prefer to use production and trade data that is reported in an internally consistent manner by the FAO. However, trade data at the bilateral level is available from Comtrade starting in 1962, whereas it is only available from the FAO starting in 1986. Thus, for the gravity equations estimated in Table C.1, we use Comtrade bilateral trade data. As a robustness check, we show in column 5 of Table F.7 that our main result is unaffected when we construct domestic expenditure share using Comtrade data.

ENSO index Annual ENSO variations can be detected using different indices, with the most commonly used being equatorial Pacific sea surface temperature (SST) anomalies. We primarily utilize 1960-2013 values of the monthly Kaplan NINO4 index which averages SST over the area 5°S-5°N, 160°E-150°W. For robustness checks in Table F.5, we also use the NINO3 (5°S-5°N, 150°W-90°W), NINO34 (5°S-5°N, 170°W - 120°W), and NINO12 (10°S-0°, 90°W-80°W) indices (Kaplan et al., 1998).[39]

Historical temperature and precipitation Global temperature (in degrees centigrade) and precipitation (in mm/month) variable constructed from monthly gridded global weather data at a 0.5° latitude by 0.5° longitude resolution was obtained from the Center for Climatic Research at the University of Delaware (Legates and Willmott, 1990*a*,*b*). 1960-2013 monthly data was first spatially aggregated from pixel to country-level using cross-sectional crop-area weights in 2000 from Ramankutty et al. (2008). For robustness checks in Table F.5, we also aggregate temperature from pixel to country-level using total country area. Annual values are then constructed by averaging January-December monthly values.

Projected temperature under climate change Global multi-model ensemble mean temperature temperature (in degrees centigrade) from monthly gridded global data at the 2.5° latitude by 2.5° longitude resolution from the Coupled Model Intercomparison Project version 5 (CMIP5).[40] 2014-2099 monthly data was first spatially aggregated from pixel to country-level using cross-sectional crop-area weights in 2000 from Ramankutty et al. (2008). Annual values are then constructed by averaging January-December monthly values.

Geography Country latitude and longitude are defined as crop area-weighted average using the global cross-sectional distribution of crop area in 2000 from Ramankutty et al. (2008). Great-circle distances between these country centroids are computed using the haversine formula.

Global oil prices Monthly West Texas Intermediate crude oil spot price obtained from the St. Louis Federal Reserve for 1961-2013.[41] Annual values are then constructed by averaging January-

[39] Available at http://iridl.ldeo.columbia.edu/SOURCES/.Indices/.nino/.EXTENDED/
[40] Available at https://climexp.knmi.nl/selectfield_cmip5.cgi
[41] Available at https://fred.stlouisfed.org/series/WTISPLC

December monthly values.

Export restrictions Export restrictions come from the United Nations Conference on Trade and Development's (UNCTAD) TRAINS database.[42]. To construct the dummy variable used in column 6 of Table 3, we employ all export-related measures (Chapter P of the International Classification of Non-Tariff Measures), excluding export subsidies. The indicator equals one for country-year observations in which a new restriction on exporting any cereal to any trading partner was introduced.

Variables in Table F.1 Time-averaged country-level real GDP per capita, TFP, capital stock, employment, and human capital index over 1961-2013 from Feenstra, Inklaar and Timmer (2015). Time-averaged country-level political stability, rule of law, and corruption indices over 1996-2013 from World Bank's World Governance Indicators.[43] Time-invariant country-level distance to nearest coastline or river and soil suitability for agriculture from Gallup, Sachs and Mellinger (1999).

C Additional empirical results

C.1 Gravity estimates for cereals trade

The theoretical model of Section 2 assumes that trade in cereals follows a gravity specification for exporter i, importer j, and year t:

$$\ln X_{ijt} = -\epsilon \ln \tau_{ij} + \ln\left(\frac{\chi_{it}}{w_{it}^{\epsilon}}\right) + \ln\left(\frac{X_{jt}}{\Phi_{jt}}\right) \tag{C.1}$$

Estimating this log-linear equation using bilateral trade flows in cereals results in patterns similar to those found in aggregate trade flows (e.g., Head and Mayer 2014). Bilateral cereal trade flows are available from Comtrade starting in 1962. We estimate a standard panel data model using bilateral distance as a (time-invariant) source of variation in bilateral trade costs (τ_{ij}) while employing exporter-year (it) and importer-year (jt) fixed effects. As in our main model, standard errors are clustered by year. Table C.1 reports the results. While the estimated distance coefficient of -1.5 shown in column 1 differs from the coefficient of -1.0 typically estimated for aggregate trade flows, the regression exhibits the typical explanatory power, accounting for the majority of the variation in cereal trade flows. In addition, 63% of countries that trade cereals in a given year both import and export cereals that year. At the level of importer-exporter pairs, 19% of trading pairs sell cereal in both directions. Thus, cereals are far from homogeneous commodities, and international trade in cereals is well described by the gravity specification. In column 2, we examine whether ENSO affects the trade elasticity ϵ by examining its effect on the distance elasticity.[44] Specifically, we include

[42] Available at http://trains.unctad.org

[43] Available at http://info.worldbank.org/governance/wgi/#home

[44] This is informative about the the trade elasticity per se to the extent that the distance elasticity of trade costs is invariant to ENSO.

an interaction between bilateral distance and a quadratic function of the sum of contemporaneous and lagged ENSO, $\text{ENSO}_t + \text{ENSO}_{t-1}$, the functional form for ENSO used for our main IV results in Table 2. ENSO does not alter the distance elasticity.

Table C.1: Gravity regression for international trade in cereals

Outcome is log import value		
	(1)	(2)
$\ln \text{distance}_{ij}$	-1.460	-1.477
	(0.046)	(0.066)
	[0.000]	[0.000]
$\ln \text{distance}_{ij} \times (ENSO_t + ENSO_{t-1})$		0.037
		(0.037)
		[0.324]
$\ln \text{distance}_{ij} \times (ENSO_t + ENSO_{t-1})^2$		0.004
		(0.029)
		[0.878]
Observations	102,787	102,787
R-squared	0.556	0.557
Country-level intra-industry trade share	0.628	0.628
Bilateral intra-industry trade share	0.185	0.185

NOTES: The dependent variable is annual bilateral (importer-reported) cereal trade value from Comtrade. The data cover 1962-2013. All models include importer-year and exporter-year fixed effects. Intraindustry trade shares are fraction of country-year and country-pair-year observations with positive exports and imports, conditional on positive exports or imports. Standard errors, clustered by year, in parentheses; p-values in brackets.

D Welfare calculations

This section details the welfare calculations in the main text.

D.1 Calculating historical variance of welfare effect

This section details the within-sample welfare calculation discussed in Section 4.2 and shown in Table 2. Recall the expression for the variance of welfare in equation (3):

$$var\left(\ln\left(C_i/L_i\right)\right) = var\left(\ln A_i\right) + 2cov\left(\ln A_i, \frac{-1}{\epsilon}\ln\lambda_{ii}\right) + var\left(\frac{1}{\epsilon}\ln\lambda_{ii}\right)$$

We employ this expression to quantify the magnitude of our reduced-form results in welfare terms. Consider the following thought experiment: suppose the spatial correlation of productivity increases

from the 1961-2013 historical mean, $\bar{I} = .214$, by one standard deviation, $\sigma_I = .0191$. What is the resulting percentage change in the cross-sectional variance of welfare, holding everything else fixed? We denote these two hypothetical states as uncorrelated state u and correlated state c.

For the uncorrelated state, we define variance productivity as the average cross-sectional productivity variance during 1961-2013:

$$var(\ln A_i^u) \equiv E_t[var_i(\ln A_{it}|t)] \tag{D.1}$$

Next, we define covariance between productivity and domestic share of expenditure during the uncorrelated state as the average cross-sectional covariance during 1961-2013:

$$cov(\ln A_i^u, \ln \lambda_{ii}^u) \equiv E_t[cov_i(\ln A_{it}, \ln \lambda_{iit}|t)] \tag{D.2}$$

We further define the variance of domestic share of expenditure during the uncorrelated states as the average variance during 1961-2013:

$$var(\ln \lambda_{iiu}) \equiv E_t[var_i(\ln \lambda_{iit}|t)] \tag{D.3}$$

Note that the values in definitions (D.1), (D.2), (D.3) can be directly computed from data since $\ln A_{it}$ and $\ln \lambda_{iit}$ are observed.

For the correlated state c, $var(\ln A_i^c)$ is also given by definitions (D.1) since we assume productivity variance is unaltered by changes in spatial correlation. $cov(\ln A_i^c, \ln \lambda_{ii}^c)$ and $var(\lambda_{ii}^c)$, however, have to be calculated as one does not directly observe data from a year in which only $I_t = \bar{I} + \sigma_I$ while everything else is fixed at the historical mean. To do this, first recall our reduced-form expression for $\ln \lambda_{it}$ from equation (7):

$$\ln \lambda_{iit} = \beta_0 \ln A_{it} + \beta_1 \ln A_{it} I_t + \mathbb{Z}_{it}\Pi + \mu_{it}$$

Our estimates of this equation can be employed to construct each component of equation (3) for the correlated state. The covariance between productivity and domestic share of expenditure during the correlated state is:

$$\begin{aligned} cov(\ln A_i^c, \ln \lambda_{ii}^c) \equiv\ & (\widehat{\beta_0} + \widehat{\beta_1}(\bar{I} + \sigma_I))E_t[var_i(\ln A_{it}|t)] \\ & + E_t[cov_i(\ln A_{it}, \mathbb{Z}_{it}\widehat{\Pi}|t)] + E_t[cov_i(\ln A_{it}, \widehat{\mu}_{it}|t)] \end{aligned} \tag{D.4}$$

The variance of domestic share of expenditure during the correlated state is:

$$\begin{aligned} var(\ln \lambda_{ii}^c) \equiv & (\widehat{\beta}_0^2 + 2\widehat{\beta}_0\widehat{\beta}_1(\bar{I}+\sigma_I) + \widehat{\beta}_1^2(\bar{I}+\sigma_I)^2)E_t[var_i(\ln A_{it}|t)] \\ & + E_t[var_i(\mathbb{Z}_{it}\widehat{\Pi}|t)] + E_t[var_i(\widehat{\mu}_{it}|t)] \\ & + 2(\widehat{\beta}_0 + \widehat{\beta}_1(\bar{I}+\sigma_I))E_t[cov_i(\ln A_{it}, \mathbb{Z}_{it}\widehat{\Pi}|t)] \\ & + 2(\widehat{\beta}_0 + \widehat{\beta}_1(\bar{I}+\sigma_I))E_t[cov_i(\ln A_{it}, \widehat{\mu}_{it}|t)] \\ & + 2E_t[cov_i(\mathbb{Z}_{it}\widehat{\Pi}, \widehat{\mu}_{it}|t)] \end{aligned} \tag{D.5}$$

Each term in equations (D.4) and (D.5) is either directly observable or can be obtained by estimating equation (7). For example, for the model estimated in column 4, panel B of Table 2, with $\widehat{\beta}_0 = 2.114$ and $\widehat{\beta}_1 = -4.144$, we have:

$$\begin{aligned} E_t[var_i(\ln A_{it}|t)] &= .453 \\ E_t[var_i(\mathbb{Z}_{it}\widehat{\Pi}|t)] &= 1.04 \\ E_t[var_i(\widehat{\mu}_{it}|t)] &= .083 \\ E_t[cov_i(\ln A_{it}, \mathbb{Z}_{it}\widehat{\Pi}|t)] &= -.497 \\ E_t[cov_i(\ln A_{it}, \widehat{\mu}_{it}|t)] &= -.026 \\ E_t[cov_i(\mathbb{Z}_{it}\widehat{\Pi}, \widehat{\mu}_{it}|t)] &= -.001 \end{aligned}$$

Applying equation (3), the percentage change in the variance of welfare in the correlated state, relative to the uncorrelated state, is

$$\frac{var\left(\ln \frac{C_i^c}{L_i}\right) - var\left(\ln \frac{C_i^u}{L_i}\right)}{var(\ln(C_i^u/L_i))} = \frac{var\left(\ln A_i^c\right) - \frac{2}{\epsilon}cov\left(\ln A_i^c, \ln \lambda_{ii}^c\right) + \frac{1}{\epsilon^2}var\left(\ln \lambda_{ii}^c\right)}{var\left(\ln A_i^u\right) - \frac{2}{\epsilon}cov\left(\ln A_i^u, \ln \lambda_{ii}^u\right) + \frac{1}{\epsilon^2}var\left(\ln \lambda_{ii}^u\right)} - 1 \tag{D.6}$$

To complete the calculation, let the agricultural trade elasticity be $\epsilon = 8.59$ (Caliendo and Parro, 2015, Table A2). Values from equation (D.6) are shown in Table 2, with standard errors calculated using the delta method.

D.2 Calculating change in variance of welfare under climate change

In Section 5.2, we calculate the percentage change in the variance of welfare between the end of our estimation period, $\bar{t} = 2013$, and the end of our projection period, $\mathcal{T} = 2099$, under climate change, holding everything else fixed. Compared with the welfare calculation described in Appendix D.1 and reported in Table 2, there is an added complication: climate change also changes the variance of productivity.

To begin, recall equation (10) for $\ln A_{it}$ during the estimation period, $t \in [1961, 2013]$:

$$\ln A_{it} = k(T_{it}) + \mathbb{X}_{it}\Psi + \nu_{it}$$

Column 1 of Table F.8 shows coefficients for $\widehat{k}()$ from our benchmark specification, which is also plotted in Figure 15. Using estimates from equation (10) and our business-as-usual CMIP5 ensemble mean projected temperatures under climate change, $\widehat{T}_{it}$, we first compute country-year agricultural productivity under climate change during the projection period $t \in [2014, 2099]$, holding everything but temperature fixed to estimated $\bar{t} = 2013$ values:

$$\widehat{\ln A}_{it} = \widehat{k}(\widehat{T}_{it}) + \mathbb{X}_{i\bar{t}}\widehat{\Psi} + \widehat{\nu}_{i\bar{t}} \tag{D.7}$$

Figure 16 shows the associated change in log agricultural productivity, $\widehat{\ln A}_{i,2099} - \ln A_{i,2013}$, for each country. In Figure 18, the gray line shows $var(\widehat{\ln A}_{it})$ while the blue line shows Moran's I, $\widehat{I}_t$ computed using $\widehat{\ln A}_{it}$, for each projection year.

To compute the change in variance of welfare from the end of the estimation period, $\bar{t} = 2013$, to any year during the projection period, $t \in [2014, 2099]$, we difference equation (3):

$$\begin{aligned} var\left(\ln(C_{it}/L_{it})\right) - var\left(\ln(C_{i\bar{t}}/L_{i\bar{t}})\right) = & [var(\widehat{\ln A}_{it}) - var(\ln A_{i\bar{t}})] \\ & - (2/\epsilon)[cov(\widehat{\ln A}_{it}), \widehat{\ln \lambda}_{iit}) - cov(\ln A_{i\bar{t}}, \ln \lambda_{ii\bar{t}})] \\ & + (1/\epsilon^2)[var(\widehat{\ln \lambda}_{iit}) - var(\ln \lambda_{ii\bar{t}})] \end{aligned} \tag{D.8}$$

We consider two scenarios for obtaining future domestic share of expenditure, $\widehat{\ln \lambda}_{iit}$. In the first scenario, the projection omits changes in the spatial structure in the sense that the spatial correlation of productivities is fixed at its value at the end of the estimation period, $I_{\bar{t}}$, throughout the projection period. In the second projection, we allow climate change to alter the spatial correlation of productivity.

Variance projection omitting changes in spatial structure Holding the spatial correlation of productivity fixed, the domestic share of expenditure during the projection period, $t \in [2014, 2099]$, is computed using our benchmark estimate of equation (7) from column 4, panel B of Table 2:

$$\widehat{\ln \lambda}^{n}_{iit} = (\widehat{\beta}_0 + \widehat{\beta}_1 I_{\bar{t}})\widehat{\ln A}_{it} + \mathbb{Z}_{i\bar{t}}\widehat{\Pi} + \widehat{\mu}_{i\bar{t}} \tag{D.9}$$

Equations (D.7) and (D.9) allow construction of $var(\widehat{\ln \lambda}^{n}_{iit})$ and $cov(\widehat{\ln A}_{it}, \widehat{\ln \lambda}^{n}_{iit})$ for each year in the projection period. These then enter into equation (D.8) to compute the change in welfare variance since 2013 over the 21st century for the projection that omits changes in spatial structure. That projected welfare variance is shown as the solid gray line in Figure 18.

Variance projection including changes in spatial structure Allowing the spatial correlation of productivity to vary under climate change, the domestic share of expenditure during the projection period, $t \in [2014, 2099]$, is computed using our benchmark estimate of equation (7) from column 4, panel B of Table 2:

$$\widehat{\ln \lambda}^{s}_{iit} = (\widehat{\beta}_0 + \widehat{\beta}_1 \widehat{I}_t)\widehat{\ln A}_{it} + \mathbb{Z}_{i\bar{t}}\widehat{\Pi} + \widehat{\mu}_{i\bar{t}} \tag{D.10}$$

Equations (D.7) and (D.10) allow construction of $var(\widehat{\ln \lambda}^{s}_{iit})$ and $cov(\widehat{\ln A}_{it}, \widehat{\ln \lambda}^{s}_{iit})$ for each year in the projection period. These then enter into equation (D.8) to compute the change in welfare variance since 2013 over the 21st century for the projection that includes changes in spatial structure. That projected welfare variance is shown as the solid red line in Figure 18.

Difference across projections For the period from $\bar{t} = 2013$ to $\mathcal{T} = 2099$, we calculate the percentage difference in the change in welfare variance between projections that include and omit changes in spatial structure:

$$\frac{var\left(\ln\left(C^{s}_{i\mathcal{T}}/L^{s}_{i\mathcal{T}}\right)\right) - var\left(\ln\left(C_{i\bar{t}}/L_{i\bar{t}}\right)\right)}{var\left(\ln\left(C^{n}_{i\mathcal{T}}/L^{n}_{i\mathcal{T}}\right)\right) - var\left(\ln\left(C_{i\bar{t}}/L_{i\bar{t}}\right)\right)} - 1 \tag{D.11}$$

When using baseline estimated parameters, and an agricultural trade elasticity of $\epsilon = 8.59$ (Caliendo and Parro, 2015, Table A2), we find that allowing climate change to alter the spatial correlation of productivities predicts a 20% greater increase in welfare variance than when spatial correlation is held fixed.

D.3 Calculating change in country-level welfare under climate change

From equation (2), the expression for welfare of country i in year t is

$$\ln\left(C_{it}/L_{it}\right) = \ln A_{it} + \gamma - \frac{1}{\epsilon}\ln \lambda_{iit}.$$

For the projection period, the productivity of country i in year t, $\widehat{\ln A}_{it}$ is given by equation (D.7). Next, we calculate the difference in welfare projections for individual countries between projections that include and omit changes in spatial structure.

Country welfare projection omitting changes in spatial structure Holding the spatial correlation of productivity fixed, the other component of welfare during the projection period, $t \in [2014, 2099]$, is:

$$\widehat{\ln \lambda}^{n}_{iit} = (\widehat{\beta}_0 + \widehat{\beta}_1 I_{\bar{t}})\widehat{\ln A}_{it} + \widehat{\kappa} I_{\bar{t}} + \mathbb{Z}_{i,\bar{t}}\widehat{\Pi} + \widehat{\mu}_{i\bar{t}} \tag{D.12}$$

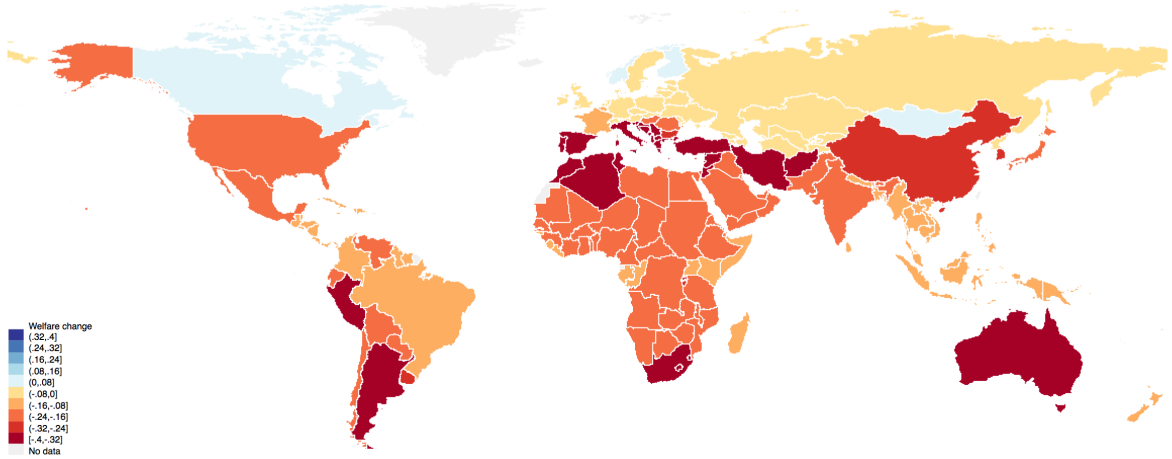
where spatial correlation affects both the average domestic share of expenditure (κ) and its relationship to domestic productivity (β_1).[45] The difference in country i welfare from $\bar{t} = 2013$ to $\mathcal{T} = 2099$ is:

$$\ln(C^{n}_{i\mathcal{T}}/L^{n}_{i\mathcal{T}}) - \ln(C_{i\bar{t}}/L_{i\bar{t}}) = [\widehat{\ln A}_{i\mathcal{T}} - \ln A_{i\bar{t}}] - (1/\epsilon)\left[(\widehat{\beta}_0 + \widehat{\beta}_1 I_{\bar{t}})(\widehat{\ln A}_{i\mathcal{T}} - \ln A_{i\bar{t}})\right] \tag{D.13}$$

Figure D.1 shows the change in welfare for each country under this projection.

[45] To obtain κ, we first recover year fixed effects from equation (7). $\kappa = 2.45$ is the coefficient from a linear regression of year fixed effects on I_t and a linear time trend.

Figure D.1: Welfare change under projection that omits changes in spatial structure (2013-2099)



NOTES: Map shows the projected 2013-2099 welfare changes from the projection that omits changes in spatial structure under a business-as-usual CMIP5 ensemble mean climate projection.

Country welfare projection including changes in spatial structure Allowing the spatial correlation of productivity to vary under climate change, the other component of welfare during the projection period, $t \in [2014, 2099]$ is:

$$\widehat{\ln \lambda}^{s}_{iit} = (\widehat{\beta}_0 + \widehat{\beta}_1 \widehat{I}_t)\widehat{\ln A}_{it} + \widehat{\kappa}\widehat{I}_t + \mathbb{Z}_{i,\bar{t}}\widehat{\Pi} + \widehat{\mu}_{i,\bar{t}}$$

Similarly, the difference in country i welfare from $\bar{t} = 2013$ to $\mathcal{T} = 2099$ is:

$$\ln(C^s_{i\mathcal{T}}/L^s_{i\mathcal{T}}) - \ln(C_{i\bar{t}}/L_{i\bar{t}}) = [\widehat{\ln A}_{i\mathcal{T}} - \ln A_{i\bar{t}}] - (1/\epsilon)\left[(\widehat{\beta}_0 + \widehat{\beta}_1 \widehat{I}_{\mathcal{T}})\widehat{\ln A}_{i\mathcal{T}} - (\widehat{\beta}_0 + \widehat{\beta}_1 I_{\bar{t}}) \ln A_{i\bar{t}} + \widehat{\kappa}(\widehat{I}_{\mathcal{T}} - I_{\bar{t}})\right]$$

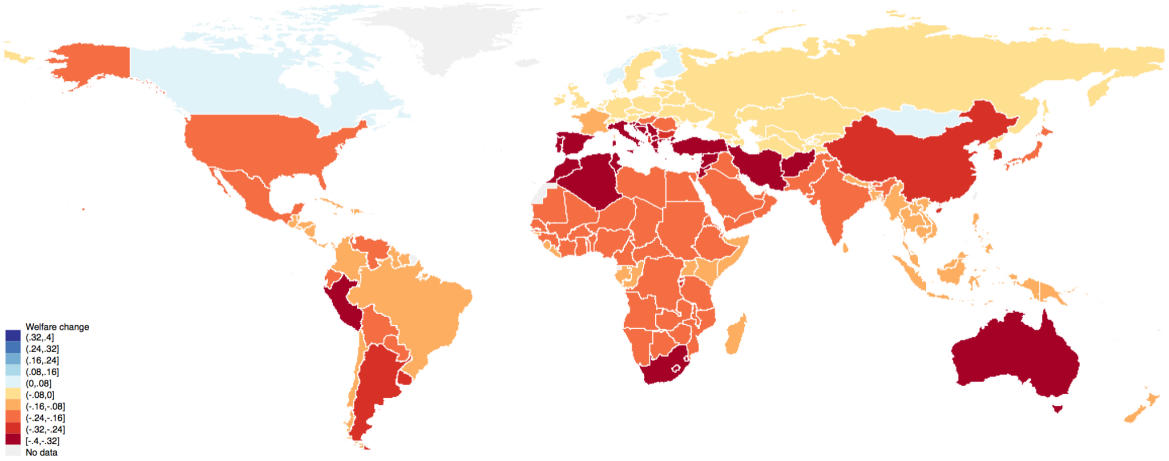
Figure D.2 shows the change in welfare for each country under this projection.

Difference across projections The difference in country welfare between projections that include and omit changes in spatial structure is:

$$[\ln(C^s_{i\mathcal{T}}/L^s_{i\mathcal{T}}) - \ln(C_{i\bar{t}}/L_{i\bar{t}})] - [\ln(C^n_{i\mathcal{T}}/L^n_{i\mathcal{T}}) - \ln(C_{i\bar{t}}/L_{i\bar{t}})] = -(1/\epsilon)[(\widehat{\beta}_1 \widehat{\ln A}_{i\mathcal{T}} + \widehat{\kappa})(\widehat{I}_{\mathcal{T}} - I_{\bar{t}})] \quad \text{(D.14)}$$

Figure 19 shows the country-level difference across projections.

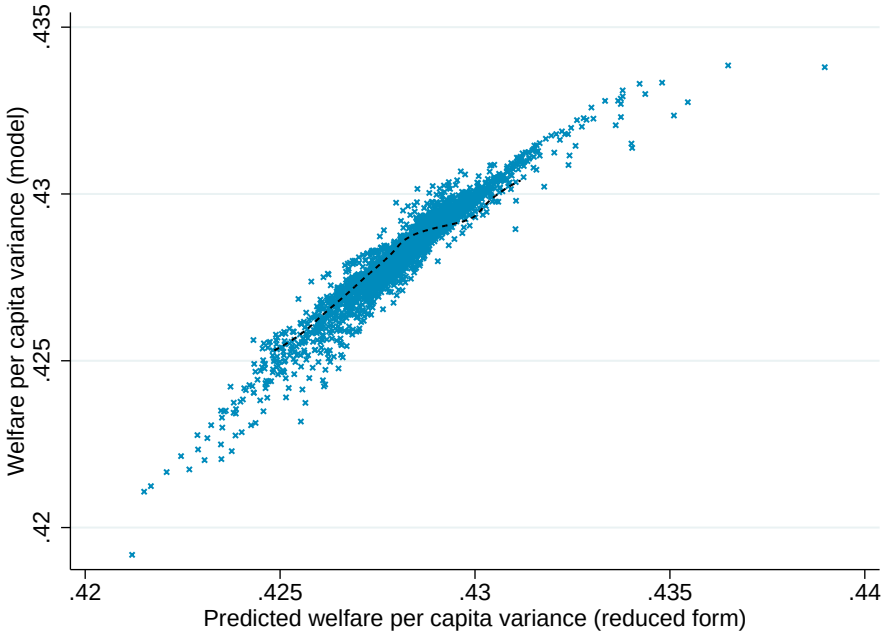
Figure D.2: Welfare change under projection that includes changes in spatial structure (2013-2099)



NOTES: Map shows the projected 2013-2099 welfare changes from the projection that includes changes in spatial structure under a business-as-usual CMIP5 ensemble mean climate projection.

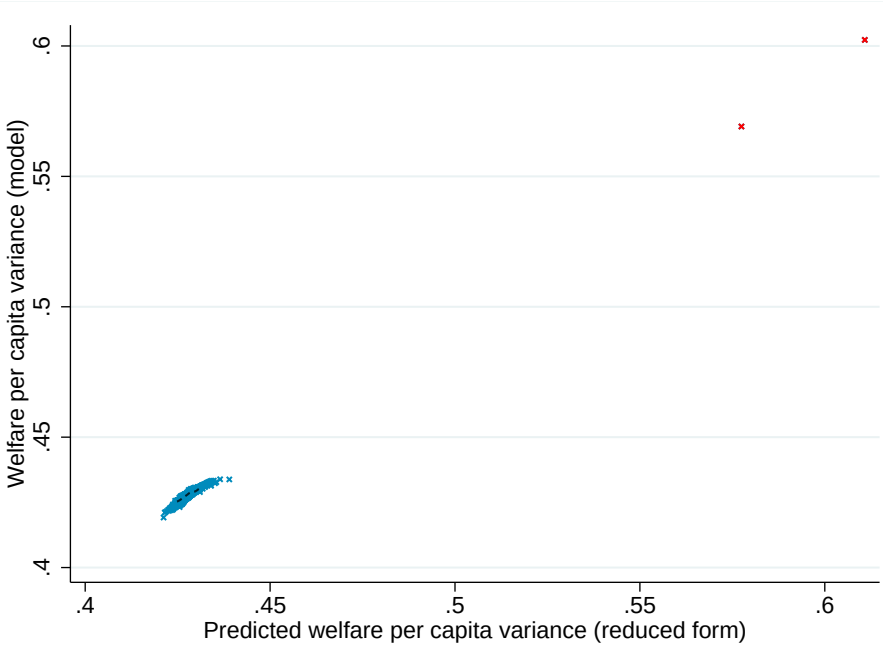
E Appendix figures

Figure E.1: Welfare per capita, model vs approximation by linear regression



NOTES: For each equilibrium depicted in Figure 7, we compute equilibrium welfare per capita in the model (vertical axis) and welfare per capita predicted by an estimated linear regression (horizontal axis). The regression specification is akin to the line of best fit depicted in Figure 7, see equation (7). Predicted welfare per capita is computed by plugging in predicted values of $\ln \lambda_{ii}$ into equation (3). The dashed series is a local polynomial fit on the 1st through 99th percentiles of predicted welfare per capita. The R^2 of the bivariate relationship exceeds .93.

Figure E.2: Welfare per capita under climate change, model vs approximation by linear regression



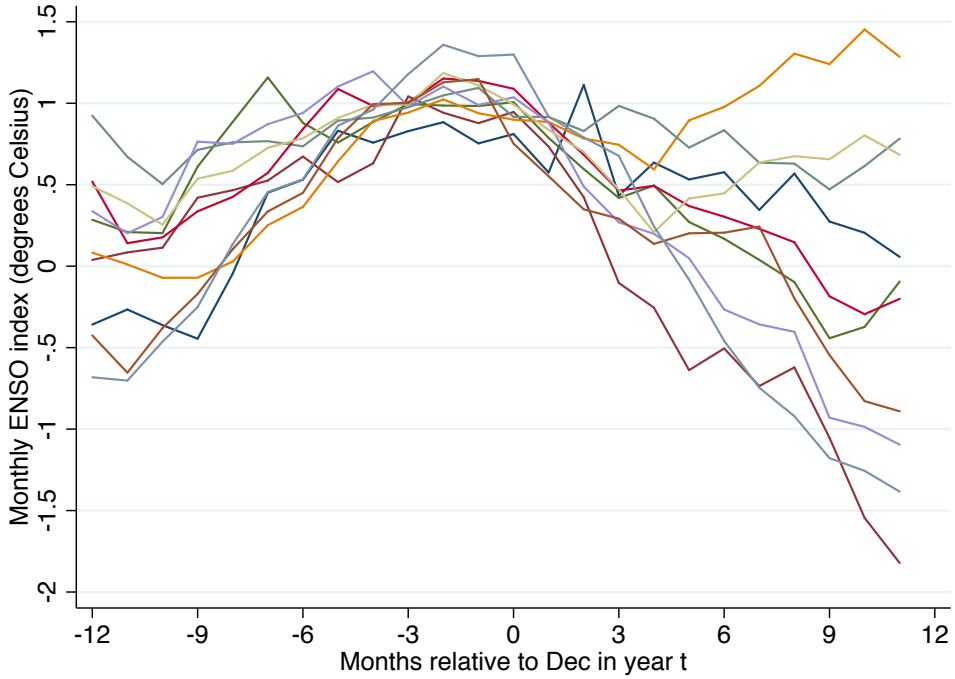
NOTES: The blue observations and black dashed local polynomial are identical to those in Figure E.1. The two red Xs denote observations in which we impose the (predicted) cereal productivities for 2013 and 2099 from equation (10) and solve for equilibrium (vertical axis). The linear extrapolation based on the blue observations predicts these values of variance in welfare per capita well.

Figure E.3: Location of ENSO sea-surface temperature measurements



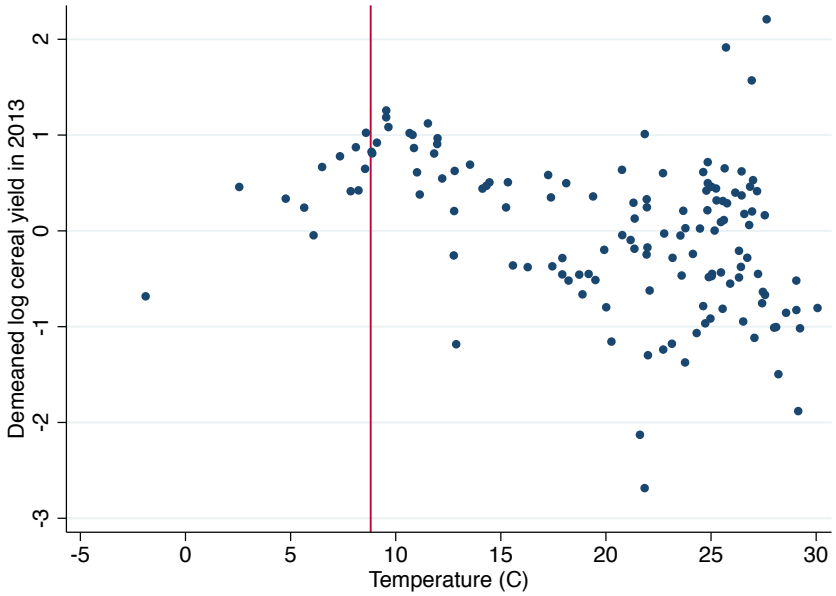
NOTES: ENSO indices defined as average sea surface temperature over a region minus the long-term mean sea surface temperature for that region. Spatial definitions for standard ENSO indices: NINO4 (5°S-5°N, 160°E-150°W), NINO3 (5°S-5°N, 150°W-90°W), NINO34 (5°S-5°N, 170°W - 120°W), and NINO12 (10°S-0°, 90°W-80°W).

Figure E.4: Monthly ENSO index for top 10 positive events



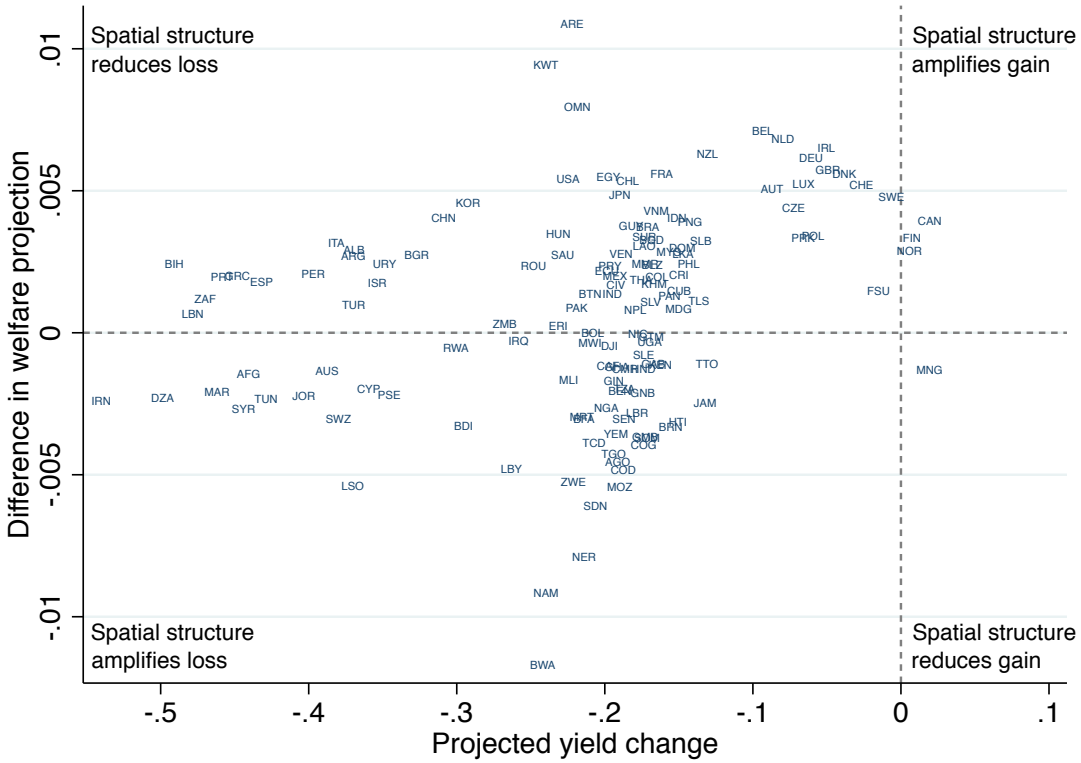
NOTES: Monthly evolution of ENSO index 12 months before and after the 10 most positive ENSO events over 1961-2013. ENSO events occur during the winters of 1965, 1972, 1982, 1986, 1991, 1994, 1997, 2002, 2006, and 2009.

Figure E.5: Observed log cereal yields and temperature in 2013



NOTES: Observed country-level log cereal yields in 2013 with cross-sectional mean removed plotted against temperature in 2013. From equation (10), observed log cereal yield is sum of the nonlinear temperature relationship $k(T_{it})$, controls $\mathbb{X}_{it}\Psi$, and the residual term ν_{it}. Vertical line shows the predicted log yield maximizing temperature from Figure 15.

Figure E.6: Differences in welfare projections due to change in spatial correlation and projected yield changes



NOTES: Scatter shows the difference in projected country-level welfare change between projections that include and omit changes in spatial correlation (from Figure 19) plotted against change in log cereal yields (from Figure 16) over 2013-2099 under climate change. Countries labeled by ISO3 identifier.

F Appendix tables

Table F.1: Spatial correlation of economic determinants

	Moran's I
Income	
log real GDP per capita[†] (top panel of Figure 1)	.247
Reshuffled log real GDP per capita[†] (bottom panel of Figure 1)	.015
Determinants	
log TFP[†]	.102
log capital stock[†]	.287
log employment[†]	.233
Human capital index[†]	.296
Political stability index[‡]	.164
Rule of law index[‡]	.19
Corruption index[‡]	.174
Temperature[§]	.236
log distance to nearest coastline or river[**]	.121
Soil suitability for agriculture[**]	.183

NOTES: Spatial correlation for income per capita and various determinants. Moran's I lies within $[-1, +1]$. [†] denotes time-averaged cross-country variables over 1961-2013 from Feenstra, Inklaar and Timmer (2015). [‡] denotes time-averaged cross-country variables over 1996-2013 from World Bank's World Governance Indicators. [§] denotes time-averaged cross-country variable over 1961-2013 from Legates and Willmott (1990*a*). [**] denotes time-invariant cross-country variables from Gallup, Sachs and Mellinger (1999).

Table F.2: Statistical significance of first-stage coefficients

	(1)	(2)	(3)	(4)	(5)
α'_{11} joint F-stat p-value	0.022	0.007	0.011	0.011	0.008
α'_{12} joint F-stat p-value	0.006	0.038	0.097	0.178	0.218
α'_{21} joint F-stat p-value	0.071	0.004	0.007	0.006	0.003
α'_{22} joint F-stat p-value	0.041	0.062	0.028	0.041	0.071
Number of temperature splines in $f()$	2	3	4	5	6
Observations	5452	5452	5452	5452	5452

NOTES: Shows p-values from joint significance F-tests across the elements of each vector of first-stage coefficients, α'_{11} and α'_{12} from equation (8), α'_{21} and α'_{22} from equation (9). Columns 1-5 correspond to the IV specifications in columns 2-6 of Table 2.

Table F.3: Alternative error structures
Outcome is log domestic share of expenditure

	(1)	(2)	(3)	(4)
$\ln A_{it}$ (β_0)	2.114	2.114	2.114	2.114
	(0.604)	(0.581)	(0.830)	(0.698)
	[0.001]	[0.001]	[0.014]	[0.004]
$\ln A_{it} \times I_t$ (β_1)	-4.144	-4.144	-4.144	-4.144
	(1.834)	(1.659)	(2.157)	(1.939)
	[0.028]	[0.016]	[0.060]	[0.037]
Clustering	year cluster	year cluster and 20 year HAC	year cluster and cntry cluster	year cluster
Bekker adjustment	No	No	No	Yes
Observations	5452	5452	5452	5452

NOTES: Estimates of β_0 and β_1 from equation (7). Column 1 reproduces benchmark estimates from column 4, panel B of Table 2 with year-level clustered standard errors. Column 2 allows year-level clustering and common serial correlation across countries within a 10-year window. Column 3 allows year and country-level clustering. Column 4 allows year-level clustering with a Bekker (1994) adjustment. Standard errors in parentheses; p-values in brackets.

Table F.4: Sample split
Outcome is log domestic share of expenditure

	(1)	(2)	(3)	(4)
$\ln A_{it}$ (β_0)	2.114	2.152	1.845	1.692
	(0.604)	(0.595)	(2.807)	(0.511)
	[0.001]	[0.001]	[0.517]	[0.003]
$\ln A_{it} \times I_t$ (β_1)	-4.144	-4.226	-4.639	-2.708
	(1.834)	(1.925)	(12.564)	(1.627)
	[0.028]	[0.033]	[0.715]	[0.108]
Include large producers?	Yes	No	Yes	Yes
Sample period	1961-2013	1961-2013	1961-1987	1988-2013
Observations	5452	4952	2655	2793

NOTES: Estimates of β_0 and β_1 from equation (7). Column 1 reproduces benchmark estimates from column 4, panel B of Table 2. Column 2 excludes the following ten countries, which together account for more than half of world cereal output in each year: China, United States, India, Former Soviet Union, France, Indonesia, Canada, Brazil, Germany, and Bangladesh. Column 3 restricts sample to 1961-1987. Column 4 restricts sample to 1988-2013. Standard errors clustered by year in parentheses; p-values in brackets.

Table F.5: ENSO and local temperature definitions
Outcome is log domestic share of expenditure

	(1)	(2)	(3)	(4)
Panel A: Crop-area-weighted country temperature				
$\ln A_{it}$ (β_0)	2.114	2.108	2.084	2.722
	(0.604)	(0.715)	(0.706)	(0.987)
	[0.001]	[0.005]	[0.005]	[0.008]
$\ln A_{it} \times I_t$ (β_1)	-4.144	-4.064	-4.465	-6.026
	(1.834)	(2.414)	(2.406)	(3.127)
	[0.028]	[0.098]	[0.069]	[0.059]
Observations	5452	5452	5452	5452
Panel B: Total-area-weighted country temperature				
$\ln A_{it}$ (β_0)	1.632	1.722	1.562	1.871
	(0.500)	(0.626)	(0.597)	(0.729)
	[0.002]	[0.008]	[0.012]	[0.013]
$\ln A_{it} \times I_t$ (β_1)	-3.960	-4.125	-4.155	-4.517
	(1.617)	(2.155)	(2.071)	(2.331)
	[0.018]	[0.061]	[0.050]	[0.058]
ENSO index	4	3	34	12
Observations	5605	5605	5605	5605

NOTES: Estimates of β_0 and β_1 from equation (7). Panel A uses crop-area-weighted country-level temperatures. Panel B uses total-area-weighted country-level temperatures. Columns 1 to 4 use NINO4, NINO3, NINO34, and NINO12 as ENSO index. Standard errors clustered by year in parentheses; p-values in brackets.

Table F.6: Using spatial correlation of temperature instead of ENSO

Outcome is log domestic share of expenditure

	(1) OLS	(2) IV	(3) IV	(4) IV	(5) IV	(6) IV
$\ln A_{it}$ (β_0)	0.284	2.486	2.540	1.918	1.647	1.686
	(0.119)	(1.310)	(1.182)	(0.600)	(0.618)	(0.624)
	[0.021]	[0.063]	[0.036]	[0.002]	[0.010]	[0.009]
$\ln A_{it} \times I_t$ (β_1)	0.758	-5.044	-5.135	-3.092	-2.348	-2.394
	(0.487)	(4.173)	(4.011)	(1.884)	(1.943)	(2.021)
	[0.126]	[0.232]	[0.206]	[0.107]	[0.232]	[0.241]
Number of temperature splines in f		2	3	4	5	6
Temperature Moran's I polynomial order in g		1	1	1	1	1
Number of instruments		4	6	8	10	12
Cragg-Donald F-stat		6.407	5.267	6.161	5.428	4.846
Stock-Yogo crit. value: 10% max 2SLS bias		7.560	9.480	10.220	10.580	10.780
Stock-Yogo crit. value: 10% max 2SLS size		16.870	21.680	25.640	29.320	32.880
Stock-Yogo crit. value: 10% max LIML size		4.720	4.060	3.780	3.640	3.580
Kleibergen-Paap F-stat		2.813	2.217	2.145	2.389	2.061
Anderson-Rubin weak-id robust joint p-value		0.000	0.000	0.000	0.000	0.000
BIC for first stage equations		-30778.99	-30789.58	-30873.67	-30862.59	-30845.54
Observations	5452	5452	5452	5452	5452	5452

NOTES: Estimates of β_0 and β_1 from equation (7) with $g(ENSO_t + ENSO_{t-1})$ in first-stage equations (8) and (9) replaced with the annual global spatial correlation of temperature, $I_t(T_{it})$. Column 1 shows OLS estimates. Columns 2-6 show LIML estimates that vary by the number of temperature spline terms in $f()$. All models include country fixed effects, year fixed effects, and country-specific linear trends as included instruments. Standard errors clustered by year in parentheses; p-values in brackets.

Table F.7: Alternative domestic expenditure share constructions

Outcome is log domestic share of expenditure

	(1)	(2)	(3)	(4)	(5)
$\ln A_{it}$ (β_0)	2.114	1.365	1.825	1.568	1.883
	(0.604)	(0.397)	(0.559)	(0.432)	(0.604)
	[0.001]	[0.001]	[0.002]	[0.001]	[0.003]
$\ln A_{it} \times I_t$ (β_1)	-4.144	-3.068	-3.622	-2.835	-4.676
	(1.834)	(1.423)	(1.585)	(1.337)	(1.938)
	[0.028]	[0.036]	[0.026]	[0.039]	[0.019]
Price data	FAO	FAO	FAO	FAO	Comtrade
Price imputation	average export	export+ producer	lowest export	highest export	average export
Observations	5452	2918	5452	5452	4937

NOTES: Estimates of β_0 and β_1 from equation (7). Column 1 reproduces benchmark estimates from column 4, panel B of Table 2 with average export-volume-weighted cereal export unit value used for imputing cereal-level prices in constructing domestic expenditure share. Column 2 uses cereal-level export unit values with missing observations imputed using producer prices to construct domestic expenditure. Columns 3 and 4 use cereal-level export unit values with missing observations imputed using the lowest and highest observed export unit value for a given country and year, respectively. Column 5 replicates column 1 but constructs domestic expenditure share using Comtrade bilateral trade data instead of FAO trade data. FAO trade data available for 1961-2013. Comtrade data available for 1962-2013. Standard errors clustered by year in parentheses; p-values in brackets.

Table F.8: Log cereal yield and local temperature
Outcome is log cereal yields

	(1)	(2)	(3)	(4)	(5)	(6)
Temperature 1st term	0.004	0.004	0.005	0.005	0.007	0.005
	(0.009)	(0.009)	(0.010)	(0.010)	(0.011)	(0.011)
	[0.686]	[0.677]	[0.629]	[0.631]	[0.519]	[0.623]
Temperature 2nd term	-0.183	-0.165	-0.222	-0.203	-0.126	-0.100
	(0.041)	(0.040)	(0.071)	(0.071)	(0.060)	(0.059)
	[0.000]	[0.000]	[0.003]	[0.006]	[0.041]	[0.093]
Temperature 3rd term	0.650	0.599	0.418	0.393	0.020	-0.031
	(0.160)	(0.159)	(0.196)	(0.196)	(0.212)	(0.205)
	[0.000]	[0.000]	[0.038]	[0.050]	[0.924]	[0.882]
Temperature 4th term	-1.162	-1.100	0.356	0.248	1.320	1.394
	(0.533)	(0.539)	(0.649)	(0.644)	(0.674)	(0.658)
	[0.034]	[0.047]	[0.586]	[0.702]	[0.056]	[0.039]
Temperature 5th term			-2.204	-1.801	-2.895	-3.370
			(1.775)	(1.760)	(1.880)	(1.864)
			[0.220]	[0.311]	[0.130]	[0.076]
Temperature 6th term					1.830	3.213
					(3.814)	(3.791)
					[0.633]	[0.401]
Precipitation		0.003		0.003		0.003
		(0.001)		(0.001)		(0.001)
		[0.000]		[0.000]		[0.000]
Precipitation squared		-0.000		-0.000		-0.000
		(0.000)		(0.000)		(0.000)
		[0.000]		[0.000]		[0.000]
Number of temperature splines	4	4	5	5	6	6
Precipitation	No	Yes	No	Yes	No	Yes
Temp. joint p-value	0.0004	0.0014	0.0009	0.0030	0.0015	0.0049
Optimal temp.	8.81	8.91	8.87	8.94	7.80	7.70
Observations	7226	7226	7226	7226	7226	7226

NOTES: Estimates of cubic spline terms for $h()$ in equation (10) during 1961-2013. The number of knots placed along the temperature support according to Harrell (2001) varies across columns. Odd (even) numbered columns exclude (include) quadratic precipitation terms. P-value from a joint significance test of temperature terms shown. Standard errors clustered by year in parentheses; p-values in brackets.